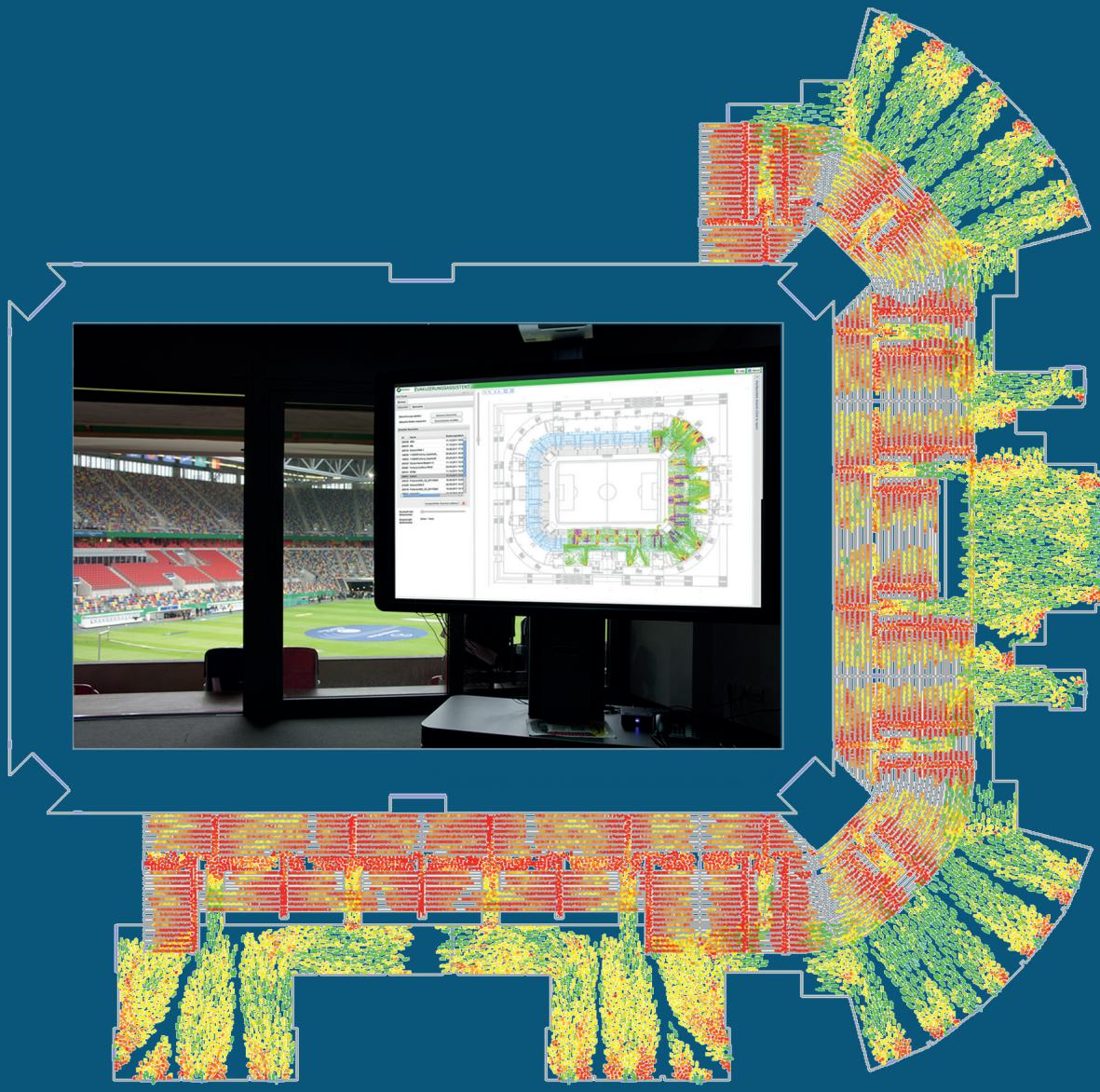

Route Choice Modelling and Runtime Optimisation for Simulation of Building Evacuation

Armel Ulrich Kemloh Wagoum

Mitglied der Helmholtz-Gemeinschaft

JÜLICH
FORSCHUNGSZENTRUM

Schriften des Forschungszentrums Jülich

IAS Series Volume 17

Forschungszentrum Jülich GmbH
Institute for Advanced Simulation (IAS)
Jülich Supercomputing Centre (JSC)

Route Choice Modelling and Runtime Optimisation for Simulation of Building Evacuation

Armel Ulrich Kemloh Wagoum

Schriften des Forschungszentrums Jülich

IAS Series Volume 17

ISSN 1868-8489 ISBN 978-3-89336-865-5

Bibliographic information published by the Deutsche Nationalbibliothek.
The Deutsche Nationalbibliothek lists this publication in the Deutsche Nationalbibliografie; detailed bibliographic data are available in the Internet at http://dnb.d-nb.de.

Publisher and Distributor:	Forschungszentrum Jülich GmbH Zentralbibliothek 52425 Jülich Phone +49 (0) 24 61 61-53 68 · Fax +49 (0) 24 61 61-61 03 e-mail: zb-publikation@fz-juelich.de Internet: http://www.fz-juelich.de/zb
Cover Design:	Jülich Supercomputing Centre, Forschungszentrum Jülich GmbH
Printer:	Grafische Medien, Forschungszentrum Jülich GmbH
Copyright:	Forschungszentrum Jülich 2013

Schriften des Forschungszentrums Jülich
IAS Series Volume 17

D 468 (Diss., Wuppertal, Univ., 2012)

ISSN 1868-8489
ISBN 978-3-89336-865-5

The complete volume is freely available on the Internet on the Jülicher Open Access Server (JUWEL) at http://www.fz-juelich.de/zb/juwel

Persistent Identifier: urn:nbn:de:0001-2013032608
Resolving URL: http://www.persistent-identifier.de/?link=610

Abstract

Increasing number of visitors at large-scale events combined with the increasing complexity of modern buildings set a major challenge for planners, operators and emergency services. Examples include multi-purpose arenas, large railway stations and airports. In this dissertation the use of modern parallel hardware in combination with optimised algorithms are for the first time used on site to speed up the simulation of large crowds. The aim is to perform real-time forecasts of pedestrian traffic. For this purpose, special neighbourhood lists and a two-stage hybrid parallelisation are used. The second part of this dissertation deals with route choice in complex structures, which plays an important role in achieving realistic computer simulations of pedestrian flows. The developed route choice process is based on visibility and perception of the local environment by the simulated agents. It has as basis a navigation graph. The generation of the graph, especially in complex structures, has also been performed within the framework of this thesis. The work is closed with an empirical study in which the route choice profiles of spectators during various football games and concert performances are analysed and compared with the proposed model. The runtime optimisation strategies and route choice algorithms have been successfully tested in the ESPRIT arena in Düsseldorf (Germany), where they have been integrated in an evacuation assistant.

Keywords: pedestrian dynamics, route choice, evacuation, high performance computing.

Zusammenfassung

Steigende Besucherzahlen bei Veranstaltungen und die wachsende Komplexität moderner Gebäude stellen für Planer, Betreiber und Rettungskräfte eine große Herausforderung dar. Beispiele sind Multifunktionsarenen, große Bahnhöfe und Flughäfen. In dem ersten Teil dieser Dissertation wird modernste parallele Hardware in Kombination mit optimierten Algorithmen benutzt um eine Fußgängerverkehrsprognose schneller als in Echtzeit zu erstellen. Zu diesem Zweck werden spezielle Nachbarschaftslisten und eine zweistufige hybride Parallelisierung eingesetzt. Der zweite Teil dieser Dissertation beschäftigt sich mit der Routenwahlthematik, welche bei der Durchführung realistischer Computersimulationen von Personenströmen eine tragende Rolle spielt. Das entwickelte Routenwahlmodell basiert auf Sichtbarkeit und Umgebungswahrnehmung von den simulierten Agenten und hat als Basis einen Navigationsgraphen. Die Erzeugung des Graphen, insbesondere in komplexen Strukturen ist ebenfalls Schwerpunkt dieser Dissertation. Die Arbeit wird mit einer Feldstudie abgeschlossen, in der das Bewegungsprofil von Zuschauern bei diversen Fußballspielen und Konzerten analysiert wird. Anschließend werden die Ergebnisse der Feldstudie mit dem Routenwahlmodell verglichen. Die Laufzeitoptimierung und das Routenwahlmodell wurden erfolgreich in der ESPRIT arena in Düsseldorf getestet, wo sie in einem Evakuierungsassistenten eingesetzt wurden.

Stichwörter: Fußgängerdynamik, Routenwahl, Evakuierung, Hochleistungsrechner.

Statement

I affirm that this dissertation is my original work and that borrowed concepts and ideas have been duly cited.

Erklärung

Hiermit erkläre ich, dass die vorliegende Arbeit von mir selbständig und nur unter Verwendung der angegebenen Quellen und Hilfsmittel erstellt wurde.

Jülich, 12 April 2012.

Acknowledgements

This doctoral dissertation would not have been possible without the help and the support of the people around me to only some of whom it is possible to give particular mention here.

First of fall I would like to thank my supervisor Prof. Seyfried for giving me the opportunity to perform such an interesting dissertation in a great team and within the framework of a great project. Special thanks to Prof. Fiedrich who kindly accepted to be my second supervisor for this thesis. Many thanks go to my working colleagues at the Forschungszentrum Jülich, specially Stefan Holl, Bernhard Steffen, Mohcine Chraibi, Maik Boltes and Andrea Portz for the very exiting discussions and critical reviews. Also, I really appreciated the quiet and peaceful working atmosphere in the Forschungszentrum Jülich facility. I also express my gratitude to the colleagues of the Bergische Universität Wuppertal and to Kai Baumann and Michael Krabbe from the ESPRIT arena in Düsseldorf.

I am very grateful to all of you who took some time, read my work, checked for mistakes and gave me very usefull remarks. Through your remarks, many things have been reformulated clearly and the quality of the work greatly improved. I am particularly thinking of Thibaut Tchinda, Yannick Tchinda and Bernhard Steffen.

Special thanks also to my parents Tidoh Angèle and Kemloh François and to my lovely niece Valmar for their termless support not only in this phase of my life. Special thanks also to two special friends Aigün Hirsch and Anna Atrás for their very motivating words in hard moments. To all of you, whose names I didn't mention here, to all of you who understood and accepted all my excuses for not having much time for you: thank you very much. Finally, to you (yes, I really mean you!) actually reading this dissertation, I hope it will give you some answers to your questions.

The researches performed in this dissertation have been done within the program "Research for Civil Security" in the field "Protecting and Saving Human Life" funded by the German Government, Federal Ministry of Education and Research (BMBF). The project has been supported under the grant no. 13N9952.

Contents

List of Figures

List of Tables

Chapter 1

Introduction

In the last decades, the study of pedestrian dynamics has gained more attention due to continuously growing urban population and cities. This growth is accompanied by an increase not only in size but also in frequencies of large-scale events. The increase sets new challenges to architects, urban planners and organizers of such events. The growing interest in large-scale events also requires increased security measures and new security concepts that are tailored to the large amount of people. In this context, simulations of pedestrian dynamics are already performed, e.g. for escape route design and/or optimising the traffic flow to allow an efficient use of the designed facility. These simulations are also used for the verification processes used in building regulations approval.

This dissertation has been done within the framework of the design, implementation and installation of a real-time evacuation assistant for large-scale events in a multi-purpose arena. It focusses on the different challenges associated to the development of the framework and presents methods that were developed to address them. This introductory chapter first gives a general introduction to the pedestrian dynamics field and its various applications. Thereafter, the evacuation assistant and its requirements are presented. The last section provides a detailed structure of the dissertation.

1.1 Pedestrian Dynamics

Pedestrian dynamics has been studied for decades. The first models and quantitative analysis can be traced back to Predtetschenski and Milinkskii in the 1970's [1]. The main motivation in the study of pedestrian dynamics is the understanding of the factors regulating the movements and more generally the behaviour of crowds. Researches performed in the pedestrian dynamics area can roughly be categorised into experiments, analysis, simulations, modelling and applications. An application area is safety and comfort, where nowadays simulations are

Period	Place	Occasion	Casualties
1896	Chodynka Field, Moscow (Russia)	Coronation, Tsar Nicholas II	1400
1903	Iroquois Theatre, Chicago (USA)	Performance	602
1982	Luschniki-Stadium, Moscow (Russia)	Football game	66
2001	Johannesburg (South Africa)	Football game	47
2004	Mihong-Park, Peking (China)	Lantern festival	37
2006	Jamarat Bridge (Saudi Arabia)	Hajj	363
...	...	...	...
2010	Duisburg (Germany)	love parade	21
2010	Phnom Penh (Cambodia)	Water festival	375
...	...	...	...

Table 1.1: Non-exhaustive chronological list of official casualties at major events over the past years. The main reported causes of death were overcrowding and stampedes.

performed for design purposes e.g. for escape route design [2–6]. Another area of interest is computer animations or virtual reality [7]. This comprises animated films and video games. Pedestrian dynamics also finds many applications in the field of robotics where similar algorithms are used, for instance for computing autonomous robots paths [8, 9]. However, the approaches used in these simulations are only the first steps to understand and model the manifold influences on human beings from the motion point of view. The study of pedestrian dynamics is important if we consider the fact that since 2006, half the world population lives in cities. If the current trend holds, by 2056 more than 75 % of the world population will live in cities [10, 11]. This is synonymous with densely populated cities, which brings us back to the security and comfort aspects mentioned earlier. The potential hazards related to dense crowds then become obvious if we consider the tragedies that happen in the past. Table 1.1 shows a non-exhaustive chronological list of disasters in the last century[1]. The link between those unfortunate tragedies is the absence of any external threats. The main causes were overcrowding combined with insufficient pedestrian facilities and not properly dimensioned escape routes, which lead to crushes and stampedes. All these factors contribute to the main idea behind the conception and the development of an evacuation assistant for mass events, which is presented in the next section.

1.2 Hermes: an evacuation assistant

The project Hermes [12, 13] has been funded by the German Federal Ministry of Education and Research. The aim is to develop an evacuation assistant for complex facilities to assist decision makers and security services in case of emergency. One target in the project is to forecast the evacuation of 50,000 pedestrians in a stadium for the next 15 minutes within 2 minutes of computation. The test venue for the system is the ESPRIT arena in Düsseldorf, North Rhine-Westphalia, Germany. Major challenges for the evacuation assistant include

[1] An extended list is available at `http://www.gkstill.com/ExpertWitness/CrowdDisasters.html`

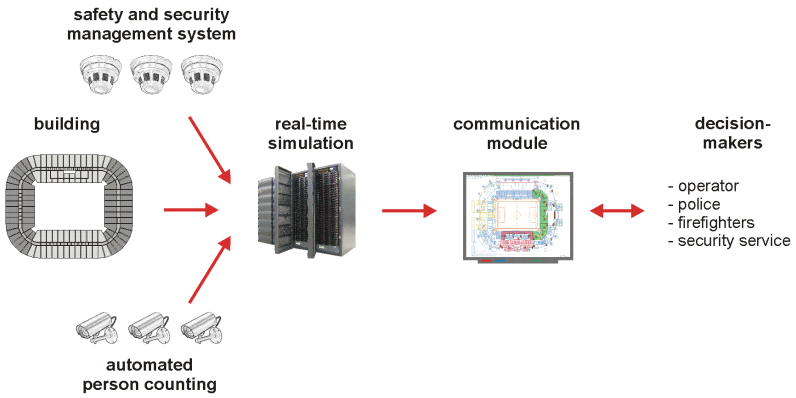

Figure 1.1: Layout of the evacuation assistant.

the proper development of microscopic models to accurately reproduce individual pedestrian motions, the proper development of a route choice model and the efficient implementation of these models with respect to the runtime. The layout of the assistant is presented in Figure 1.1. It features 3 main blocks: the first block matches all data input sources for a simulation. The second block consists of the simulation engine itself. The third block consists of the output devices. The assistant is steered from the communication module installed on one output device. The communication module collects all necessary information from the different input sources and merges them. It also launches a simulation if required and displays the results on a smart-board. The operational interface of the evacuation assistant displaying the results (analysis of pedestrians' trajectories) of a simulation is presented in Figure 1.3.

1.2.1 Experiments

The key features of models are their capability of reproducing the reality. For that purpose, empirical data for calibration and verification are needed. In the field of pedestrian dynamics, such data are scarce and they often show disparities [14]. Considering this aspect one of the goals followed by the Hermes project is to compile an outstandingly large database of experimental data. To achieve that goal, more than 300 different configurations of experiments were performed over three days involving more than 400 test persons. The venues for the experiments were the ESPRIT arena and the trade fair centre in Düsseldorf. In the fair centre two-dimensional experiments were performed including uni- and bidirectional flows in corridors, bottlenecks with different widths, merging of pedestrian streams at T-junctions. Three-dimensional experiments were performed in the stadium area. They included the merging of pedestrian streams at the gate of a tribune area and the velocity analysis of pedestrians on stairs. Three such experiments are presented in Figure 1.2. The moving direction is given by the arrows. The test persons are wearing a cap that facilitates the analysis of the footages. In Figure 1.2(a) three pedestrian streams merging at a gate are displayed. All pedes-

trians are walking on stairs. The streams from left and right (pedestrians in red and black shirts) are descending; the stream in the middle (pedestrians in grey shirts) is ascending the stairs. Figure 1.2(b) shows two pedestrian streams merging in a T-junction. This experiment was performed on level terrain. Pedestrians descending a circular stair are presented in Figure 1.2(c). The data obtained from the experiments in terms of video footages are publicly available[2]. In addition, the extraction of the information, in this case the trajectories, from experiments' video footages using pattern recognition techniques [15] has been performed. The tool PeTrack[3] was used for that purpose. The results are high accurate three-dimensional pedestrians' trajectories.

1.2.2 Population distribution

In a hazardous situation, it is often required to know the exact or approximated distribution of the persons in the location. This is essential for choosing the best evacuation strategy and optimally distributing the resources available between the responders. In the case of a closed door event, the total number of attendees is usually determined by the number of sold and scanned tickets or by using turnstiles at the gates. On a free (open air) terrain, one or more cameras can be used to have an overview of the distribution. For indoor events in complex structures, an arena for instance, where people can be distributed in several different locations this procedure is rather cumbersome. Despite the different camera views, it is difficult to approximate the number of persons. It also applies for outdoor events. This is particularly true for high density. This is a reason why in critical situations with high densities and casualties, it has always been a problem to estimate the real number of persons in the location. An example is given by the Love Parade in Duisburg 2010, Germany (see Table 1.1).

For the project Hermes, a nearly accurate distribution of spectators in the arena is required. This is part of the input data for the simulation. A method to obtain the distribution is to scan some devices usually carried by people such as Bluetooth devices or cell phones. The main issue is usually the covering range of the scanners and the percentage of people carrying such devices. Another option is to integrate RFID (Radio-frequency identification) chips in tickets. This solution however requires that the spectators would have to keep their cards during the complete event, which is very unlikely. In addition, such chips usually show problems in high densities. To obtain a nearly accurate distribution of the spectators in the different sections of the arena, an automatic persons counting system based on cameras has been developed and installed[4]. The counting system also delivers route choice data that can be used to make general assumptions over the exits usage by the spectators in the arena during an event. The collected data are also publicly available. It is important to mention here that these data do not contain any person related information, just the number of persons passing through a

[2]The data can be downloaded from `http://www.fzj.de/jsc/ped`
[3]PeTrack can be downloaded from `http://www.fzj.de/jsc/petrack`
[4]`http://www.vitracom.de`

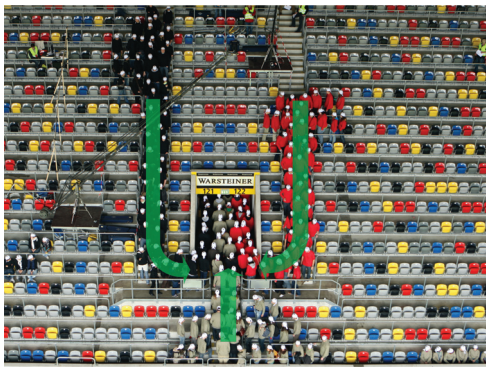

(a) Three pedestrian streams merging at a gate

(b) Two pedestrian streams merging at a T-junction

(c) 180 grad bends on a circular stair

Figure 1.2: Three samples of experiments performed in the preparation phase of the project Hermes. The arrows indicate the moving direction.

particular exit at a specific time.

1.2.3 Information acquisition and fusion

The input information for the evacuation assistant is divided in three streams (see Figure 1.1). The first stream contains information related to the geometry. There are two different configurations for the geometry for different events: seats only and mostly seats with some standing areas. Different formats of the geometry are needed to fulfil the requirements for the different pedestrian models used for the simulation. The second stream of information comes from the safety and security management system. This is dynamic and changes with each run of the system. The information about the state of the escape routes, which is important in a hazardous situation, is made available. This information includes the states of the different doors and areas, for instance, which doors are still usable (not blocked for instance) and which areas of the building are smoke-filled. In order to avoid any possible interference with the installed / operational system, which could be dangerous in a test phase, a clone of the already installed system has been made. The third stream of information comes from the automatic persons counting system. The output is the number of pedestrians in each section of the arena. Other input for the simulation includes the type of the event, concert or football game for instance and the type of clearing that should be simulated. We have routine clearing and emergency clearing. Depending on the clearing type, different route choice strategies are applied. All this information is merged and transmitted to the simulation core using web services. This solution is flexible and rapidly deployable.

Another non-negligible point raised in this project is the efficient display of information during a crisis. This is solved by condensing the information to a minimum, for instance no animations are displayed. The simulations results however can be displayed in time slices. Five-minute time slices have proven to work well in this case. The simulation results are shown using different Level of Services (LOS) [16]. LOS is a common measure used in traffic to determine the effectiveness of elements of transportation infrastructure, for instance pathways. The LOS of the areas is displayed in three colours: red, yellow and green. Red stands for high density and green for low density. Figure 1.3 depicts a live representation of simulation results on a smart board. The LOS of the different sections is displayed.

1.2.4 Real-time computation

The forecast of the congestion areas should be by a factor of 7 faster than real-time. This gives enough time to the security services and other responders to react. They can redirect the congested pedestrian flows to different exits or areas. Also, they can split or direct the pedestrian streams at the beginning of the evacuation process, such that the forecast congestions do not occur. In order to achieve the faster than real-time computation, a computer cluster has been set up and different optimisation techniques have been used. The high dynamics of the system with local and global interactions makes it difficult to use standard domain decomposition techniques. After the real-time simulation, the results are forwarded to the communication

Figure 1.3: Evacuation assistant displaying simulation results.

module which analyses and properly displays the results. Those results are finally visualised on a smart board (see Figure 1.3) where they are discussed by the decisions makers.

1.2.5 Route choice

Route choice modelling in pedestrian dynamics is essential for choosing the appropriate route choice strategy and reproducing the correct behaviour in simulations. The problem statement is the following: given a set of possible routes, which criteria influence pedestrians' choice for a particular route? This is essential for reproducing route choice in computer models and is difficult due to the many underlying subjective influences on this choice. The manner in which pedestrians choose their way in a simulation has a direct influence not only on the predicted evacuation times but also on the average time they spend in a jam. Also, the route choice in general is often bounded to a certain history of the pedestrian. When entering a building, much information is subjectively recorded, for example the chosen way or a closed door along the path is remembered. This history is usually not available in simulation environments. At the current stages, many models and simulation tools concentrate their validation criteria on locally reproducing the correct flows at exits and the fundamental diagram (relation between density and velocity). However, when it comes to estimate evacuation times or to forecast congestion areas during an evacuation process, route choice and specially the history of the simulated agents may play an important role. In the implementation of the evacuation assistant, some restrictions must be considered. As we are simulating an evacuation scenario, we assume that all pedestrians have the same motivation, to leave the facility. The practice tests of the system will hopefully only see routine clearings, not emergency evacuations. In this case, the route choice is not necessarily the shortest path out of the building, instead a lengthy but

comfortable way along the promenade towards the parking lots and the train station.

1.3 Aim and Structure of the Dissertation

1.3.1 Aim of the work

The hereby presented dissertation follows three goals. The first goal is the development and use of existing runtime optimisation techniques and their application in pedestrian dynamics. Due to the very high dynamics of the system with both local and global interactions, a great challenge consists of finding the optimal partitioning mechanism that makes use of parallelisation. The local interactions are related to the fact that pedestrians use for instance locally available information for collision avoidance mechanisms. The global interactions are obvious and are mainly used for route choice. Another effect is that pedestrian flows are usually directed (in an evacuation scenario for example), the result is an inhomogeneous distribution and a gathering at exits which makes it difficult to use standard partitioning schemes. The second goal is the development of route choice strategies for an evacuation scenario in a complex facility. The first task is the construction of a navigation graph for the pedestrians in the facility and the connecting of this graph to a force based model. The second task is the modelling and implementation of route choice procedures in the constructed graph. The third goal is an empirical study of pedestrians' route choice in a stadium. The data are collected during various football games and concert performances using the automated person counting system introduced in the previous section.

1.3.2 Structure of the work

The present chapter is the general introduction to this dissertation. Chapter 2 gives an insight into different pedestrian models with respect to the runtime and their requirements concerning the geometry resolution. The advantages and drawbacks of the models are presented. The focus is set on the generalized centrifugal force model [17] which is a force based model and has been developed for the Hermes project. The last section presents an open source framework for the development of pedestrian models. An emphasis is set on the visualisation environment and the importance of visualisation. Chapter 3 focusses on runtime optimisation techniques for short range force based models. The first step is the optimisation of serial codes using special neighbourhood search techniques that benefit from short range characteristics of the forces present in the system. The second step consists of using a hybrid parallelisation. The Message Passing Interface and the Open Multi-Processing application programming interfaces are used. The speedup obtained is analysed. The developed route choice strategies are presented in Chapter 4. The strategies operate on a navigation graph and use criteria such as the patience time of individual pedestrians and their visibility range to direct them in the sim-

ulated environment. Chapter 5 deals with the generation of visibility graphs for navigation. Standard approaches are presented followed by the solution adopted for a complex structure like the tribune of a stadium. This is followed in Chapter 6 by an empirical study of pedestrians' route choice in the arena. The study is done for two types of events: football games and concerts. The modelling approaches presented in Chapter 4 are compared with the obtained data. Outlooks and future works are elaborated in Chapter 7.

Chapter 2

Pedestrian Models Framework

There are many classes of pedestrian models used for describing pedestrian dynamics, each with its own advantages and drawbacks. In this chapter, the general pedestrian model framework is described. The different classes of models are presented and discussed with respect to the runtime efficiency and the resolution of the simulated space. The focus is thereby set on the generalized centrifugal model, which is a force based model in a continuous space. The last section of the chapter introduces an open source framework, which has been launched for promoting models developments.

2.1 Motion Description

The general framework used for describing pedestrian traffic can be divided in a three-tier structure. According to Hoogendoorn et al. [18] one distinguishes between the strategic, the tactical and the operational levels. This subdivision is illustrated in Figure 2.1. The start and the end trip for each pedestrian are usually known in advance. At the strategic level, after considering their final destinations, pedestrians choose their self-estimated best route, among a collection of different alternatives. This can be done based on experience. Examples could be the global shortest path or the familiar path to a given destination. Short- terms decisions are taken at the tactical level, avoiding jams and obstacles or switching to a faster route for instance. Basic rules for motion are defined at the operational level. These rules include accelerating, decelerating and stopping. There are undoubtedly overlaps between the different tiers. In Chapter 4 and Chapter 6 modelling approaches and analysis for the strategic and tactical levels will be presented. The next section focusses on models at the operational level.

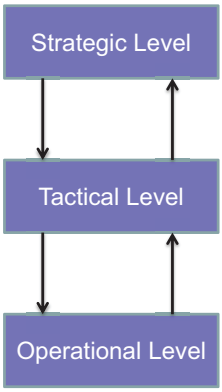

Figure 2.1: Hierarchy of motion structure [18].

2.2 Models Classes

There are essentially two classes of models for describing pedestrians' properties/characteristics depending on their degrees of freedom: microscopic and macroscopic models [14]. In microscopic models, each pedestrian is represented separately with individual properties such as walking velocity or route choice behaviour. Also, the pedestrians interact with each other. There are mainly four different classes of microscopic models for pedestrian dynamics: cellular automata (CA) models [19–22], rule based models [2, 4], force based models [23, 24] and hybrid models [25–27]. In CA models, the geometry is decomposed in cells (usually 40 cm $\times$ 40 cm) and the pedestrians move from cells to cells according to some predefined transitions probabilities. Usually a cell can only be occupied by one pedestrian at a time. With this representation, a maximal density of ≈ 6 persons/ m^2 can be simulated. The common metrics used are the Moore and the Manhattan norms. CA models have the advantage of being computationally efficient, but the resolution of the simulated geometry is limited by the size of the cells. Other types of decompositions include smaller cells size [28] and the use of hexagonal decompositions [29]. The discretization with smaller cell size also means an increase of the complexity.

Force based models usually operate on a continuous geometry. They need more computational resources but have the advantages of working on a geometry that is the exact representation of the real geometry. For more about the advantages and disadvantages of the individual models we refer to [14, 30]. Figure 2.2 shows a discretization of the ground plan of a room connected to a corridor for a CA model. Only the white cells can be occupied by pedestrians. The black cells are walls and other not traversable objects. To illustrate what implications the resolution of the geometry can have, let's consider a 100 cm wide exit. This exit cannot be represented by a discretization using the aforementioned cell size of 40 cm. In most of the

cases, the geometry is then narrowed down to fit in the smallest representable space using the cells. Up to now the effects of the 'lost' 20 cm (or the 'exceeding' 20 cm in the case the exit was broaden) are not investigated. This may indeed affect the flows at exits and have huge impacts on evacuation times in simulations. In other to cope with that eventual problem, CA models may reduce their cell size as proposed in [28], thereby increasing the computation complexity. No space discretization is required for force based models in continuous space implying no possible artefacts caused by the procedure.

Macroscopic models do not distinguish between individuals. The description is based on aggregate quantities, e.g. appropriate densities. Typical models belonging to this class are fluid-dynamic approaches [31,32]. Hand calculation methods [1,16,33,34] which are often used in the field of (fire-safety) engineering belong to this class as well. For other various pedestrians modelling techniques and especially behavioural agent based models we refer to [7] and the references therein.

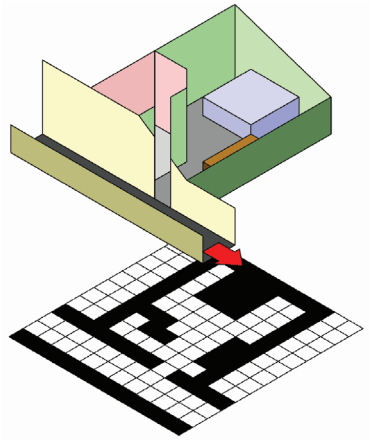

Figure 2.2: Discretization of the ground plan of a room and a corridor [3]. Only white cells can be occupied by pedestrians.

2.3 Generalized Centrifugal Force Model

The generalized centrifugal force model (GCFM) [35] describes pedestrians' motion at the operational level. In the GCFM, pedestrians are described with ellipses having velocity dependent semi-axes. The motion is ruled by the so-called social forces [23, 36]. The forces can be attractive, for instance forces between pedestrians and their destinations, a door for instance. They can be repulsive, for instance interaction forces among pedestrians, or between a pedestrian and a wall. At each simulation step the forces between the pedestrians and the obstacles (e.g. walls) are computed. The GCFM is an extension of the Centrifugal Force Model [24] (CFM) in which pedestrians are defined with a hard core radius. The CFM also

expresses collision avoidance mechanism in its definition of the repulsive forces. The GCFM also gives pedestrians more flexibility. Given a pedestrian i with coordinates $\overrightarrow{R_i}$, the equation of motion is:

$$m_i \ddot{\overrightarrow{R_i}} = \overrightarrow{F_i} = \overrightarrow{F_i^{\text{drv}}} + \sum_{j \in \mathcal{N}_i} \overrightarrow{F_{ij}^{\text{rep}}} + \sum_{w \in \mathcal{W}_i} \overrightarrow{F_{iw}^{\text{rep}}}, \tag{2.1}$$

where $\overrightarrow{F_{ij}^{\text{rep}}}$ denotes the repulsive force from pedestrian j acting on pedestrian i, $\overrightarrow{F_{iw}^{\text{rep}}}$ is the repulsive force emerging from the obstacle w and $\overrightarrow{F_i^{\text{drv}}}$ is a driving force. m_i is the mass of pedestrian i. $\mathcal{N}_i$ is the set of all pedestrians that influences pedestrian i and $\mathcal{W}_i$ the set of walls or borders that act on pedestrian i. The obstacles to be considered are within a certain cutoff radius $r_c = 2$ m. One should note here that it is not a hart cutoff as the repulsive forces are Hermite interpolated, so that they smoothly reach the values 0 at the distance r_c (see Figure 2.3(b)).

The driving force is defined by:

$$\overrightarrow{F_i^{\text{drv}}} = m_i \frac{\overrightarrow{v_i^0} - \overrightarrow{v_i}}{\tau}, \tag{2.2}$$

with $\overrightarrow{v_i^0}$ the desired velocity of pedestrian i, $\overrightarrow{v_i}$ the current velocity and τ a constant reflecting the reaction time. The repulsive force is given by

$$\overrightarrow{F_{ij}^{\text{rep}}} = -m_i k_{ij} \frac{(\eta {v_i}^0 + v_{ij})^2}{\text{dist}_{ij}} \overrightarrow{e_{ij}}, \tag{2.3}$$

where

$$\text{dist}_{ij} = \| \overrightarrow{R_{ij}} \| - r_i(v_i) - r_j(v_j), \tag{2.4}$$

$$\vec{e}_{ij} = \frac{\vec{R}_{ij}}{\|\vec{R}_{ij}\|}, \vec{R}_{ij} = \vec{R}_i - \vec{R}_j, \tag{2.5}$$

$$v_{ij} = \frac{1}{2}[(\vec{v}_i - \vec{v}_j) \cdot \vec{e}_{ij} + |(\vec{v}_i - \vec{v}_j) \cdot \vec{e}_{ij}|], \tag{2.6}$$

and

$$k_{ij} = \frac{1}{2}\frac{\vec{v}_i \cdot \vec{e}_{ij} + |\vec{v}_i \cdot \vec{e}_{ij}|}{\|\vec{v}_i\|} \tag{2.7}$$

v_{ij} is the projection of the relative velocity of pedestrian i and j onto the direction of the vector connecting their centres as presented in Figure 2.3(a). This expression from the relative velocity minimises the effects of pedestrians moving in the front at a higher velocity. $\|\vec{R}_{ij}\|$ is the distance between the centres of the pedestrians i and j whereas dist_{ij} is the effective distance between pedestrian i and j. The effective distance is obtained by subtracting the polar radii r_i and r_j from the distance between the centres. The coefficient k_{ij} reduces the action-field of the repulsive force to 180° in the direction of movement. A motivation for the modelling of pedestrians with velocity-dependent semi-axes is that on one hand faster pedestrians require more space in their walking directory than slower pedestrians. On the other hand, slower pedestrians sway laterally stronger than faster pedestrians. The relation between the semi-axes and the velocity are given by Equation 2.8. b_{min} is the minimum shoulder width, b_{max} denotes the maximum swaying range for a pedestrian. The minimal space need in the moving direction is expressed by a_{min}. The calibration of the parameters for the GCFM is thoroughly explained in [37, 38].

$$\begin{aligned} a &= a_{\min} + \tau_a v_i \\ b &= b_{\max} - (b_{\max} - b_{\min})\frac{v_i}{v_i^0} \end{aligned} \tag{2.8}$$

As presented in Equation 2.3 the repulsive force is inverse proportional to the distance between pedestrians and therefore should take its maximal value when the pedestrians are close enough and its minimal value where the pedestrians are out of the cutoff radius. This is achieved by means of interpolation. The magnitude of the repulsive force is illustrated in Figure 2.3(b). One of the main ideas behind the model is the consideration of volume exclusion between the ellipses. This is synonymous to minimising overlaps between the ellipses. To model the idea, a distance of closest approach (DCA) was introduced in [17] and the repulsive forces are interpolated to be high in the neighbourhood of that distance. The DCA is the minimal distance dist_{ij} between two pedestrians before they start to overlap. This can be expressed as the optimisation of the volume exclusion principle. For circles or parallel aligned ellipses, the value of the DCA is then ~ 0. The DCA $\tilde{l}$ between two ellipses is sketched in Figure 2.4, further details are discussed in [17]. The same constraints apply for repulsive forces between pedestrians and walls.

The process of determining the DCA is the most computing intensive part of the simulation involving several trigonometric operations combined with square root extractions. A simulation with a small amount of pedestrians can be obtained in a reasonable computing time. The simulation of large amount of pedestrians can be cumbersome especially if there are some time constraints, as the requirement for a real time computation for instance. Methods to speed up

the computation will be discussed in the next chapter.

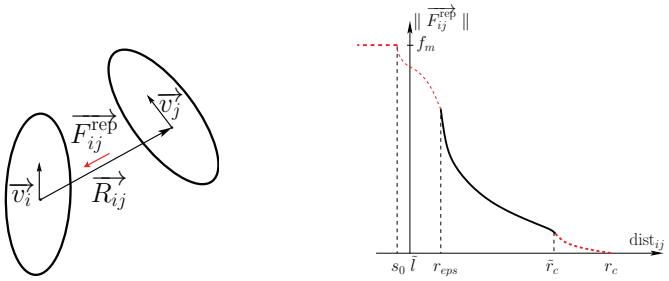

(a) Repulsive force and distance between two ellipses

(b) Interpolation of the repulsive force

Figure 2.3: Repulsive force between two ellipses combined with interpolation in the GCFM. The force smoothly reaches 0 at the cutoff radius [17].

2.4 Open Pedestrian Simulation Framework

The motivation for starting the Open Pedestrian Simulation (OpenPedSim) is the following: in many universities and thesis projects, a lot of time is spent on setting up a proper environment for the development of the new approaches. Although the main objective is for instance the development of a new pedestrian model, the work on utilities like an editor for the geometry or for the input of data, a tool for visualising the results is an enormous entry barrier. Another side issue is the definition of file formats. It is only after those steps have been successfully taken that the real work starts. Usually this work has to be done as fast as possible. Most of the time, the result is a code which is neither reusable, nor maintainable, nor scalable. In this context, the OpenPedSim (Open Pedestrian Simulation), an open source framework for performing pedestrian simulations, is hereby introduced. The primary goal of OpenPedSim is to provide students and researchers with a toolbox that will allow them to focus on their main task, i.e. the development, calibration, and validation of new models or model features. Also, some standards and benchmark scenarios for evaluation of pedestrian simulations are under development. This task is closely linked to RiMEA [39] and the IMO validation cases [40].

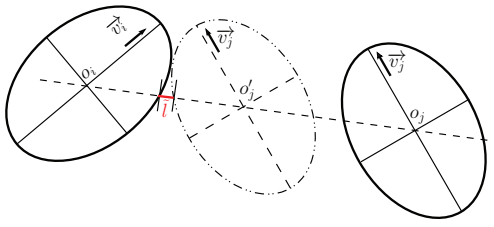

Figure 2.4: Distance of closest approach $\tilde{l}$ between two ellipses [17].

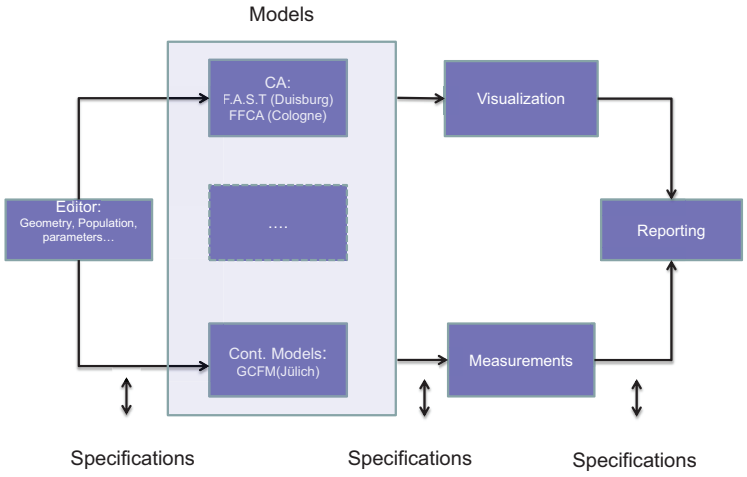

Figure 2.5: Structure of the Open Pedestrian Simulation framework. Some well-known models from the literature are implemented: two space discrete and one space continuous models.

2.4.1 Description

The OpenPedSim framework is described in Figure 2.5. It consists of loosely coupled modules. The modules can be used individually, but then only part of the workflow described above is covered. The editor allows the creation of new scenarios for a simulation. A scenario comprises a geometry, information about the pedestrians and other constraints. Constraints can be the state of rooms or doors, blocked doors or inaccessible rooms for instance. These are the input to the models. The results of the models are then visualised using the module designed for that purpose. The results are the trajectories of the individual pedestrians in the simulation. Other models can output other types of results as well, density for instance. In addition, a measurement tool analyses the results and generates a report. The measurement tool uses high quality methods based on the Voronoi cell decomposition [41,42]. A very important point here is the specification of the different interfaces. A clear and open specification facilitates the integration of new components, in this case of new models. Some specifications are under development.

2.4.2 Modules

The OpenPedSim framework actually consists of the following modules:

1. OPSed: it provides geometries for continuous models as well as for cellular automata.

2. OPSgcfm: it is an implementation of the Generalized Centrifugal Force Model [17].

3. OPSffca: it is a cellular automaton model discrete in time, space and state variables. It is based on the *Floor Field Cellular Automaton* (FFCA) [21, 43, 44].

4. OPSfast: it is an implementation of the F.A.S.T. cellular automaton model described in [45, 46].

5. OPStraVisTo: it is a visualisation tool.

6. OPSreport: it is a reporting tool integrated in the overall workflow.

2.5 Visualisation of Trajectories

The main advantage of visualisation methods is their ability to communicate large amounts of information in a short time period, recall the saying "one picture is worth a thousand words". There is no better, quick and simple way to assess a model than a snapshot of the results. However, depending on the information one is interested in, a single snapshot might be insufficient. In the field of pedestrian dynamics, just like in many other fields, an animation of the whole simulation is often required to properly assess the dynamics of the system. As a result, visualisation is often used as the first primary validation technique and it eases the calibration of the models.

For visualisation purposes, we developed the Trajectories Visualisation Tool, which is built on top of the Visualisation Toolkit (VTK) libraries [47]. VTK is an open source and platform independent library for computer graphic and provides many algorithms for visualisation and data analysis as well as an interface to the C++, Java, Python and Tcl languages. OPStraVisTo reads a file containing the simulation results (coordinates, velocities, orientations, ...) together with geometry information and allows the user to interact with this information in form of an animation, for instance focusing on an area of interest or masking views. OPStraVisTo can also be used in an online mode, where simulation results are directly streamed to the application. The user interface is designed using the QT libraries [48].

Several problems of force-based models that are discussed in [17] can be detected by a good visualisation of the trajectories produced by the simulation. Problems such as the wrong sorting of pedestrians at a door or the dynamic torque shown by the ellipses become visible. Individual pedestrians can easily be tracked and other issues such as the unrealistic blocking between individual pedestrians in a jam situation can be visually analysed. Another aspect is a visual control of the qualitative aspect of pedestrian dynamics produced by the model, e.g. lanes formation or clogging at exits. Some examples of the problems described in [17] are shown in Figure 2.6. Extreme values of η, which denote the strength of the repulsive forces, lead to strong overlaps between pedestrians and oscillations. The colour of the pedestrians

is correlated to their current velocity. The red colour denotes a low velocity and represents congestions areas. Green corresponds to the maximum desired velocity of the pedestrians.

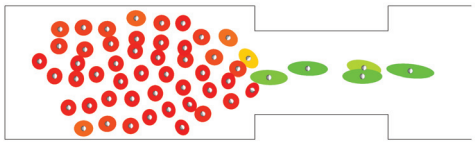

(a) Pedestrians blocking each other at the bottleneck. The bottleneck width is not effectively used.

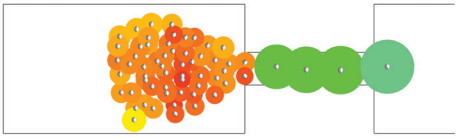

(b) Strong overlaps between pedestrians ($\eta = 0.1$) due to weak repulsive forces.

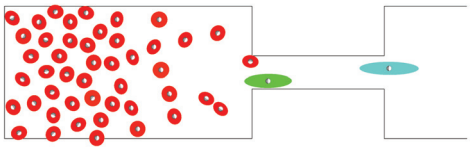

(c) Oscillations between pedestrians ($\eta = 0.7$), strong repulsive forces cause some pedestrians to perform backwards movement (Note the orientation of the pedestrians in the rear of the bottleneck). In addition some pedestrians have overcome the wall forces and passed through the walls due to these extreme forces.

Figure 2.6: Blocking, overlaps and oscillations between pedestrians. The simulation is performed with 60 pedestrians. The colour and shapes of the ellipses are correlated to their instant velocity. Slow ellipses appear red [17].

Chapter 3

Runtime Optimisation

Force based models in continuous spaces are particularly computation intensive in comparison to cellular automata or rules based models. For instance a naive implementation of the generalized centrifugal force model (GCFM) requires for stability reasons a time step $dt = 0.001$ s whereas $dt = 0.3$ s are usually enough for cellular automata [43]. In the GCFM, each simulation step includes arithmetic operations like computing the forces between the pedestrians, the forces to the walls and other obstacles, the new velocities and positions. Each of which comprises several trigonometric and square root functions. This is due to the elliptical shape of the pedestrians. Detailed information about the operations and performance are found in [17, 49] as well as in Chapter 2. In this chapter, optimisation techniques are described to speedup simulations with force based models. Results obtained in the ESPRIT arena are presented.

3.1 Neighbourhood List Methods

A naive implementation of the GCFM has the complexity of $O(N^2)$, N being the number of simulated pedestrians. The complexity is attributed to the fact that at each simulation step, the neighbourhood of each pedestrian has to be determined. This is done by computing the distances between all pedestrians. The complexity can be reduced to $O(N)$ using special neighbourhood lists such as the Verlet lists or the linked cells commonly used in molecular dynamics [50, 51].

The Verlet lists principle is explained in Figure 3.1. For each pedestrian the neighbours in the region with radius $R_c + R_s$ are saved in a list. R_c gives the cutoff radius of the force while R_s is the skin-radius determining the size of the reservoir. Only interactions with pedestrians in the list are considered. The list must be updated in time intervals given by R_s and the maximal speed of the pedestrians. Some runtime results obtained with the Verlet lists and applied to the GCFM are presented in [13, 52].

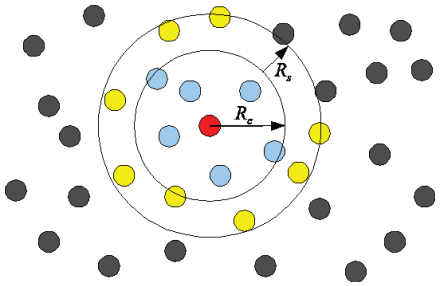

Figure 3.1: Illustration of the Verlet list method. The cutoff radius R_c and the reservoir size R_s are displayed [52].

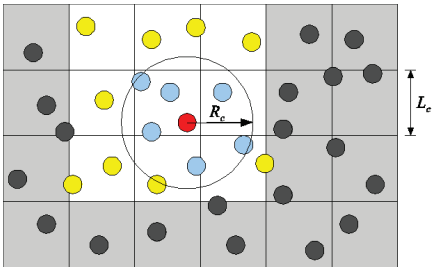

Figure 3.2: Illustration of the linked cells [52]. The cutoff radius R_c is displayed together with the 9 adjacent cells of the red marked pedestrian (located at the centre of the circle with radius R_c).

The principle of the linked cells is represented in Figure 3.2. Similar to the Verlet lists, it is based on a cutoff radius. With a given range R_c for the interaction forces, the simulated space is decomposed in cells of size $R_c \times R_c$. Only the interactions with pedestrians in adjacent cells have to be considered. At each simulation step and for each pedestrian, at most 9 times the maximal number of pedestrians in a cell are involved in the forces computations. It can be obtained by the maximal density in the system. The complexity is thus reduced to $O(N)$.

The complexity applies to the neighbourhood search (distances computation) and the forces computation. The performance comparison of the two list types and some of the results achieved are presented in [52, 53]. The linked cells provided better results than the Verlet lists in terms of memory requirements. Both lists types perform equally in terms of speedup. The speedup is measured with respect to the brute force method, which can be implemented in several manners. A naive method will be to compute the forces between all pedestrians. The forces between the pedestrians outside the cutoff radius will vanish automatically due to the extrapolation presented in Figure 2.3. Another implementation is, for optimisation purposes, to compute only the square of the distances between the pedestrians, thereby avoiding expensive square root extractions.

3.2 Parallelisation

3.2.1 Domain decomposition techniques

The next step in this optimisation process is the use of parallelisation on a multicore system. The most suitable parallelisation strategy for an application is usually coupled to the underlying hardware architecture. Some techniques on GPUs are presented in [54], and results obtained on the Cell-broadband Engine in [55]. More general techniques for particles in molecular dynamics are found in [56] and especially for pedestrian dynamics in [57, 58]. Independently of the underlying hardware architecture, there are several parallelisation techniques with different complexities in the computation, the memory required and the communication respectively the data exchange between the processors.

One technique is the replicated data approach [59]. Each processor keeps a copy of all data in its memory, but works only on the portion it is responsible of. This method has a large communication complexity. At each step, all processors have to actualize their data. For P processors and N pedestrians this algorithm achieves a parallel complexity of the order $O(N/P)$ (N thanks to the linked cells) for the CPU time, but its communication and memory complexities are of the order $O(N)$. The replicated data approach does not scale with P and the total runtime is dominated by the communication.

Another approach is parallelisation by data partitioning. Here, each processor only stores the data of the pedestrians required during the computation. These are the N/P pedestrians that are assigned to the processors in the parallel computation, and the other pedestrians that interact with those pedestrians, i.e. the pedestrians in the neighbourhood (see Equation 2.1). The data partitioning method scales as $O(N/P)$ for computation and communication as long as P is so small that latency is negligible.

A similar approach to the data partitioning is achieved by static domain decomposition [60, 61]. The main goal here is to limit the communication between the processors. For that purpose, the simulation domain is decomposed into subdomains and each processor is assigned a subdomain. The data are partitioned and distributed to processors in such a way that as little communication as possible is needed. In each communication step, only the pedestrians from neighbouring subdomains have to be communicated. Using the linked cells, the number of neighbouring pedestrians can be further reduced. Only the pedestrians within the interaction range (cutoff radius) are exchanged between the processors. The areas shared by the processors are called ghost areas. Figure 3.3 shows an example of ghost areas between three processors in a static domain decomposition. The size of the ghost areas is proportional to the width of the boundaries between the subdomains and is expressed in terms of cells. For example, the size of the ghost area shared by process P1 and process P2 in Figure 3.3 is 6 cells. The ghost area shared by process P2 and process P3 is 4 cells. With this procedure, the number of pedestrians for which data have to be received or sent decreases to $O(\sqrt{N/P})$. The complexity

of the entire computation is of the order $O(N/P)$. One should note that this applies only when the pedestrians are uniformly distributed. In the case where the pedestrians are not uniformly distributed, dynamic decompositions [62–64] might be required to obtain a balanced load by ensuring an almost uniform distribution of the N pedestrians on the P processors.

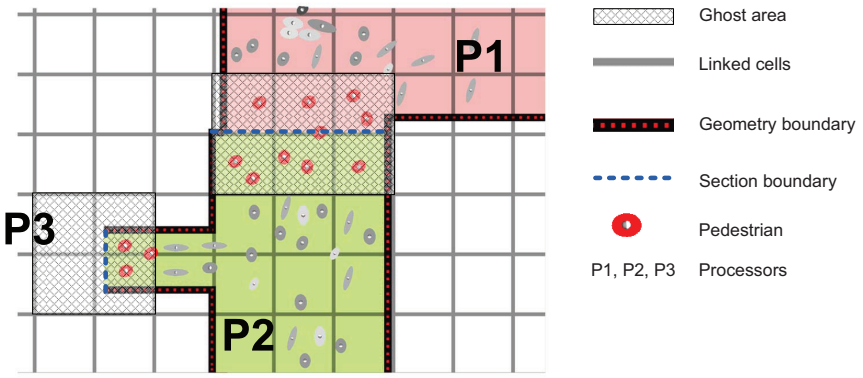

Figure 3.3: Ghost areas shared by three processors: the red pedestrians are present on more than one processor. Six ghost cells are shared by P1 and P2, four ghost cells are shared by P2 and P3. The different processor areas are represented by the colours green and purple. The grid is formed by the linked cells.

3.2.2 Hybrid parallelisation

The Message Passing Interface (MPI) [65] and Open Multi-Processing (OpenMP) [66] application programming interfaces can be combined in a hybrid architecture. MPI is based on distributed memory whereas OpenMP is based on shared memory. It means that data does not have to be explicitly exchanged between the processors as they all have access to the same memory. The structure of the hybrid parallelisation is shown in Figure 3.4 and is usually a good choice in multi-threaded environments. The step from a sequential program to parallel program using OpenMP is done by inserting macros in the sequential program. This has the advantage of leaving the sequential program almost untouched. Also, such macros are ignored if a suitable parallel environment is not found at compile time, making the program more portable. A restructuring of the sequential code is usually necessary for using MPI.

3.2.3 Load balancing

Load balancing is important to parallel programs for performance reasons. All processors should have approximately the same amount of work to do. This is not always possible in the case of a static partitioned simulation area. One solution is to use a dynamic partition-

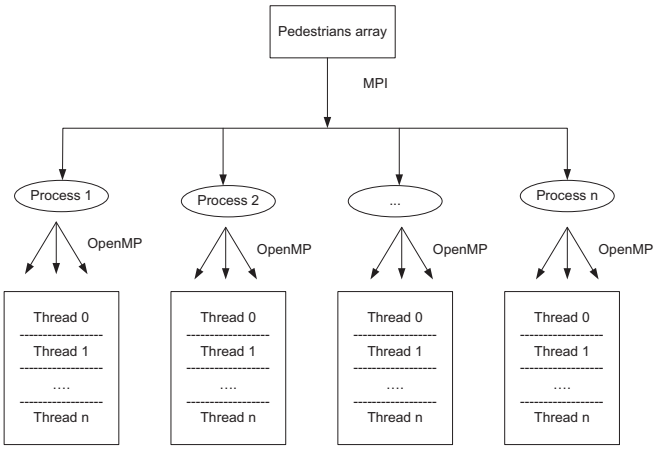

Figure 3.4: Hybrid parallelisation structure using MPI and OpenMP.

ing as presented earlier. This is done at the cost of a higher communication between the processors. The common practice of achieving load balancing is to distribute the number of computed particles or entities evenly to the different processors. This procedure assumes that the computational load pro entity is the same. This assumption unfortunately does not apply in the pedestrian dynamics field. Firstly, there are more interaction forces to be computed with increasing density. It means that a smaller room with fewer pedestrians may need longer to computer than a larger room with more pedestrians. Secondly, the geometrical boundaries and restrictions also play a role. Consequently, a simulation area with many obstacles (walls, furniture) will also influence the computational load per entity. Thirdly, there is a fundamental difference with common particles simulation, in that sense that each pedestrian is unique and therefore subjected to different influences at a time. The simplest way to illustrate this is to consider the route choice. Different route choice procedures, for instance the global shortest path or the quickest path (see Chapter 4), require different amount of computation depending not only on the geometry and the density in the location but also on the internal state of the pedestrians. An example is that the route choice of a pedestrian is influenced by the time he/she is caught in a jam. The jam time is not the same for all pedestrians. All these factors make it impossible to achieve a balanced load on the different processors by simply assigning them the same amount of pedestrians to compute on each simulation step.

3.3 Performance Analysis

Two common values to measure the performance of a parallel application are the speedup and the efficiency. The speedup is defined by

$$S(P) = T/T(P) \tag{3.1}$$

where T is the time needed by the serial application and $T(P)$ the time needed by the parallel (optimised) application using P processors. An ideal speedup would be reached if $S(P) = P$.

The efficiency is defined as

$$E(P) = S(P)/P \tag{3.2}$$

and it describes how good the processor are used to solve the problem in comparison to the resources lost in communication and synchronisation. The ideal value for the efficiency is 1. Although the speedup mostly applied to parallel programs, it will also be used to measure the performance of the linked cells algorithm presented earlier.

The performance analysis setup scenario is given in Figure 3.5. The geometry is a $50 \times 50\ m^2$ square with a 5 m exit in the middle of a side. 10.000 pedestrians are initially distributed in the area leading to a density of 4 persons / m^2. The density ρ is calculated using Equation 3.3 where N is the number of pedestrians and A_{room} the area of the room. The speedup is determined by measuring the simulation runtime in relation to an increasing number of pedestrians. The results for the speedup of the serial code are presented in Figure 3.6. It is almost linear and reaches the value of 72 by 7000 pedestrians.

$$\rho = \frac{N}{A_{\text{room}}} \tag{3.3}$$

By assuming that the runtime mainly consists of the calculations of the interaction forces the expected speedup can be estimated in advance. Therefore, by combining Equation 3.1 and Equation 3.3 it follows

$$S = \frac{t_{BF}}{t_{NL}} \approx \frac{N(N-1)}{N(N^*-1)} = \frac{N-1}{\rho\pi R_c^2 - 1} = \frac{N-1}{\frac{N}{A_{\text{room}}}\pi R_c^2 - 1} \xrightarrow{N\to\infty} k\frac{A_{\text{Room}}}{\pi R_c^2} \tag{3.4}$$

where t_{BF} is the runtime using the optimised brute force method and t_{NL} the runtime with the linked cells algorithm.

These assumptions seem to speak against the linear speedup presented in Figure 3.6. Two facts must be considered: firstly, by increasing the number of pedestrians up to the maximal

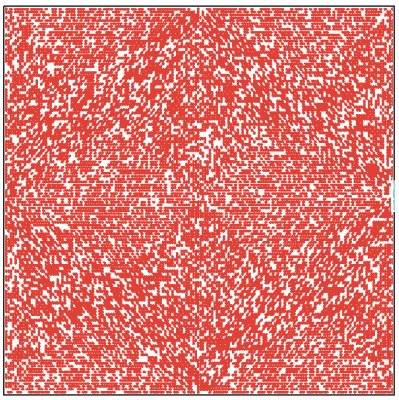

Figure 3.5: Initial distribution of 10000 pedestrians in a 50 m x 50 m room. The density is 4 persons / m^2.

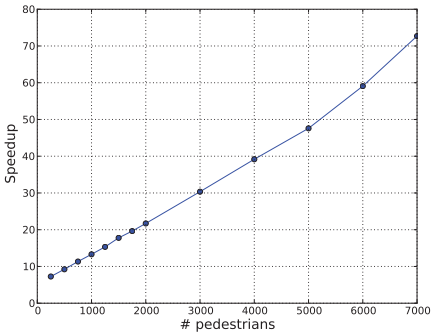

Figure 3.6: Speedup of the linked cells over the brute force method.

density possible, the scenario will converge to a homogeneous scenario. The actual density of 2.8 is still far from the maximal density which is of ≈ 8 persons/m^2. Secondly, the case of convergence of the speedup in an homogeneous scenario has been demonstrated by [13, 52]. Considering these two facts, it can be expected that the speedup function rises with its current slope (of) and stagnates around 160×k. The factor k added here has a damping role and can be determined by simulations.

The runtimes using different numbers of processors are given in Figure 3.7. The corresponding speedups are in Figure 3.8. A perfect linear speedup is not reached in this case, which according to Amdahl's law [67] is due to the portion of the code that cannot be parallelised and thus has to run in serial. This is for instance the updating of the linked cells. The maximum speedup achieved is 9 using 12 processors. We should mention here that the obtained results

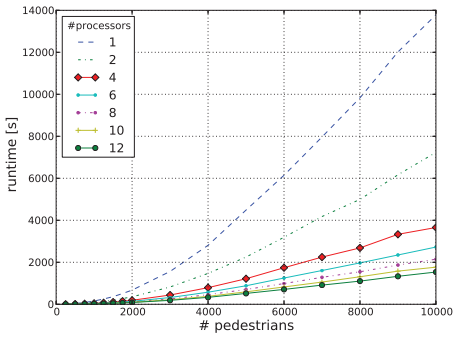

Figure 3.7: Runtime using different numbers of processors.

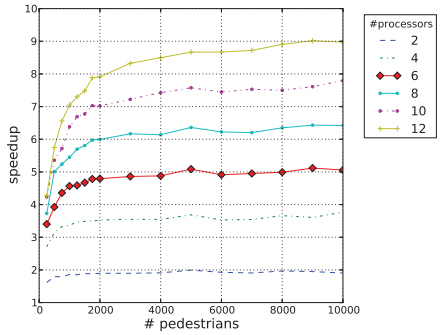

Figure 3.8: Speedup using different numbers of processors.

are not directly applicable to other scenarios, which might for example have other geometrical restrictions (see the previous section on load balancing).

3.4 Case Study: ESPRIT arena

3.4.1 Simulation area

The simulation domain (part of the arena) is presented in Figure 3.9. It is subdivided in 15 sections which are mapped into the detection areas of the automatic person counting systems. The promenade is divided in 5 sections. The sections HRI030 and HRI010 are connected to the tribune with three gates each. The remaining three sections are connected to 2 gates each. The promenade has a maximal capacity of $\sim$ 9500 pedestrians. The tribune is divided in 9 sections. The last section is the playing field. The individual maximal capacities of the different sections are shown in Table 3.1. This division will also be used as domain decomposition technique for

section name	max. capacity
HRI010	2472
HRI020	2072
HRI030	2494
HRI040	1580
HRI050	1722
HRI070	1600
HRI080	1713
HRI090	1615
HRI150	∼17500

Table 3.1: Maximal capacity with seats configuration for some sections (see Figure 3.9). The capacity for standing places configuration differs.

the parallelisation as shown in the next sections.

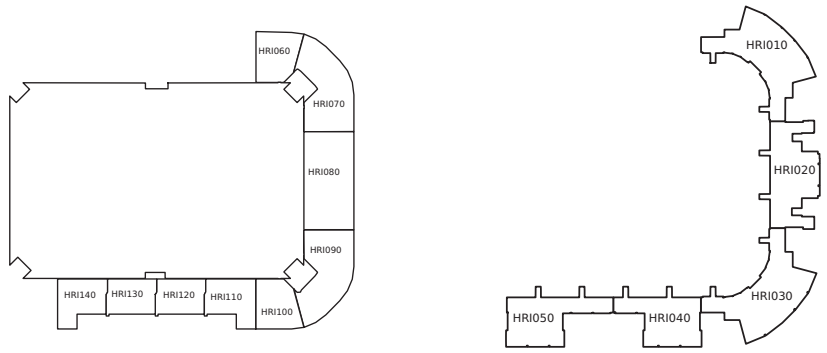

(a) Tribune and playing field divided in 10 sections (b) Promenade divided in 5 sections

Figure 3.9: Simulation area subdivided in 15 sections.

3.4.2 Computer architectures

3.4.2.1 Cell Broadband Engine - CBE

The first architecture the simulation was supposed to run on was the Cell Broadband Engine Architecture (CBEA) [68]. First introduced in the PlayStation 3® from Sony Computer Entertainment, the CBEA has a wide range of applications in the high performance computing domain including large crowd simulations [55]. The neighbourhood lists methods presented above have been tested on an IBM BladeCenter®. Each blade features two CBEAs (see Figure 3.10), each of which has 9 elements: 1 Power Processor Element (PPE) and 8 Synergistic Processing Elements (SPE) all connected to a high bandwidth bus, the Element Interconnect Bus (EIB). The SPEs give the CBEA its computational power and the work is usually coordi-

nated by the PPE which is a standard 64 bit PowerPC CPU operating at a nominal frequency of 3.2 GHz.

The approach of running the simulation on this architecture was discontinued to the benefit of a general purpose architecture: the Xeon® processor from Intel® [69]. The discontinuation had many reasons. Firstly, the development of the CBEA was discontinued itself [70, 71]. Secondly, the CBEA is optimised for pipeline computation and is very sensitive to branching, i.e. *if-statements* (see section 4.6 and 8.5 in [68]). These statements are the basis of the cellular automata models, which also use the same architecture to perform their simulation. Finally, since the discontinuation the price/performance ratio of the CBEA has dropped.

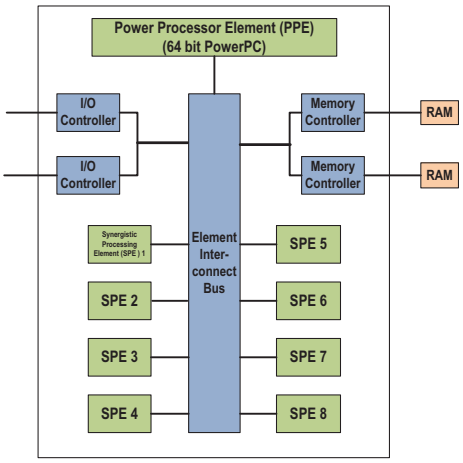

Figure 3.10: Cell Broadband Engine Architecture featuring 1 Power Processor Element (PPE) and 8 Synergistic Processing Elements (SPE).

3.4.2.2 Intel® Xeon® Processor

A more general purpose processor has been preferred for the simulation in Hermes for the reasons mentioned earlier. Another advantage is that the code can be optimised in a more general fashion. The simulations are performed on a cluster consisting of 15 PowerEdge M610 blade servers. Each server features 2 six-cores Intel(R) Xeon(R) CPU X5670 clocked at 2.93GHz and disposing of a 12 MB cache. Figure 3.11 shows the cluster used for the project.

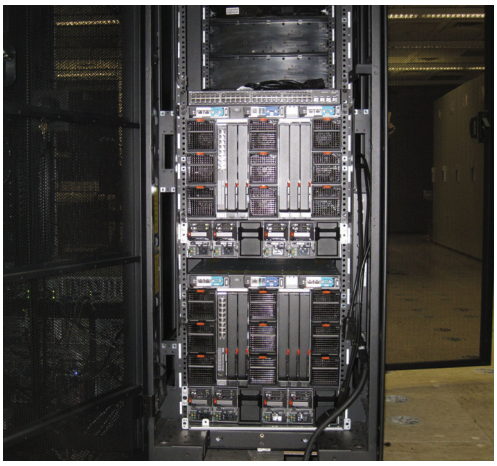

Figure 3.11: Cluster used for the simulation in the ESPRIT arena in Düsseldorf, Germany.

3.4.3 Parallelisation results

3.4.3.1 Parallelisation strategy

To achieve the real-time requirement, the optimisation of the serial code is performed at three levels. The Message Passing Interface is used to run the simulation across the computing nodes. The simulation code on each node is run in a multi-threaded environment using OpenMP. Finally, special neighbourhood list algorithms are used to consider the short range character of the repulsive forces. In this case the linked cells is used with a cutoff radius of 2 m. Recall that ideally the cell size should be at least equal to the cutoff radius (see Chapter 2).

Two main reasons speak in favour of a static domain decomposition on the geometry presented in Figure 3.9. The first reason is the relative low communication requirements and also due to the natural partitions given by the persons counting system. This partitioning was done to achieve as little communication as possible between the domains. This is done by choosing the boundaries between the domains, which are also the counting lines for the system, as small as possible, thus mainly at doors. We also assume an initial almost uniform distribution of the pedestrians in the simulation area. The ghost areas, which hold the data shared by different processes, are presented in Figure 3.3. They are computed with the help of the linked cells. Only the red pedestrians are present on more than one processor. The second reason is the route choice algorithm which is the main topic of the next chapter. The algorithm needs information about the pedestrian distribution in a specific decision area (in this case a room) at each simulation step. With a static domain decomposition in rooms, all this information is always available on the same processor. The simulation of pedestrians as particles differs from the simulation of the general N-Body systems. One difference is that in pedestrian dynamics the pedestrian stream and direction of movement are predictable. Predictable in

the sense that at a certain time in the simulation, they will gather at exits. Therefore, the concept of splitting the simulation area into static areas is well suited (see Section 3.2.3 on load balancing). Another reason is the production machine dedicated to the application. 15 nodes are available for the space continuous model in the evacuation assistant. In addition, the results of the simulation, i.e. the trajectories of the pedestrians are written with respect to those areas. Thus, the nodes can independently perform IO operations without any need of synchronisation.

In the case of the evacuation assistant, the initial number of pedestrians is received via sensors (see Figure 1.1) of an automatic persons counting system. The received pedestrians are then homogeneously distributed in their respective areas. The workflow diagrams for the master processor and the slave processors are shown in Figure 3.12. All processes read the same geometry file and logically have the same constraints on that geometry. The constraints are for example the doors states (closed/open) and the block states (smoked/smoke-free). Thereafter the master shares the works, depending on the number of computing nodes available. Each node receives $\lfloor \frac{\#sections}{\#nodes} \rfloor$. The last node in the list might receive more. When a node receives more than one section to operate on, it is guaranteed that the sections are contiguous. This also limits the data exchange between the processes.

3.4.3.2 Promenade area

The following results have been obtained on the cluster dedicated for the project presented in Figure 3.11. Similar results published in [49, 72] have been obtained previously on JUROPA [73], an Intel based cluster installed at the Jülich Supercomputing Centre from the Forschungszentrum Jülich GmbH. At that time the Hermes cluster was not available, furthermore JUROPA offers more debugging tools. The Hermes cluster is more efficient as attested by the results presented below. The main differences are the higher CPU frequency, the increase cache size and the number of cores per nodes (12 cores versus 8 cores). For the results presented here, only the promenade has been simulated and the pedestrians are always equally and homogeneously distributed in the 5 sections. The runtime for the different number of pedestrians applies to a complete simulation i.e. all pedestrians have left the facility. The evacuation times are presented in Figure 3.16 for comparison purposes. There is a linear dependence between the number of pedestrians and the evacuation times. 8000 pedestrians need ≈ 3 minutes to clear the area. The slope of the evacuation time curve, which is also the flow over all exits, is estimated at 44.5 persons per second.

Figure 3.13 shows a comparison of the brute force method and the linked cells on a single node using different numbers of processors. OpenMP is used in this case for the shared memory parallelisation. The overall speedup obtained for 5×1600 Pedestrians in this case is 200 for 1 processor and 750 using 12 processors. The convergence speed of the speedup is also related to the number of processors. Using 1 processor the maximal speedup is already obtained by

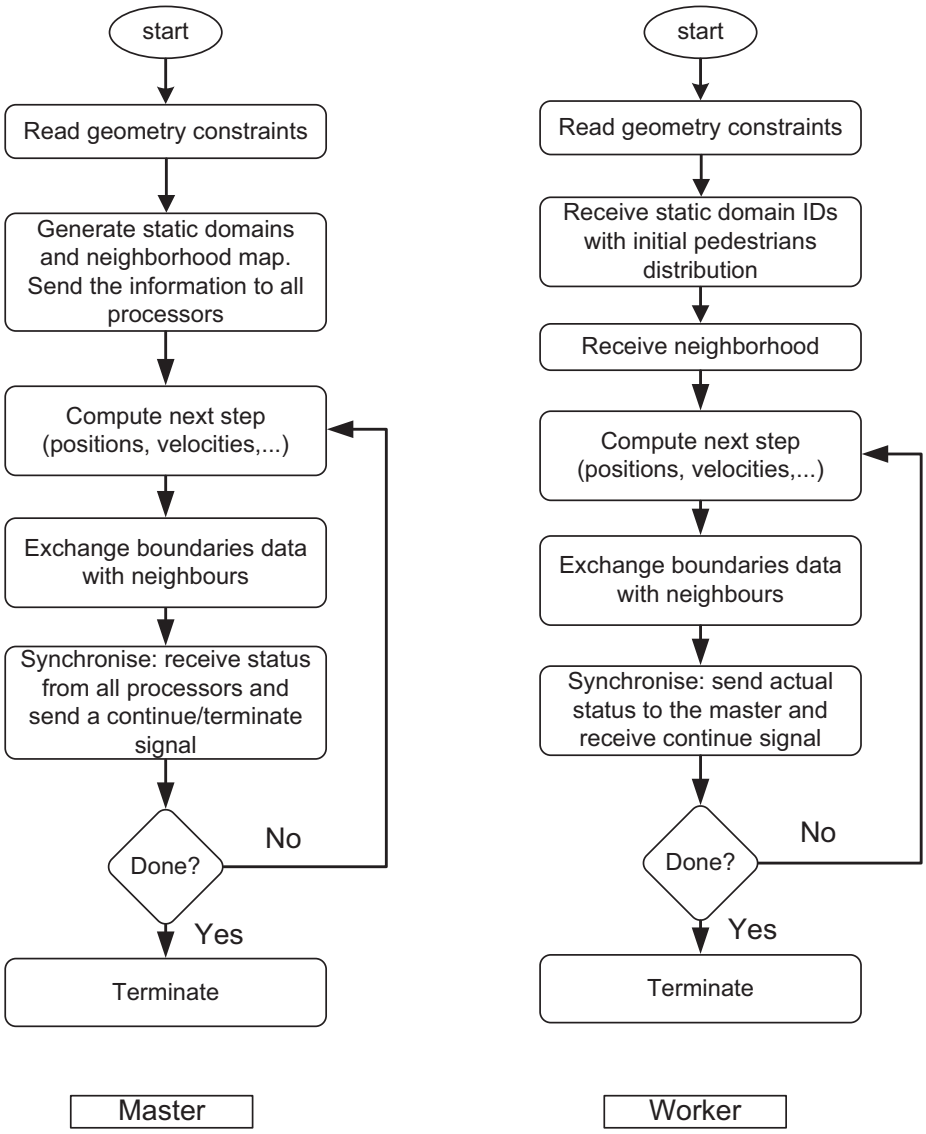

Figure 3.12: Parallelisation algorithm for the master and worker processors.

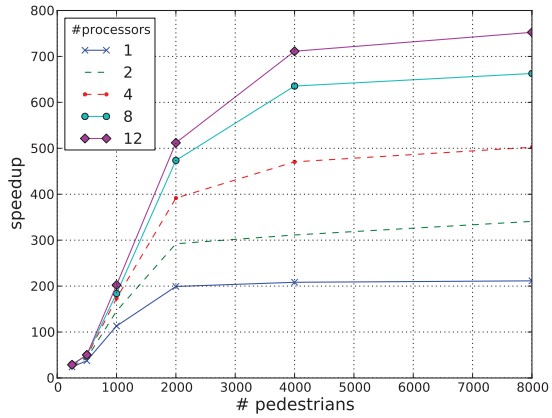

Figure 3.13: Speedup of the linked cells with different number of threads over the serial brute force method.

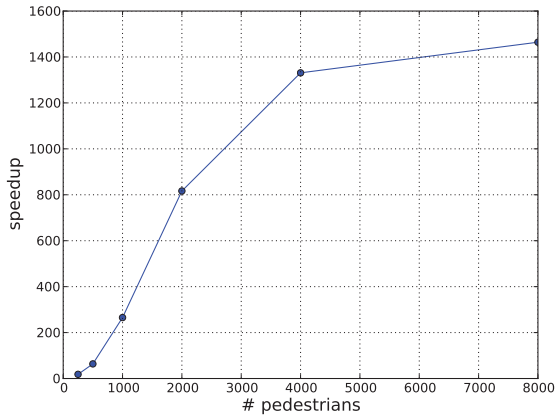

Figure 3.14: Speedup of the hybrid program (MPI + OpenMP + linked cells) over the serial brute force method.

2000 pedestrians. On the contrary, by using 12 processors the full convergence is not reached for 8000 pedestrians. One should note here that the brute force is only in the neighbourhood detection, not on the force computations between the pedestrians. In addition, the brute force has been 'naturally' optimised by the area partitioning in sections, which means that by the neighbourhood search, not necessarily all pedestrians in the simulation are investigated, but only those in the same room including directly connected rooms.

Figure 3.14 shows the results obtained using a hybrid MPI+OpenMP parallelisation approach using 5 computing nodes. The overall speedup obtained in this case for 8000 pedestrians is 1450

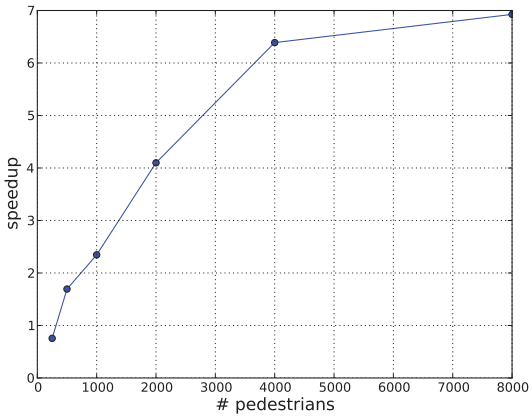

Figure 3.15: Speedup of the hybrid program (MPI + OpenMP + linked cells) over the serial linked cells.

#pedestrians	BF	LC	Hybrid
250	231	9	12
500	436	11	6
1000	2117	18	7
2000	7960	39	9
4000	30663	147	23
8000	220000	1040	150

Table 3.2: Runtime in seconds in the promenade using the brute force (BF), the linked cells (LC) and a hybrid parallel implementation.

over the brute force serial program. The maximal speedup obtained when compared with the serial code optimised with the linked cells and the parallel code is 7. The convergence values are presented in Figure 3.15. The individual runtime in seconds are presented in Table 3.2. In addition, the overhead for very small amount of pedestrians is noticeable. The hybrid method needs more time for 250 pedestrians than the serial code. The conclusion is that the most speedup is gained from the used of the linked cells. In other terms, the most computation time is required for determining the neighbourhood.

3.4.3.3 Tribune area

The tribune and the promenade differ in many ways. There is more freedom concerning route choice possibilities in the promenade than in the tribune area. From each section of the tribune, there is only one gate to reach the promenade. Also, the sitting rows are defined as rooms i.e. bounded by walls. Therefore, interactions between pedestrians and walls will dominate the computation. In the promenade, we have more interaction among pedestrians. Finally,

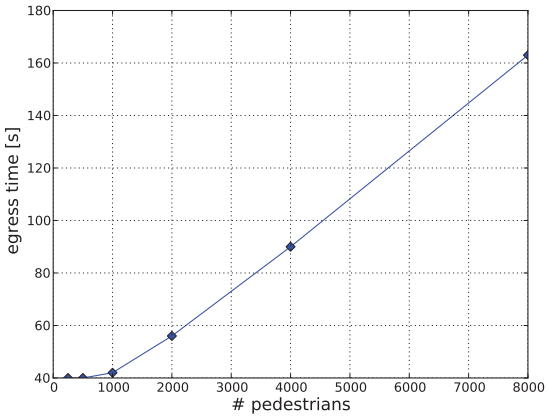

Figure 3.16: Evacuation times in the promenade.

the tribune is subdivided in 9 sections compared to 5 sections in the promenade. Due to these differences, different values for speedup and runtime are expected. In order to obtain reliable results for comparison only five sections of the tribune have been filled and the same number of processors was used. The results applies for complete evacuation i.e. all pedestrians have left the arena. The evacuation times are presented in Figure 3.17. The clearing times are much larger compared to the promenade, $\approx$ 14 minutes for 8000 pedestrians. Linearity in the times is also noticeable. The slope of the curve is 5.45 persons per second. The runtime is given in Table 3.3. For 250 pedestrians, the overhead brought by the parallelisation dominates over the computation and lead to a higher computation time.

Figure 3.18 shows the speedup achieved over the serial brute force using different number of processors and OpenMP. The values are four times lower than the values obtained in the promenade. The code scales up to 4000 pedestrians on 12 processors and up to 1000 pedestrians on 1 processor. This is on one hand due to the nature of the computed forces: more pedestrians-wall forces in the tribune and more pedestrian-pedestrians forces in the promenade. On the other hand, we have a natural optimisation in the implementation of the brute force. The sitting rows are modelled as rooms in the geometry file and the brute force implementation loops through the rooms and considers only pedestrians in neighbouring rooms.

The speedup obtained over the linked cells using the hybrid implementation is presented in Figure 3.19. A speedup of 18 is reached for 8000 pedestrians. The results obtained using the hybrid implementation over the serial brute force are presented in Figure 3.20. There is a stagnation of the speedup at the value of 550 for 4000 pedestrians. The obtained results are improved if the same amount of pedestrians is homogeneously distributed in the complete 9 sections of the tribune.

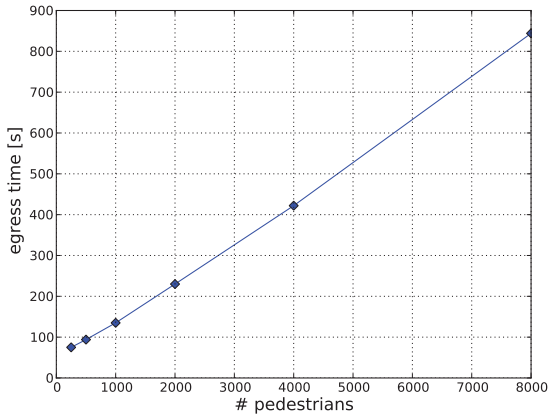

Figure 3.17: Evacuation times in the tribune.

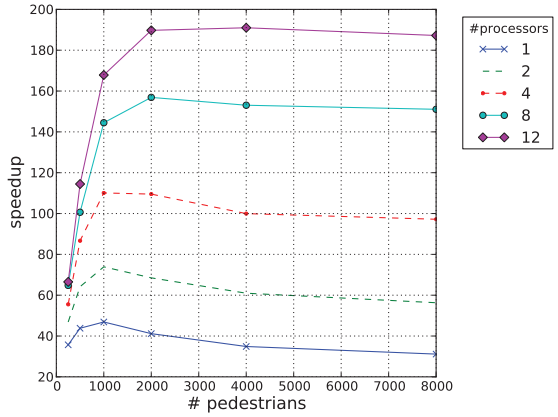

Figure 3.18: Speedup of the linked cells with different numbers of processors/threads over the serial brute force method.

#pedestrians	BF	LC	Hybrid
250	426	11	27
500	1106	25	8
1000	3071	65	12
2000	8636	209	21
4000	25305	725	46
8000	82160	2637	145

Table 3.3: Runtime in seconds in the tribune using the brute force (BF), the linked cells (LC) and a hybrid parallel implementation.

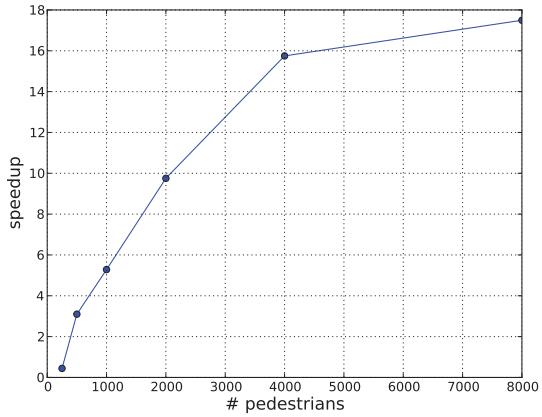

Figure 3.19: Speedup of the hybrid program (MPI + OpenMP + linked cells) over the serial linked cells.

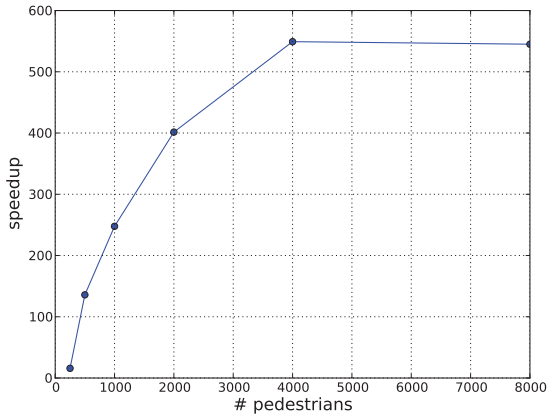

Figure 3.20: Speedup of the hybrid program (MPI + OpenMP + linked cells) over the serial brute force method.

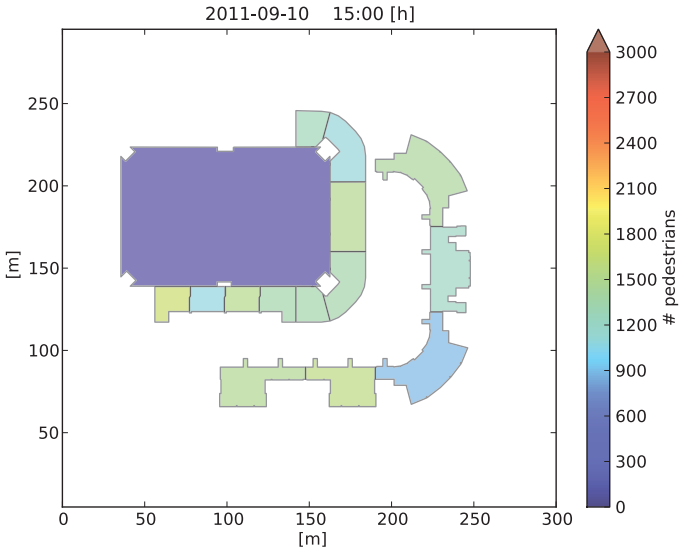

Figure 3.21: Simulation area divided in 15 sections. The initial configuration prior to a simulation is represented by the number of pedestrians inside the sections. These are real input data coming from the automated person counting system. Camera teams and players for instance are also accounted to the pedestrians in the playing field area.

3.4.3.4 Complete arena

Finally, we investigate the runtime of a typical starting configuration for a simulation in the evacuation assistant framework. The typical start configuration is presented in Figure 3.21. The runtimes achieved using different numbers of processors is shown in Figure 3.22. The runtimes apply to a complete simulation i.e. all pedestrians have left the facility as also investigated for the tribune and the promenade separately. The measured evacuation times are 580 seconds for 20000 pedestrians and 332 seconds for 10000 pedestrians. The simulation times are 130 and 43 seconds respectively. One should note that an evacuation scenario was simulated in this case. It means that there is no direct way of validating the obtained evacuation time. The times measured during a routine clearing (after a concert is over for instance) are usually bigger. This can be attributed to the fact that people might spend more time in the facility celebrating their teams and stars or at the fan shops for instance. The results computed by the assistant are presented in Figure 1.3. The congestions areas are displayed. The assistant interface is web based making it flexible and location independent.

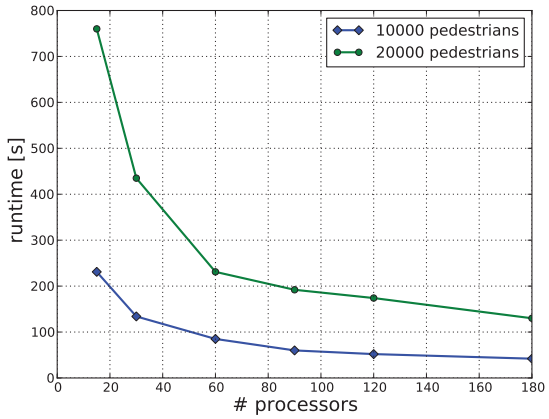

Figure 3.22: Runtime using different numbers of processors. The evacuation times are 332 seconds for 10000 pedestrians and 580 seconds for 20000 pedestrians.

3.5 Summary

In this chapter, runtime optimisation techniques have been presented. The test case is an irregular structure given by the ESPRIT arena. The runtime measurements take into account the linked cells and a hybrid parallelisation using MPI and OpenMP. The requirement of performing a faster than real time computation has been achieved by combining the techniques. Still, a closer look at the simulation with appropriate debugging tools of the Scalasca toolset [74] shows that the communication between the processors offers further possibilities of optimisation. The simulation cluster supports hyper-threading allowing up to 360 virtual processors. However, the use of hyper-threading has been shown to be very inefficient in this case. Other investigated runtime optimisation approaches include the use of other solvers for the differential equations. For instance, the implementation of solvers which allow a larger step size like the Verlet or the Leapfrog Algorithms. Unfortunately, no satisfactory results have been obtained. The next chapter will focus on the routing strategies used.

Chapter 4

Route Choice

This chapter deals with an event driven way finding algorithm for pedestrians in a graph-based structure. The events used to (re)direct pedestrians include the identification of a jam situation and/or the identification of a better route than the current. The modelled strategies are the shortest path (local and global); they are combined with a quickest path approach, which is based on the perception of the environment. The pedestrians take their decisions based on the observed environment and are routed dynamically in the network, generated from the building, using an appropriate cost benefit analysis function. The motivation of each pedestrian is to leave the facility, i.e. an evacuation scenario is considered. The influences of the different strategies on the evacuation time, the individual times spent in jam, the jam size evolution and the overall jam size itself are investigated.

4.1 Definition and Psychology

A route is defined as a way or course taken from a starting point to a destination. Route choice in pedestrian dynamics can be very dynamic and also unpredictable. Besides, the route choice underlies many subjective factors including the actual crowd density, the perception, the internal states, the experience and the history of the pedestrians. Most of those factors cannot directly be measured. Nevertheless, they have to be taken into consideration for reproducing a realistic behaviour in simulations. Table 4.1 shows a categorisation of different paths in a facility according to their perception and the criteria that influence them. They are classified in subjective and objective paths. We are aware that a strict categorisation is not possible. The shortest, the quickest and the given paths are more objective than subjective and might be easier to capture and model than the others. In most simulation software, pedestrians are initialised without any history. It means for instance that the pedestrians have no idea about the route they have chosen to enter the facility, completely ignoring the aspect of experience. This may indeed have some influences on their decision while being evacuated from the facility.

	Type	Criteria
Objective	Shortest path (global, local)	exits in sight range, signs, experience, ...
	Quickest path	jam in sight range, experience,...
	Given path	directives from signs or panels, personal,...
Subjective	Pleasant path	design, clarity, lighting, experience, emotional state,
	Safest path	experience, overview, walking in group...
	Known path	experience, overview, (re) identification of signs,...
...	...	...

Table 4.1: Examples of path types classification inside a facility and possible influencing criteria.

4.1.1 Psychology of crowd

We are modelling and simulating crowds composed of individual agents and the study of crowds has been done in the past. Usually people want to fit in a group and conform to it as demonstrated by Asch [75]. It has been shown from a psychological point of view that pedestrians act in a coordinated fashion using only little communication [75–77]. Apparently, people conform for two main reasons: because they want to fit in with the group which is called normative influence. They may believe the group is better informed than they are, which is known under informational influence. Crowds may also create new norms for interacting with each other as presented by Turner [77]. It is clear that social behaviour emerges from interactions between people as acknowledged by Allport [76]. He discussed topics such as emotions, conformity to a group and the effects of an audience on other persons.

4.1.2 Incorporating the psychology of crowds in models

For all the aforementioned psychological factors to be taken into account, pedestrians have to be modelled as a group as well as individuals. Modelling human behaviour is a difficult task and models are often simplified due to this difficulty as Sime argued [78]. To fill the gap psychology and computer science are often associated resulting in cognitive models. Several modelling techniques are presented by Thalmann et al. [7, 79]. He proposes three ways of controlling crowds in a simulation: scripts, rules with events/reactions and external control. Decision Field Theory [80] characterises pedestrians as unique and individual agents, with their own attributes and a certain level of cognition for making their own or personal decisions. Depending on the modelled scenario, different types of crowd are observed: commuters, visitors and local inhabitants. The Multi-Agent Communication for Evacuation Simulation (MACES)

developed by [81] integrates some psychological features, where three categories of people can be simulated: trained leaders, untrained leaders and untrained non-leaders (followers). Different results are obtained depending on the percentage representative of each group among the simulated pedestrians. Furthermore, it offers high level way finding and inter-agent communication, which allows message transportation between the simulated entities. The Performance Moderator Functions Server (PMFserv) [82, 83] developed by the Barry Silverman Laboratory at the University of Pennsylvania, is a concept-modelling system for pedestrians. It models four psychological areas of the human behaviour: psychobiology, personality psychology, social psychology, and cognitive psychology. It integrates several features including personality modelling, biological modelling and stress, group Identity, membership. One drawback is the lack of learning ability. The Microscopic Human Factors (MHF) approach introduced by Henein et al. [84] improves the behavioural repertoire of microscopic models. It has been successfully coupled to the basic Floor Field Model.

4.2 Route Choice Modelling

Cellular Automata (CA) models generally (but not necessarily) use floor fields (static and/or dynamic) to direct pedestrians to a destination point. Route choice in continuous models can be achieved by means of a network which consists of a set of destination points. This type of way finding is known as graph-based routing [36, 85–88]. The destination points can be predetermined (exits for instance) or adjustable (crossings, turning point at the end of a corridor for instance). The minimal network is usually a visibility graph (see [9] for more details) which ensures that any location on the facility is within the visibility range of at least one node. The initial network can be refined by adding more adjustable points converging to CA [89]. This graph can be extended to a navigation graph by adding more adjustable points. The generation of such graph is a complex process. Some efficient methods are presented in [90,91]. Once built, the shortest path is usually determined using well established algorithms such as Dijkstra [92] or Floyd-Warshall [93]. Such networks are widely spread in motion planning by robots as well [94, 95].

In the case of an evacuation, it is generally assumed that the intrinsic behaviour of the crowd is to follow the seemingly (self-estimated) quickest path. The quickest path in pedestrian dynamics describes the process of minimising the travel time to a given a destination. This is indeed a subjective notion as it depends on some prerequisites, e.g. whether or not the pedestrian is familiar with the facility. Even cultural factors can affect this behaviour. Chattaraj et al. [96] showed the influence of different cultures on the fundamental diagram, which denotes relation between the density and the velocity. It is clear that those influences can be extrapolated to the route choice behaviour as well. The question to answer is how and to what extent. A sample study of route choice from a psychological point of view about pedestrians' perceptions of their environment is presented in [97]. In the case of incomplete in-

formation, following other pedestrians can lead to better performance. This process is achieved with dynamic floor fields [21] where moving pedestrians increase the probability of using that path thereby making it more attractive for other pedestrians. This method may also worsen jams, if the followed pedestrians make a bad choice. The modelling of the quickest path is achieved by systematically avoiding congestions. In CA models, this can be obtained by means of enhanced dynamic floor fields. The enhancements include density in front of the moving pedestrians within their sight range [98] as well as the payload and distance to exits [99–101]; other approaches include navigation fields [29, 102]. Continuous models usually optimise the travel time in the constructed network. In [18] pedestrians minimise their travel time by solving the Hamilton-Jacobi-Bellman equation yielding to the optimal paths for pedestrians at each time step. A combination of a graph-based routing with CA is presented in [90] where the fastest path for pedestrians is computed using a heuristic $A*$ algorithm [103]. In [104] visibility graphs and the Dijkstra method are used to determine the route of pedestrians in discrete space. In [105] the optimal paths for pedestrians are found by using a queue principle that minimizes their respective waiting times. Timmermans et al. describe a model [106, 107] which deals with the choice of destinations and appropriate routes to reach those destinations. Additional approaches of modelling the route choice of pedestrians, especially for multiple exit selection, based on game theory are given in [100, 108]. A combination between a microscopic and a macroscopic model for determining the optimal operating on a graph egress time from a building is presented in [109].

4.3 Events Driven Modelling

In this section, an event driven way finding in a graph-based structure is introduced. The pedestrians observe their environment and take their final decisions based on the obtained data. With this observation, an approximation of the quickest path is achieved. The modelled strategies are the local shortest path (LSP), the global shortest path (GSP), the local shortest combined with the quickest path (LSQ) and finally the global shortest combined with the quickest path (GSQ). The idea has been presented in [110, 111].

In this pedestrian framework, the operational level of the walking pedestrian is described by the Generalized Centrifugal Force Model [17,35] which operates in continuous space. We focus here on the strategic level only, i.e. the pedestrians are solely given the next destination point, which is the next intermediate destination for the self-estimated optimal route. This is also the direction of the driving force (see Equation 2.2).

4.3.1 Pedestrian characteristics

We simulate pedestrians that are familiar with the facility and pedestrians unfamiliar with the facility. For those two groups we identify criteria to reproduce their route choice. Those criteria are the local/global shortest path and the quickest path. The dynamic change of the strategies is modelled. This emulates the internal state of the pedestrians and the strategies are subject to change during the evacuation process. In addition, one of the challenges consists of finding a good balance between the number of parameters and the numbers of criteria. The model should be as simple as possible with the parameter space kept as small as possible while considering as many criteria as required. This is important for model understanding and stability. In addition, for our implementation for evacuation, we assume a rational behaviour of the crowd, as we are not having any external threat or a fighting for resources. The rational handling imposes for instance no aggressiveness. As a result, no pedestrian will force his/her way through a pedestrian stream coming from an opposing direction.

4.3.2 Graph construction

In the framework used here, pedestrians move from one decision area to the next one. The decision areas are connected with nodes, which are interchangeable with destination points. A decision area is a place where the pedestrian decides which way to go or change their current destination. For a simple geometry it is an abstraction for rooms and corridors. In addition, we restrict ourselves to the case where the destination points are exits and corridors end. Figure 4.2 illustrates this procedure and is a mapping of the facility presented in Figure 4.1. The pedestrians are moving from the decision area 1 to the decision area 2. The two areas are connected with one node n_1. The network is automatically generated from the facility based on the inter-visibility of the exits. This automation is limited to structures as the one presented in Figure 4.9. For more complex structures, we refer to Chapter 5 where some methods are presented. The Euclidean distance between the nodes is used as weight as done by Molnár [36].

Well established algorithms like Floyd-Warshall are used to determine the default optimal paths. The default paths are only optimal when there is no congestion. In that case the, global shortest and the quickest path to a given destination are the same. The graph used is a directed graph. It means that each node is only connected to a node that leads (in the shortest way) to one of the desired final destinations. To optimise the runtime, each node of the graph stores information such as the

- connected nodes and distances,
- distance to all final destinations,
- shortest paths to reach all final destinations.

4.3.3 Shortest paths

4.3.3.1 Local shortest path

The most straightforward route choice approach is the local shortest path. Once a node in the navigation graph is reached, the local nearest node is chosen as next destination. Pedestrians without global information choose the local shortest path. If we reconsider the criteria given in Table 4.1 a method of achieving this would be to follow the signs or landmarks in the facility. They generally lead to the nearest exit. Those unfamiliar pedestrians could be first time visitors in a stadium, at a concert for example. This approach will lead to the outside. In many cases however, pedestrians have a preferred destination, a parking lot for instance. The appropriate strategy will be the global shortest path, provided the pedestrians show some knowledge the facility.

4.3.3.2 Global shortest path

The global shortest path is determined by running the Floyd-Warshall algorithm with path reconstruction [93] on the navigation graph built. The runtime of $\mathcal{O}(n^3)$ is not an issue since we only have a small amount of nodes. From every node on the graph, the global shortest path to reach the outside can be determined. Pedestrians familiar with the facility, regular spectators from a football game for instance, have the global map i.e. the constructed network and may approximate the global shortest path to their final destination independently of their current location. They have a better analysis of the current situation.

4.3.4 Quickest path

In contrast with the shortest path, the quickest path is dynamic and changes with time throughout the simulation. The business logic of the routing algorithm is shown in Figure 4.3. The main events used in this routing algorithm to redirect pedestrians are the entering of a new room and the identification of a jam situation. The pedestrians are first routed using the shortest path, global or local depending on their knowledge stand about the location. The key elements of a quickest path routing approach are the estimation of the travel time, the estimation of the gain and an assessment of this gain. Three functions are developed to model those key elements. We first define four values which will be used throughout this section.

Definition 1 *Re-routing time t_r*
The re-routing time t_r for a pedestrian i with position $\vec{x}_i$ is the time where one of the following conditions holds:
$\|\vec{v}(t)\| \leq v_{min}, \forall t \in [t_r - t_{min}, t_r] \quad \vee \quad \|\vec{x}(t_r) - \vec{n}_i\| \leq d_{min}$ *where v_{min} is the threshold jam*

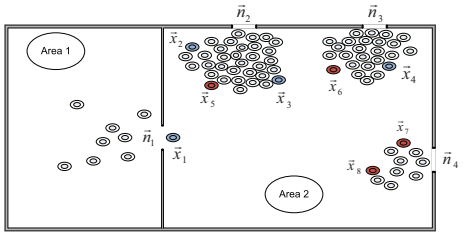

Figure 4.1: Process of selecting a reference pedestrian prior to a route change. Pedestrians are denoted with their positions. The pedestrian $\vec{x}_1$ selects $\vec{x}_5$, $\vec{x}_6$ and $\vec{x}_8$. The pedestrian $\vec{x}_2$ has no clearance of the current situation and will not select any. The pedestrian $\vec{x}_3$ selects $\vec{x}_6$ and $\vec{x}_8$. The pedestrian $\vec{x}_4$ will only select $\vec{x}_7$ as reference.

velocity [112] , t_{min} the patience time and d_{min} the minimal distance to the node to consider it as reached.

Definition 2 *Reference pedestrian $Ref(i,\vec{n}_i)$*
Let i and j be two pedestrians with positions $\vec{x}_i$ and $\vec{x}_j$. The reference pedestrian j selected by the pedestrian i with respect to the node $\vec{n}_i$ is defined as:
$Ref(i,\vec{n}_i) = \{j : j \in \mathcal{Q}(\vec{n}_i), \vec{x}_j$ *visible from* $\vec{x}_i \wedge \|\vec{x}_j - \vec{x}_i\| = min\}$, *where $\mathcal{Q}(\vec{n}_i)$ is the jamming queue at the node $\vec{n}_i$. If more than one pedestrian satisfies the condition, one is randomly chosen.*

Definition 3 *Jamming queue $\mathcal{Q}(\vec{n}_i)$*
Let $\vec{n}_i$ be a node in the navigation graph, the jamming queue $\mathcal{Q}(\vec{n}_i)$ at the node $\vec{n}_i$ is defined as
$\mathcal{Q}(\vec{n}_i) = \{\forall i : \vec{n}_i$ *destination of the pedestrian* $i \wedge \|\vec{v}_i\| \leq v_{min}\}$ *where v_{min} is the threshold jam velocity [112].*

Definition 4 *Visibility range $\mathcal{V}(\vec{x}_i)$*
$\mathcal{V}(\vec{x}_i)$ represents the set of all nodes within the visibility range of the pedestrian i considering the actual location $\vec{x}_i$ in the facility and other pedestrians. It is determined using the Algorithm 4.1.

At any time t_r (see Definition 1) during the simulation, a new orientation process is started for the pedestrian i. A reference pedestrian j (see Definition 2) is selected from the queue (see Definition 3) and observed during an observation time t_{obs}. At the end of the observation, the expected travel time $t(\vec{x}_i, \vec{n}_j)$ via all nodes in the visibility range $\mathcal{V}(\vec{x}_i)$ (see Definition 4) is approximated using Equation 4.1.

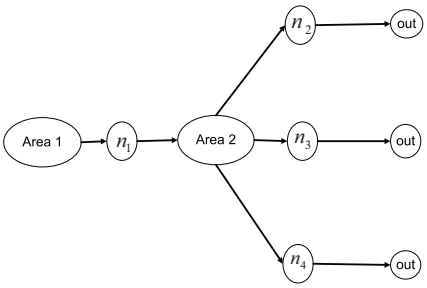

Figure 4.2: Network mapping of the facility presented in Figure 4.1 with 2 decisions areas and 4 nodes.

$$t(\vec{x}_i, \vec{n}_j) = \begin{cases} \frac{\|\vec{x}_i - \vec{x}_j\|}{\|\vec{v}_i\|} + \frac{\|\vec{x}_i - \vec{n}_j\|}{\|\vec{v}_{ja}\|}, & \text{if a reference } \vec{x}_j \text{ with average velocity } \vec{v}_{ja} \text{ was found;} \\ \frac{\|\vec{x}_i - \vec{n}_j\|}{\|\vec{v}_i\|}, & \text{if the node } \vec{n}_j \text{ is free (there is no reference in that case).} \end{cases} \tag{4.1}$$

$$\|\vec{v}_{ja}\| = \frac{1}{t_{obs}} \int_{t_r}^{t_r + t_{obs}} v_j(t) dt \tag{4.2}$$

$\vec{v}_{ja}$ is the average velocity of the reference pedestrian over the observation time defined by Equation 4.2. t_{obs} is randomly chosen between 1 and 3 seconds.

The minimal distance d_{min} is set to 0.20 m and the threshold for the jam velocity v_{min} is 0.2 ms^{-1}. This value comes from empirical studies performed in [112]. The estimated travel time is converted to a gain using Equation 4.3.

$$g(\vec{x}_i, \vec{n}_j) = \frac{1}{t(\vec{x}_i, \vec{n}_j)} \tag{4.3}$$

The cost benefit analysis (cba) function defined in Equation 4.4 determines whether it is worth changing the current destination. The gains g_1 and g_2 are calculated with Equation 4.3 and g_1 is always the current destination and g_2 the other evaluated alternative. The benefit returned should be greater than a threshold (g_{min}) in order for the pedestrian to consider the change. The thresholds taken here are 0.20 for familiar and 0.15 for unfamiliar pedestrians.

$$cba(g_1, g_2) = \frac{g_1 - g_2}{g_1 + g_2} \tag{4.4}$$

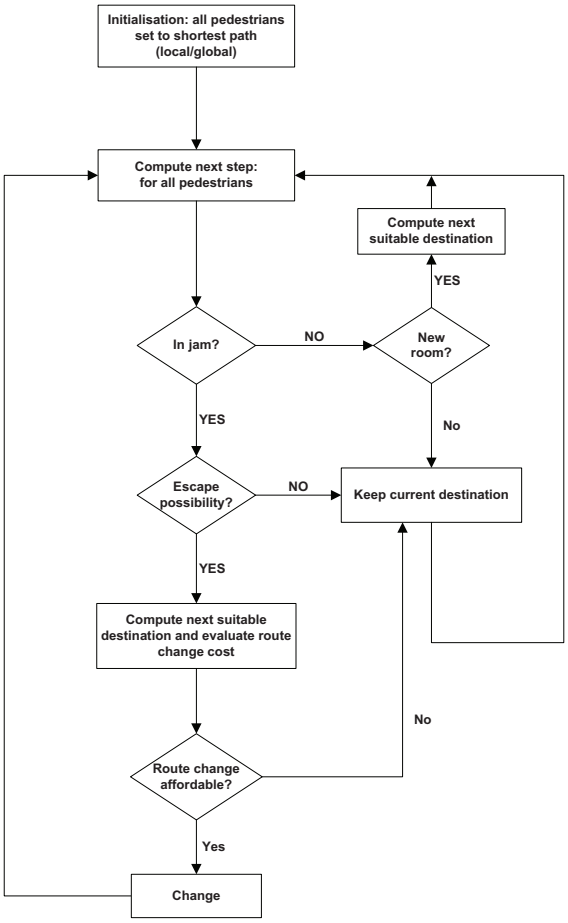

Figure 4.3: Business logic of the quickest path.

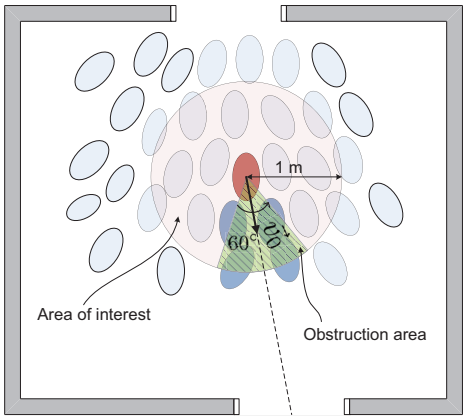

Figure 4.4: Process of escaping from a jam situation. The number of pedestrians in the obstruction area (4 in this case) determines the escape ability. The dashed line is the direction of the desired velocity $\vec{v}_0$.

When a pedestrian is caught in a jam for a period t_{min} (patience time) which varies depending on the pedestrian, he/she looks for alternatives in the decision area and in the sight range as described in Figure 4.1. The initial value for t_{min} is 10 seconds. It is increased by 1 second with any unsuccessful attempt to escape the jam. The value is kept until the room is changed. This amortizes the number of routes changes in the same room.

The process of escaping from jam is presented in Figure 4.4. Pedestrians in the obstruction area are considered as obstacles. The obstruction area is a circular arc with a radius of 1 m and a spanning angle of 60°. The obstruction area is constructed such that its bisectrix is the desired velocity $\vec{v}_0$ pointing to the exit the pedestrian is analysing. A pedestrian is unable to escape from a jam situation if the number of pedestrians in this area is larger than a threshold. We have assumed a threshold of 2 pedestrians for our simulation. With larger values of obstacles, pedestrians change their current destinations, but do not move due to the repulsive forces from other surrounding pedestrians. The pedestrians in the obstruction area are determined by their centre only.

The process of selecting a reference pedestrian is explained in Figure 4.1. The pedestrian $\vec{x}_1$ has entered a new room. The pedestrians $\vec{x}_2$, $\vec{x}_3$ and $\vec{x}_4$ have identified a jam situation. Pedestrian $\vec{x}_1$ selects the reference pedestrians $\vec{x}_5$, $\vec{x}_6$ and $\vec{x}_8$ for the exits $\vec{n}_2$, $\vec{n}_3$ and $\vec{n}_4$ respectively. The pedestrian $\vec{x}_4$ has a restricted visibility and will have only $\vec{x}_7$ as reference. There is no possibility for $\vec{x}_2$ to change. The references selection is based on the Euclidean distance and visibility range. The visibility is implemented by drawing a line from the concerned pedestrian to the pedestrians in the queue. There should not be any intersections with other pedestrians or walls in the room (see Definition 4 and Figure 4.1). It is important to mention here, that the queue size does not play a major role; more important is the processing speed of the queue.

Algorithm 4.1 Visibility Range of Pedestrian $\vec{x}_i$: $\mathcal{V}(\vec{x}_i)$

Input: Pedestrian $\vec{x}_i$
Output: $\mathcal{V}(\vec{x}_i)$

```
P ← all pedestrians \ {x_i}
W ← all nodes connected to the actual decision area of x_i
V ← ∅
obstacles_min ← 2
for all nodes n_j in W do
  obstacles ← 0
  u ← queuing pedestrians at node n_j
  for all pedestrians x_j in u do
    for all pedestrians x_k in P \ {x_j} do
      if [x_i x_j] intersects with the ellipse shape of the pedestrian x_k then
        obstacles ← obstacles + 1
      end if
    end for
    if obstacles ≤ obstacles_min and n_j ∉ V then
      V ← V ∪ {n_j}
    end if
  end for
end for
```

Unlike other algorithms, the approach presented here is not specialized to a particular case (asymmetric exits choice for instance), i.e. not bounded to the geometry. It is also not dependent on the initial distribution of pedestrians.

4.4 Evacuation Process Assessment

An important point less discussed in literature is the criticality of an evacuation process. Evaluation criteria like the building itself, the population size and the initial distribution of the evacuees, the evacuation time are discussed in [113]. Criteria related to the single pedestrians such as the individual travel time and waiting times are investigated in [105, 114]. The criteria most often used for evaluation building egress in case of emergencies are the overall evacuation time and a visualisation of the evacuation process from a simulation at specific times. Usually evacuation processes are assessed with a visual proof of simulations and evacuation time within a feasible range. In this context, Nelson and Mowrer [115] use the Available Safety Egress Time (ASET) and the Required Safety Egress Time (RSET) to analyse buildings in case of fire. The ASET is the time after which the life conditions in the building are no longer guaranteed and is commonly obtained from simulations and some experiments. The performance of a building is then evaluated with the difference between these two values. Unfortunately, these methods do not tell anything about the quality of the evacuation process, for instance the size of the jam during the evacuation process and whether this size could have been reduced by considering other options. Also, the state of an evacuation can be critical for

a certain group of the population, senior citizens and children for example, but rather harmless for a different group. Also the same results can be interpreted differently depending on the surrounding conditions, smoke or high temperature for instance.

In this section, we elaborate other criteria to address the criticality of an evacuation simulation. The analysed criteria are the individual time spent in jam, the jam size evolution over time and the total jam size defined as the area under the jam size evolution.

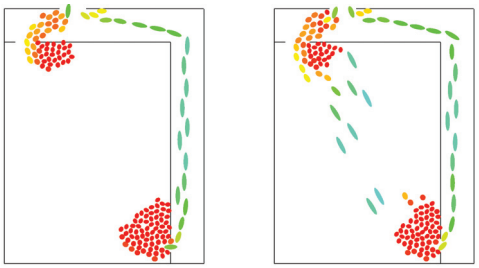

(a) Local shortest path (LSP)

(b) Local shortest with quickest path (LSQ)

(c) Global shortest path (GSP)

(d) Global shortest with quickest path (GSQ)

Figure 4.5: Dynamics of the system after 60 seconds. Congestions areas appear red. In (a) pedestrians follow the local nearest exit. In (c) the global nearest exit is chosen. In (b) and (d) pedestrians are allowed to change their current destination.

4.4.1 Evacuation time

The evacuation time is given by the last person leaving the facility. Another definition can be a clearance of the building up to 95% of the occupants. We consider the former definition here. A visual assessment of the evacuation dynamics for a simple scenario after 60 seconds is given by Figure 4.5. The colour of the pedestrians is correlated to their current velocity. Red means slow and represents congestions areas. Green corresponds to the maximum desired velocity of the pedestrians. The desired velocities are Gaussian distributed with mean 1.34 ms^{-1} and standard deviation 0.26 ms^{-1} [116]. The evacuation times distribution is presented in Figure 4.6(a). The smallest variance is achieved by the GSP. This is quite normal as the

GSP remains the same for all pedestrians irrespective of their initial positions. The largest variance is given by the LSP. The dynamics brought by the quickest path leads not only to a reduction of the overall evacuation time and a reduction of the width but also to realistic shapes in the simulation.

4.4.2 Jamming time

Up to now little importance has been brought to jam analysis itself i.e. how long pedestrians stay in jam ? This is strongly coupled with the implemented routing strategy. The keyword jam is unfortunately not well defined in pedestrian dynamics. A rather crude definition would be to have an absolute zero velocity over a minimal time interval. The minimal time interval is needed to avoid very short velocity reduction at a sharp turn for instance. We consider pedestrians moving at a speed lower than $0.2\,ms^{-1}$ [112] for a period of at least 10 seconds as being in a jam situation. The total time in jam is recorded for each pedestrian and a distribution of the recorded times is calculated. The jamming time distribution for the simulation scenario given by Figure 4.5 is presented in Figure 4.6(b). As expected, the width of the distribution is smaller for the quickest path.

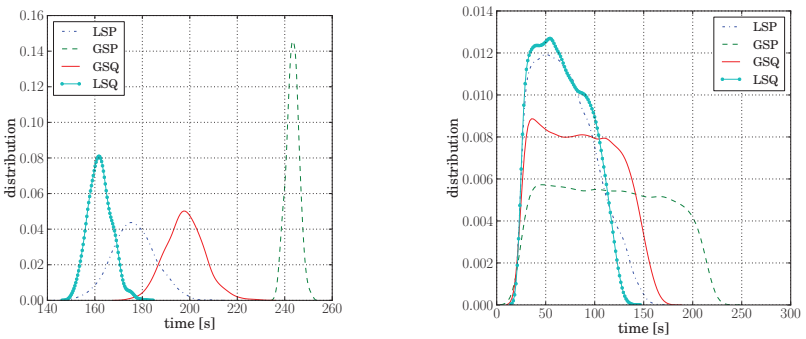

(a) Evacuation time

(b) Time in jam

Figure 4.6: Evacuation time and time in jam distribution for 200 pedestrians in the scenario in Figure 4.5.

4.4.3 Jam size

4.4.3.1 Definition

The jam size and its evolution cannot directly be derived from the evacuation time and/or the individual times spent in jam. It has to be analysed separately and for each exit individually. Short-lived jams are rather uncritical, the same holds for short-sized jams. We are particularly

interested in big jams with a long lifetime. They can be the origin of dangerous situations and should be checked not only against the characteristics of the evacuees for instance their ages, but also against the environmental conditions, the temperature for instance. The jam size is calculated by summing up the effective areas occupied by the pedestrians in jam at each time step. This is easily done by summing up the ellipses areas representing the pedestrians in the Generalized Centrifugal Force Model. Another method could be to build the envelope of the pedestrians and calculate the area of the resulting polygon. Figure 4.7(a) shows a straightforward example of a jam size analysis scenario after the first time step (0.001 second). The colour corresponds to the states. Red pedestrians are waiting for a possibility to move. Other pedestrians are already moving. The initial density is on average 1 $pedestrian/m^2$. The corresponding average jam areas are presented in Table 4.2. The values for the global and local shortest path are the same. There are some differences in their corresponding combination with the quickest path. At first look the values for the different routing strategies do not differ much from each other, but one has to consider the difference in the evacuation time, which is more than one minute in this case. There is a distribution of the overall load from the congested exits to the uncongested ones.
The jam size evolution at the different exits using the quickest path is shown in Figure 4.7(b). There is a sharp increase at the beginning of the simulation. Peaks of approximately 100 m^2 are reached at the exits which are 0.90 m, 1.20 m and 2.40 m wide. At the 5 m wide exit the peak is 70 m^2. The values then decrease with a slope correlated with the routing strategy used. The slope is constant with the static strategies and the peak lies by 160 m^2. The quickest path shows a less constant slope because some pedestrians are changing their destinations.

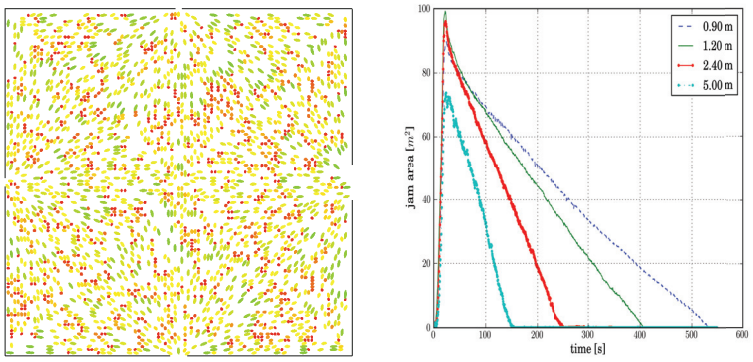

(a) Initial homogeneous distribution

(b) Jam size evolution at the four exits for the local shortest path combined with the quickest path depending on the exit width

Figure 4.7: Initial distribution and jam size evolution of 2500 pedestrians in a 50 m x 50 m room with four exits on each wall side. The exits width are 90 cm, 120 cm, 240 cm and 500 cm.

Door width b_j $[m]$	Jam area A $[m^2]$			
	LSP	GSP	GSQ	LSQ
0.90	53.7	53.7	48.8	49.3
1.20	52.8	52.8	48.2	42.5
2.40	27.4	27.4	31.3	28.1
5.00	13.2	13.2	20.3	18.1

Table 4.2: Average jam size at different exits of Figure 4.7 for the four strategies.

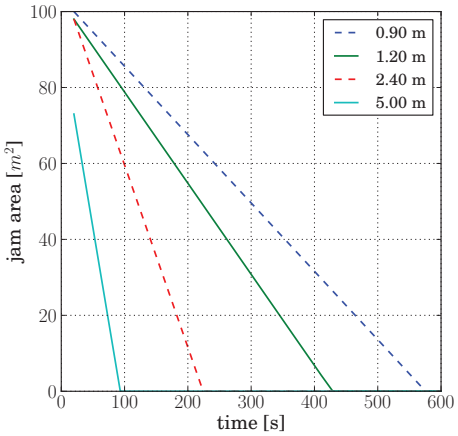

Figure 4.8: Approximation of the jam size evolution with respect to time using the specific flow as specified in Equation 4.5. The initial distribution is shown in Figure 4.7(a).

4.4.3.2 Estimation

The jam size evolution can be divided in two distinct states according to the slopes: monotonically increasing and then monotonically decreasing. At $t_1 = 20$ seconds the jams in front of the exits are fully developed. After that the jam area A decreases almost linearly in time with different slopes. The different slopes are proportional to the different door widths b_j. We assume that

$$A(t) = A_0 - k_j \times t \tag{4.5}$$

where A_0 is the jam area at time t_1 and k_j a constant proportional to the width of the exit b_j. To test this model we determine k_j with a special definition for the specific flow. We assume k_j to be

$$k_j = b_j \times J'_s \tag{4.6}$$

The classical specific flow J_s quantifies the throughput of persons per meter per second. With J'_s we define the specific flow in unit of areas taken by a person per meter per second. The

classical specific flow could be transformed by

$$J'_s = J_s \times A_j \tag{4.7}$$

where A_j is the area taken by a pedestrian in the jam and defined as

$$A_i = 1/\rho_{\text{jam}} \tag{4.8}$$

It follows that

$$k_j = 1/\rho_{\text{jam}} \times b_j \times J_s \tag{4.9}$$

From the scenario following values are measured: $J_s = 1.1\ Pers/m/s$ and $\rho_{\text{jam}} = 5\ Pers/m^2$. The jam density is obtained by counting the number of pedestrians in a square of $1 \times 1\ m^2$ in the jam area. Other methods for measuring densities including the Voronoi method are presented in [41]. The obtained results are presented in Figure 4.8. The jam size evolution is correctly described for the exits that are $0.90\ m, 1.20\ m$ and $2.40\ m$ wide. For the $5\ m$ wide exit, the jam size decreases faster compared to that of the simulation. With the estimation presented the linearity dependence of the jam size with respect to the time is described.

4.5 Simulations and Analysis

The strategies discussed in the previous section are now tested on the structure described in Figure 4.9 with different initial distributions. The simulation area is a simplified model of a section of the ESPRIT arena in Düsseldorf. The rooms R1 to R4 are the grandstands with dimensions 10 x 20 m^2. The tunnels are 2.40 m wide and 5 m long. The exits are 1.20 m wide. The rooms R4 and R6 are 10 m wide. The criteria used to evaluate the simulation results were presented in the previous section.

4.5.1 Example: partially filled facility

In the first simulation case, we are interested in the evacuation of a single block of the stadium. Figure 4.9(a) shows the initial homogeneous distribution of this test with 250 pedestrians. The dynamic of the evacuation after 60 seconds for the four strategies is presented in Figure 4.10. With the shortest path, only two exits are effectively used whereas the quickest path approach takes advantage of fours exits leading to a faster evacuation.

The results of the evacuation time analysis are summarised in Figure 4.11(a). 1000 runs are performed for the evaluation. The dynamic brought by the quickest path leads to a faster evacuation, on average 1 minute faster. As depicted in Figure 4.10 other (less congested or free) exits are used, as will be expected in a real evacuation scenario. There is not much difference between the results given by the global and the local shortest path, this is due to

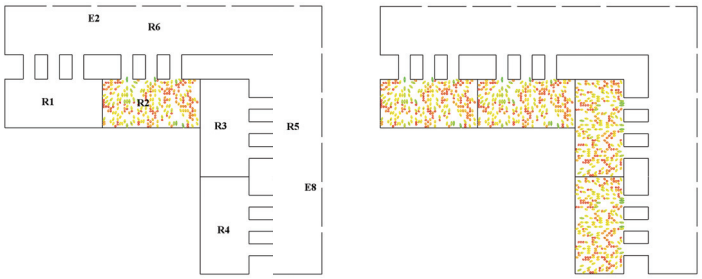

(a) 250 pedestrians distributed in a single block.

(b) 1000 pedestrians distributed in four blocks.

Figure 4.9: Investigated facility with initial homogeneous distributions of pedestrians. The total simulation area is 2144 m^2.

the shape of the investigated facility. The second value analysed is the individual distributions of time spent in jam. The results are presented in Figure 4.11(b). As expected, the results are correlated to the evacuation time. With the quickest path, pedestrians spend less time in jam, 30 seconds on average. This time is almost tripled using the static strategies. Figure 4.12 shows the evolution of the jam size at different exits. Exits without congestions have been left out. The static strategies show five long lasting jams. The quickest path alternatives shows more jams but short lived. The later ones are less critical. The total jam size distribution is taken from Figure 4.11(c). The average jam size for the static strategies is 11 m^2 and 9 m^2 for the quickest path. The similarities between the distributions are attributed to the fact that both global shortest and local shortest path are the same for this particular geometry.

4.5.2 Example: completely filled facility

The second test consists of the simulation of the evacuation of the complete facility with 1000 pedestrians. The initial distribution is shown in Figure 4.9(b). A snapshot of the simulation after 60 seconds is shown in Figure 4.13. The results of the jamming time and the evacuation time are summarised in Figure 4.14(a) and Figure 4.14(b) respectively. There is not much difference between the mean values of the distributions as in the previous case. This is due to the highly congested situation. There is no such "quickest path" in this case and most of the pedestrians just have to follow the flow. Those results are confirmed by the time in jam distribution. The total jam size distribution is taken from Figure 4.14(c). The mean jam sizes are 46 m^2 for the static and 40 m^2 for the dynamic strategies.

4.5.3 Example: broken route

In the third simulation scenario, the response of the system to a disturbance is simulated. The exits E2 and E8 (see Figure 4.9(a)) are broken and cannot longer be used. The initial

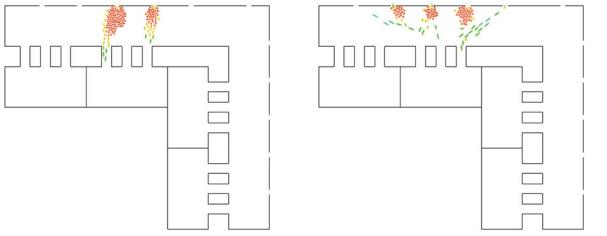

(a) Local shortest path

(b) Local shortest with quickest path

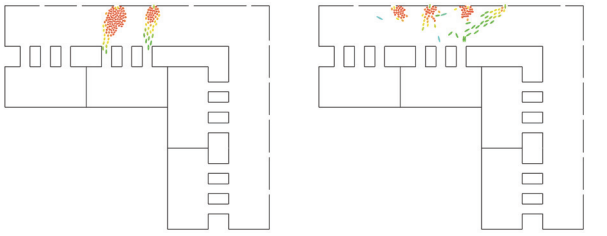

(c) Global shortest path

(d) Global shortest with quickest path

Figure 4.10: Dynamics of the system after 60 seconds for the initial distribution in Figure 4.9(a). Congestion areas appear red.

distribution is given in Figure 4.9(b). The results of evacuation time and time in jam are presented in Figure 4.15(a) and Figure 4.15(b) respectively. There is now an asymmetry in the escape route scheme and this is reproduced by the modelling approach. The quickest path leads to a faster evacuation and to less time in jam. This behaviour is also the expected one as pedestrians are still able to find the quickest path to escape from the building. The total jam size distribution is taken from Figure 4.15(c). All mean values are lower than the previous case without disturbance.

4.6 Sensitivity Analysis

This section presents a sensitivity analysis of the different parameters of the route choice model. The influence of the gain threshold for the scenario defined in Figure 4.5(d) is presented in Figure 4.16. If the gain threshold is taken large enough (1.0 for instance), pedestrians will hardly change their current destinations to switch to a fastest route. The quickest path in this case is reduced to the conventional global or local shortest path. A small gain threshold (0.0 for instance) will make the pedestrians to always take the fastest route, even if it is only 2 seconds faster than the current one. This is rather an unrealistic behaviour. Moreover, it implies that each alternative route is bounded with zero effort, which is also not the case. This is related to the fact that the quickest route is not necessarily the shortest one, so the pedestrians may have

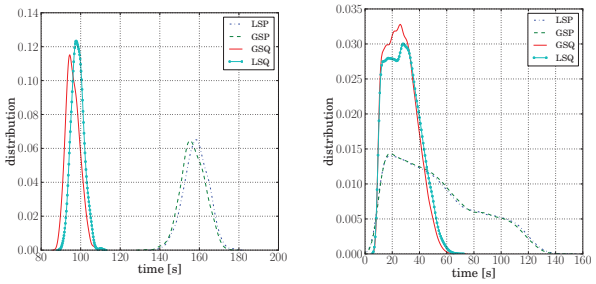

(a) Evacuation time distribution (b) Jam time distribution

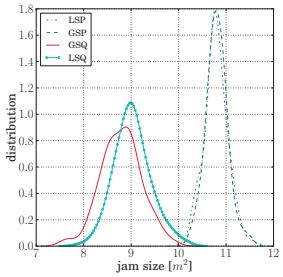

(c) Jam size distribution

Figure 4.11: Evacuation time and time in jam distribution for 250 pedestrians after 1000 runs. The initial positions are presented in Figure 4.9(a).

to walk a longer distance, which in synonymous to more energy investment. With increasing gain threshold the evacuation times are also increased and the distributions are shifted to the right. There are only minor differences in the evacuation time distribution in the threshold ranges [0.1, 0.3] and [0.4, 0.5]. The differences however appear in the dynamics of the egress process, where more or less pedestrians keep switching their routes.

For other parameters, the observation time for instance, a plausibility consideration has to be taken into account. To our knowledge, no empirical data are available so far for such special situations, where people observe their environment before making any decision. This seems however to be a normal process. Small changes of the observation time values have no large influences on the quantitative results i.e. the evacuation times. They do influence the qualitative simulation, where people for instance come out of a room and after 2 seconds choose a different destination. This phenomenon is also observed in supermarkets for example, when people have to choose between many queues. An observation time is always needed to analyse the processing speed of the different queues before making the final choice. We assume that the values chosen here reflect this behaviour. Another possibility could have been to keep the observation time values large enough and to allow the pedestrians to stop for a moment and literally observe the situation. This is unfortunately at the moment not supported by the

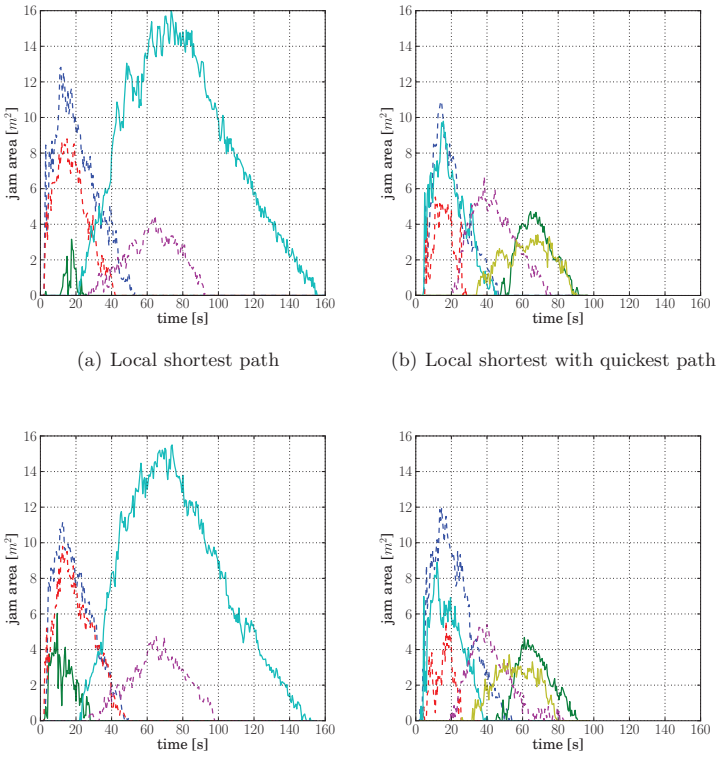

(a) Local shortest path

(b) Local shortest with quickest path

(c) Global shortest path

(d) Global shortest with quickest path

Figure 4.12: Jam size evolution for 250 pedestrians at different exits for the initial distribution in Figure 4.9(a). The colours correspond to the different exits. Exits without congestions have been left out of the plots. In (b) and (d), there are more but short-lived jams than in (a) and (c).

underlying pedestrian model at the operational level.

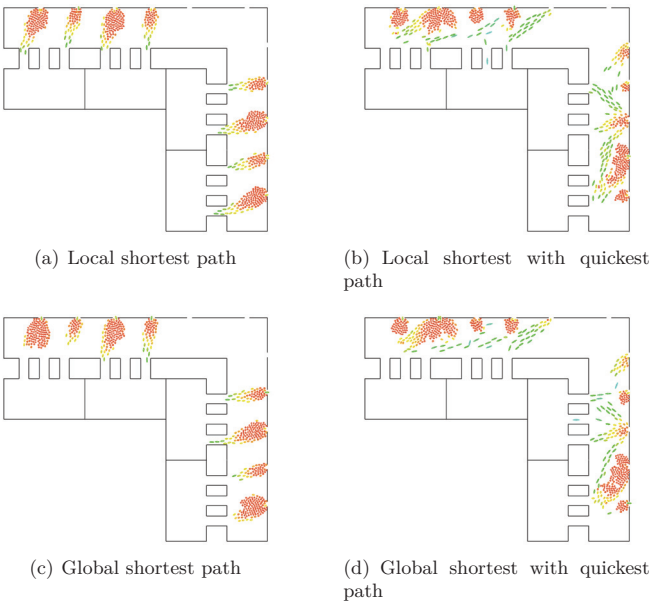

(a) Local shortest path

(b) Local shortest with quickest path

(c) Global shortest path

(d) Global shortest with quickest path

Figure 4.13: Dynamics of the system after 60 seconds for the initial distribution in Figure 4.9(b). Congestions areas appear red.

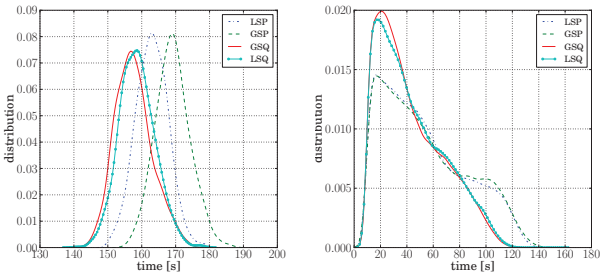

(a) Evacuation time distribution

(b) Jam time distribution

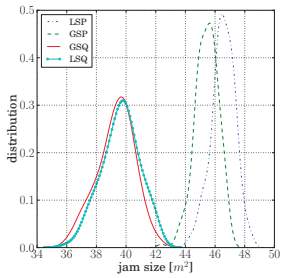

(c) Jam size distribution

Figure 4.14: Evacuation time, time in jam and jam size distribution for 1000 pedestrians. The initial positions are presented in Figure 4.9(b).

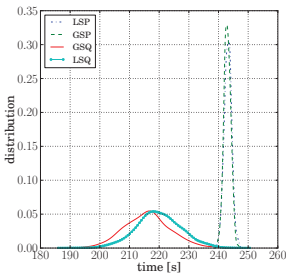

(a) Evacuation time distribution

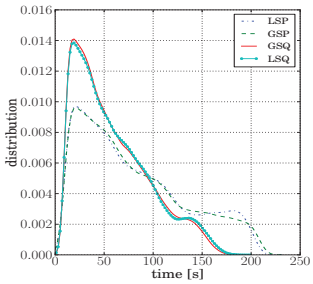

(b) Jam time distribution

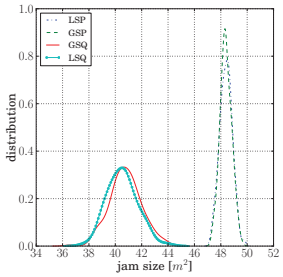

(c) Jam size distribution

Figure 4.15: Evacuation time and time in jam distribution for 1000 pedestrians after a system disturbance. The exits E2 and E8 have been closed (broken escape route). The initial positions are presented in Figure 4.9(b).

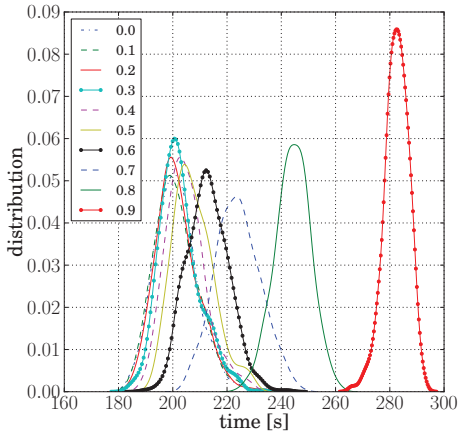

Figure 4.16: Gain variation for the scenario presented in Figure 4.5(d) using the GSQ.

4.7 Summary

This chapter presented four strategies to model the route choice of pedestrians in a combination of shortest and quickest paths. The quickest path approach, which is based on the observation of the environment, is not sensitive to initial distribution of pedestrians or special topologies like symmetric exits, making it quite general. In addition, criteria to assess the criticality of an evacuation simulation process have been elaborated. We investigated the evacuation time distribution, the time in jam distribution and the average jam size of pedestrians during an evacuation process. The approaches have been tested on different scenarios with different complexities involving symmetric, asymmetric or even broken escape routes. Faster evacuations, reduced times in jams and a plausible dynamics in the evacuation simulation have been achieved. The jam area has been expressed as a function of the time using the specific flow. The psychological preferences of pedestrians with regards to different routes were not analysed here due to the lack of any experimental data. Nevertheless, the obtained results can be used as a measure for the criticality of an evacuation process. In our modelling approach based on visibility, we did not consider other factors that could limit the view of pedestrians, for instance eyes condition or lighting. The visibility was solely limited by the crowd and the geometry. For an open air simulation in a very large complex, it might be necessary to limit the sight range of the pedestrians, or at least to scale it down. Another point, which was not considered in our modelling approach, is the anticipation of other pedestrians' decisions, resulting in a possible anticipation of jams. At the beginning of the simulation, each pedestrian assumes to have taken the best choice. The quality of this choice however obviously depends on how many other pedestrians made the same choice. This can be solved using approaches from the field of game theory. Overall, the exit choosing behaviour of pedestrians under different scenarios has been well reproduced by the model.

Chapter 5

Navigation Graph

We discussed in Chapter 4 routing strategies in a complex structure. The strategies are based on a navigation graph. The graph is generated based on the inter-visibility of the exits. This method assumes that the building has been decomposed in basic structures like rooms and corridors with no obstacles. It is not always possible to (automatically) achieve such decompositions and it can be very cumbersome for structures like the one given in Figure 5.5. In that case, other methods are used. In this chapter, the importance of navigation graphs for force based models is explained and some methods for generating such graphs on a complex structure are presented.

5.1 Problem Statement

Let's consider the simulation scenario given in Figure 5.1. The pedestrian can see the target through the glass wall. The problem statement is how to choose the direction of the desired velocity $\vec{v_0}$ (see Equation 2.2) in such a way that the pedestrian reaches the target while realistically avoiding obstacles (walls in this case).

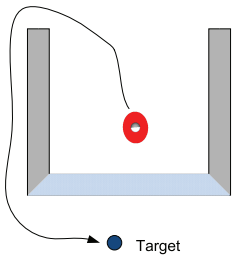

Figure 5.1: problem statement of force based models when there is no direct connection between the actual position and the target.

A possible path is sketched on the figure. In order to achieve such a navigation path, intermediate destinations usually have to be inserted or computed between the actual position of the pedestrian and the target. This modelling step belongs to the tactical level in the pedestrian modelling framework presented in Figure 2.1.

5.2 Visibility graph for navigation

The idea of navigation graph is to construct a (hopefully) minimal graph, where the vertices are the possible destinations and the edges represent the visibility between these destinations. The graph representation is $G := (V, E)$ with V vertices and $E \subseteq V \times V$ edges (see [117] for further details about graphs). This navigation graph is usually a visibility graph [9, 91] which is a common approach in the field of robotics used for autonomous robots navigation [8]. We discuss three approaches for generating such graphs. The first step in this process consists of creating the vertices of the graphs. They are usually derived from the polygonal obstacles. A visibility graph is generated in a second step.

Molnar's approach

Route choice as described by Molnár [36] is done on a simple weighted graph G with V vertices and E edges. The vertices represent the different destinations points on the geometry and the edges represent the visibility between any two of these destinations. The geometry is first decomposed into simple structures like rooms and corridors. The graph is weighted by the Euclidean distances between the vertices. A sample decomposition taken from [36] is shown in Figure 5.2. Using this representation, sharp turns can be observed at 90 degree bends, which lead to unrealistic patterns in simulations. By low density for instance, pedestrians walk parallel to corridors and right after passing the target line, make a sharp turn to the next target line. Artificial congestions are observed at high densities. A smoothing algorithm to damp these effects is presented in Section 5.5.

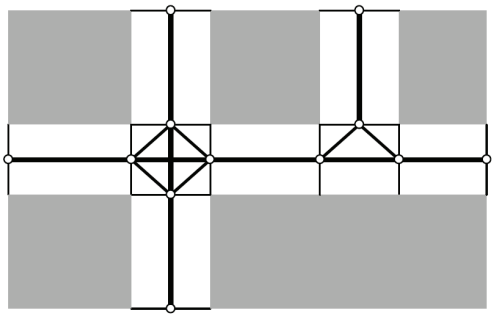

Figure 5.2: Decomposition of domain by Molnár in basic structures for navigation [36].

Stucki's approach

Stucki [118] used a similar approach than Molnár but generalised the approach. The structure

is decomposed in polygons and the vertices of the visibility graph are derived from the polygons vertices. A minimal distance d is kept to the vertices. An example taken from [118] is shown in Figure 5.3. The left side of the figure shows the complete visibility graph. The right side shows the graph that is used to reach a certain destination point. It emerges from a reduction of the initial graph (on the left). Graphs can be automatically generated for arbitrary sets of polygons by using this procedure.

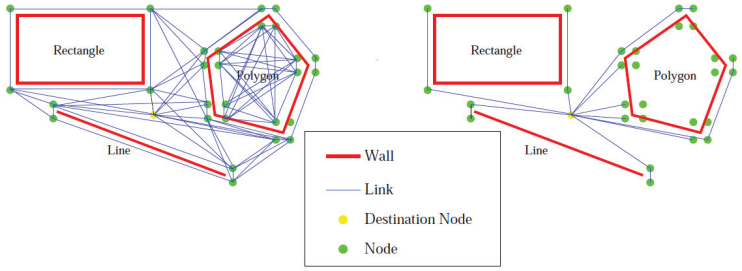

Figure 5.3: Visibility graph as generated by Stucki for navigation [118].

Höcker's approach A*

Höcker [90] proposed a method based on Molnár and Stucki approach to automatically generate a visibility graph for navigation. He uses a heuristic A^* method introduced by [103] enhanced with a reduction algorithm to compute the visibility graph from a building represented by a set of polygons. An example generated by his algorithm is presented in Figure 5.4. The complete graph is presented in the left hand side of the figure. The right hand side shows a reduced graph with a smaller number of edges used for navigation.

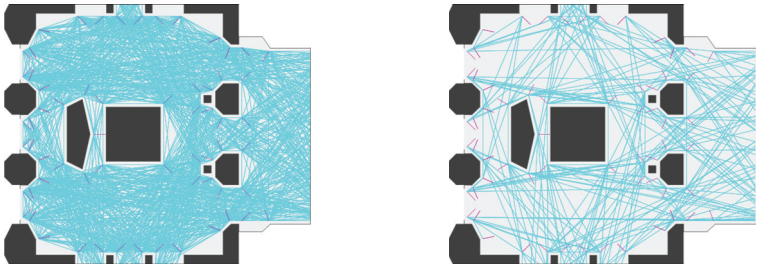

Figure 5.4: Visibility graph for navigation as generated by Höcker [90]. The graph on the left is without a reduction whereas the graph on the right has been reduced.

Other algorithms for generating a (reduced) visibility graph from a graph $G := (V, E)$ are given by Lee [119], Overmars [95], Welzl [120], Ghosh and Mount [121]. Concerning the complexity, Kitzinger [122] has shown that the Ghosh and Mount's algorithm (which is based on triangulation) outperforms by implementing, tuning and testing the algorithms on several geometry configurations. Following complexity were obtained: $\mathcal{O}(n^3)$ for a naive implementation, $\mathcal{O}(n^2 \log n)$ for Lee, $\mathcal{O}(n^2)$ for Overmars/Welzl and $\mathcal{O}(|e| + n \log n)$ for Ghosh/Mount, $|e|$ being the number of edges in the visibility graph.

5.3 Tribune Area

An example of a complex structure is given in Figure 5.5. This is part of a tribune from a stadium. The green strip shows a sample place that can be occupied by pedestrians. The arrows give the main flow directions to the exits when leaving the structure. The navigation task consists of choosing the direction of the desired velocity $\vec{v}_0$ so that a realistic motion from any sitting range to the outside is made. This is achieved by inserting navigation lines as presented in Figure 5.6. Two possible paths for two pedestrians using the navigation lines are sketched on the figures. The direction of the desired velocity $\vec{v}_0$ is orthogonal to the target navigation line. If the orthogonal projection is outside the line segment, the nearest point is chosen. The process could not be automated, as the orientations of the lines are different and independent from each other's. Also, the geometry shows a considerable amount of polygons. There are two types of lines. A room must be envisioned as a set of virtual sub-rooms. The main purpose of this subdivision is to allow an initial flexible distribution of the pedestrians before a simulation. The red navigation lines mark the limits between the sub-rooms. The green navigation lines are allowed within a sub-room. A combination of both types of lines allows a smooth navigation and preserves a good structure. The Algorithm 5.1 is also used for this purpose. After the lines are positioned Dijkstra or Floyd-Warshall are used to find the optimal path (shortest path) to the outside. The quickest path approach presented in the aforementioned chapter is applied on this graph. The result is a uniformly directed flow as observed in a stadium clearing at end of the events.

5.4 Promenade Area

The promenade is presented in Figure 5.7. The process of generating the navigation lines is the same as explained in the previous section. All possible destinations can be reached by using the lines. A sample path from the tribune area to the outside is sketched on the figure.

5.5 Smoothing Sharp Turns

One issue caused by the direction of the desired velocity is shown in Figure 5.8. The red and the green pedestrians are in the transition between a sitting range and the stairs leading to an exit. For both pedestrians the next target line is at the bottom. However, because of the repulsive forces from other pedestrians and especially from the obstacles (sitting range), the red pedestrian is stuck. This can be for instance mitigated by scaling down the strength of the repulsive forces at the costs of more overlaps and oscillations.

In order to achieve realistic motion at sharp bends (90° for instance) more navigation lines

Figure 5.5: Original CAD drawing of a section of the tribune. The green strip is a sample of a sitting row. The arrows give the main flow direction when leaving the area.

can be added. In [123] this method is applied on 90° and 180° bends. Another approach is to use a smoothing technique as depicted in Figure 5.9. The functioning for this technique is presented in Algorithm 5.1. This method also facilitates pedestrians sorting from the sitting row to the connected stairs when simulation high density in the tribune area. This solution however is tailored to the geometry of the arena and to the application of the evacuation assistant. Further investigations are needed to generalize the concept.

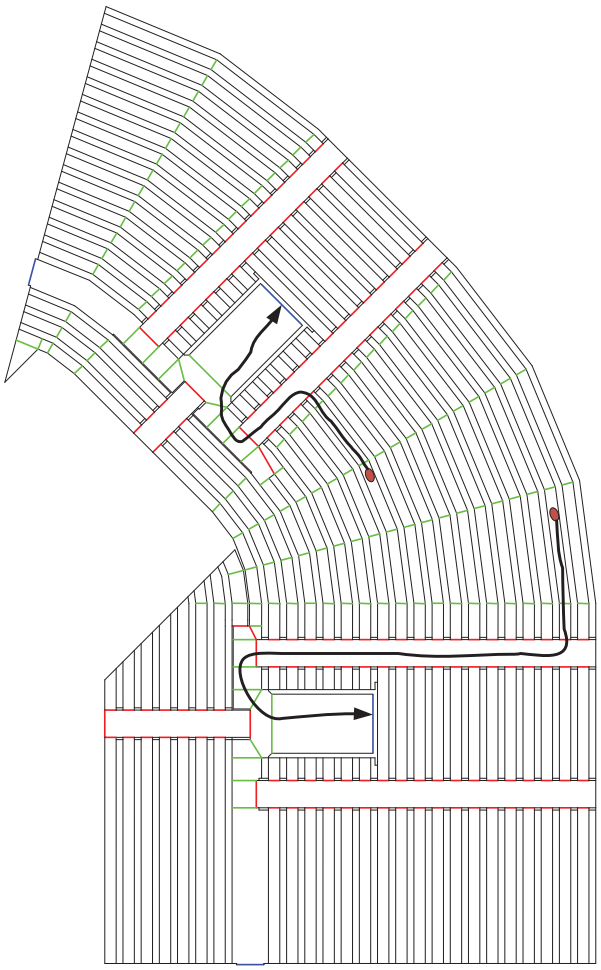

Figure 5.6: Original CAD drawing of the section HRI070 of the tribune with navigation lines in red and green colours. The blue lines are exits. Two possible paths using the navigation lines are sketched.

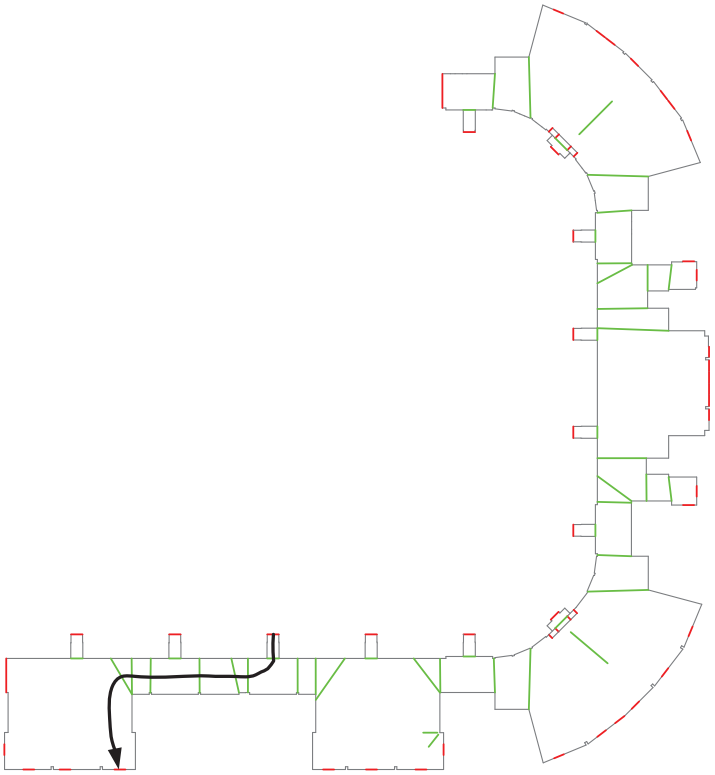

Figure 5.7: Original CAD drawing of the promenade with navigation lines in red and green colours. The red lines are exits. A possible path from the tribune to the outside using the navigation line is sketched.

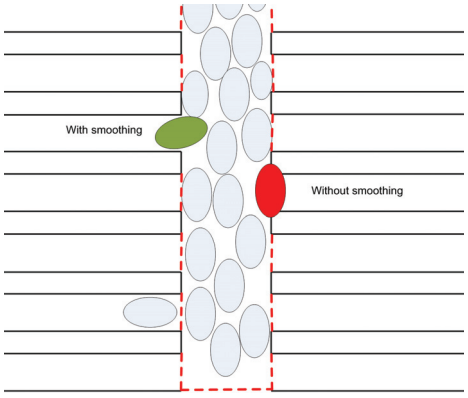

Figure 5.8: Smoothing process in the tribune.

Algorithm 5.1 Smoothing process at sharp turns

$smoothing\_duration \leftarrow 2$
$smoothing\_grad \leftarrow 15$
$drift\_velocity\_max \leftarrow 0.9$ {m/s}
$smoothing\_steps \leftarrow smoothing\_duration / simulation\_step\_size$

$\alpha_{min} \leftarrow 60$ {degree}
$\alpha \leftarrow \angle < \vec{V}_0^{old}, \vec{V}_0^{new} >$
if $\alpha \leq \alpha_{min}$ **then**
  END
end if

$\vec{V}_0^{new} \leftarrow \vec{V}_0^{old}$
$\alpha_i \leftarrow \alpha / smoothing\_grad$
while $k \leq smoothing\_grad$ **do**
  $v_{new} \leftarrow$ current pedestrian's velocity
  if $v_{new} \geq drift\_velocity\_max$ **then**
    END
  end if
  $\vec{V}_0^{new} \leftarrow \vec{V}_0^{new}$ rotated by α_i
  $k \leftarrow k + 1$
  Next Simulation step
end while

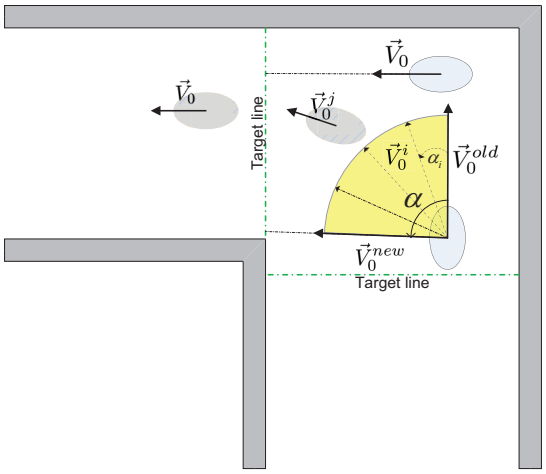

Figure 5.9: Smoothing sharp turns in a 90° bend. The direction of the desired velocity $\vec{V}_0$ is adjusted using the Algorithm 5.1.

Chapter 6

Empirical Study of Pedestrians' Route Choice

This chapter presents an empirical analysis of pedestrians' route choice in a complex facility. The study has been done within the framework of the real-time evacuation assistant described in Chapter 1. The investigated facility is part of the promenade of the ESPRIT arena in Düsseldorf, Germany. The route choice data are obtained from an automatic person counting system consisting of cameras. The cameras are distributed at all main entrances and passages of the promenade and tribune. The collected data are presented in terms of frequencies, i.e. the number of persons passing a counting line or exit per minute in the direction "in" and "out" of a section. The sectioning is the same as adopted for the parallelisation presented in Chapter 3. Using that information, the proportional usages of the different exits of the promenade are calculated. The results for different football games and concert performances are presented and analysed in this chapter. We focus on a football game played on the 4^{th} November 2011 with a more detailed analysis. The modelling approach introduced in Chapter 4 is validated against the empirical results obtained wherein some restrictions must be considered. We need to distinguish between a routine clearing of the arena and an emergency clearing. Only an emergency clearing is modelled in this case. This has two major impacts: first all pedestrians are directly going outside without any intermediate destinations that will make their path longer. In a normal clearing (at the end of an event for instance), they may have a preferred destination, the parking lots for instance. The second impact is that the pedestrians will choose the quickest path to reach the outside. We have only simulated an emergency clearing and will then set the comparison focus on the exit usages instead of the route choice patterns inside the investigated area.

6.1 Introduction

In order to calibrate and later validate models, empirical data are needed. In the field of pedestrian dynamics (and especially for route choice), there are three main sources of data. The first source is surveys. The issue with this method is usually the size of samples obtained and their representativeness. Besides, many types of information cannot be captured by surveys and information always has to be acquired afterwards. These can be the criteria influencing the choice of a particular route asked at the end of the trip. The interrogated person might not be able to give accurate responses or to remember all details. The second source is controlled indoor/outdoor experiments. Several indoor experiments were performed in the framework of the Hermes project. The results obtained from such experiments are not always directly applicable to real life situation, because they are controlled. It is likely that people behave differently under laboratory conditions. In addition, extreme cases might not be reproduced for ethical or safety reasons. Nevertheless, only under well controlled laboratory conditions, some features can be analysed without endangering the crowd, for instance the emergence of critical states by high densities. Another reason speaking in favour of controlled experiments is that the study can be focussed on the influences of a particular parameter. For example, the flow through exits of different widths can be studied without worrying on the influences other external parameters like the individual motivations. Also, different configurations of scenarios are easily performed. The third source is observations from real life scenarios. In comparison to experiments, many factors are needed to fully understand the observations, for instance the motivation of the individual pedestrians. Independently of the source of data (surveys, experiments, observations), the information has to be extracted. For surveys, participants may be asked to draw their trip on a map. For experiments and observations video surveillance are often used. Other alternatives include the tracking of digital gadgets like cell phones or GSM (Global System for Mobile Communications) log files [124] or Bluetooth devices [125, 126]. While accurate data can be obtained, the number of sample depends on the number of devices present in the investigated areas. The technique used here for collecting data is based on video surveillance.

In this chapter, we are interested in indoor empirical data. There are two main categories of events that are held in the arena: football games and concert performances. The differences can be summarised in two points. The events feature different types of visitors. Visitors for concerts are usually first/one time visitors. The contrary can be assumed for football game visitors. The number of season tickets provides a proof to this assumption. The second point is the occupancy of the stadium. For concerts people are allowed in the field and the entrances and exits configurations are different and are subjected to continuous changes. In a first step only one football game has been analysed. Although the promenade and the tribune areas are entirely covered by the cameras, we only investigate the promenade area. The motivation is that the promenade serves as distributor for the tribune and actually shows the most interesting route choice patterns. We analyse both types of events which took place between the 18^{th} July

and the 4^{th} November 2011 in the arena.

6.2 Automatic Person Counting System

6.2.1 Cameras position

The distribution of the cameras at main entrances, exits and passages leads to a logical partitioning of the promenade area in 5 sections, which are mapped to the detection areas of the automatic people counting system. The counting system consists of 45 mono and 51 stereo cameras installed in the tribune and the promenade. Each camera is merely responsible for one exit, which means that at each time the information (in this case the number) about the pedestrians passing through that exit is available. Also, the passing direction for each exit is identified, making it possible to calculate the number of pedestrians inside a specific section. Throughout this chapter, we will be referring to promenade as a combination of the five sections. The position of 52 cameras in the promenade is presented in Figure 6.1. They are represented with green filled circles.

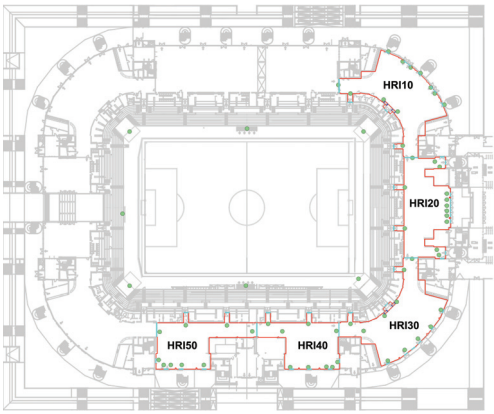

Figure 6.1: Position of the cameras in the investigated part of the promenade of the arena. The cameras are represented with green filled circles.

6.2.2 Site location

The promenade has five sections totalling $\approx 5200\ m^2$ with a maximal allowed capacity of $\approx$ 10350 persons. The gates connecting the promenade and the tribune area have a width of 2.5 m and a length of 5 m. The connections between the sections have a width of 7.4 m. The exits to the outside have a width of 2.4 m. The geographical situation of the promenade is shown in Figure 6.2. The location of the parking lots and the train station are marked. This information is needed to correctly interpret the route choice patterns obtained.

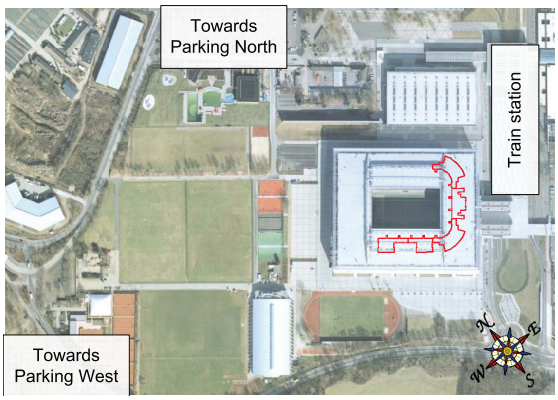

Figure 6.2: Geographical location of the promenade (image made with Google Earth™, Feb. 2012). The direction to the parking places and the train station are marked.

6.2.3 Tracking data

The cameras are all connected to a server in a local area network. The server collects and aggregates the data in real-time and makes them available through web services. The data are presented in terms of frequencies, i.e. the number of persons passing the corresponding counting line or exit per minute in the direction "in" and "out" of a section. Using that information, the proportional usages of the different exits of the promenade are calculated. In order to comply with privacy regulations, no images are stored by the system, only counting values. Data have been collected for various football matches and concerts and are presented in the next sections.

6.3 Case Study: Football Event

The following data are obtained from the automatic person counting system on the 04. November 2011 during a football match in the arena opposing Fortuna Düsseldorf and Dynamo Dresden, two teams of the 2^{nd} division of the German *Bundesliga*. A first look at the data as given by the system is presented in Figure 6.4. The data are recorded at the beginning of the event between 16:00 and 18:00. Figure 6.4(a) shows the number of spectators entering the section and Figure 6.4(b) the number of spectators leaving the section during the same period. A naive approach to determine the occupancy of the section would be to sum up the data from each door. For this particular section, the amount of pedestrians entering would be ≈ 13664 and the amount of pedestrian leaving would be ≈ 13502. However, a closer look at Figure 6.4(a) reveals that ≈ 907 spectators are coming from the tribune. This makes sense since many spectators first go to their seats and then come out again for buying some articles and food or going to the toilets for instance. The same applies for spectators leaving the

section at the beginning. Some walk out for smoking and then come in again. The resulting effects are the bi-directional flows observed at the exits.

6.3.1 Data filtering process

The unwanted effects (bidirectional flows e.g.) are mitigated by applying a two stages filtering process. In a first stage, the event running is divided in different phases. In a second stage, the bidirectional flows observed are removed by using a simplified model of a section as presented in Figure 6.3. In this model only the main flow directions are considered. The described filtering steps are required since a later comparison with a route choice model is envisaged and the model only considers a clearing scenario. In addition, we are only interested in this case study in the general pedestrians' profile, which can be resumed to entering the promenade and going to the tribune at the beginning and leaving the tribune, passing through the arena towards their cars or the train station. For the filtering process, it is logical to divide the event running in different phases corresponding to the different main flow directions. Following phases are considered:

- Phase I: entering the arena between 16:00 and 18:00
- Phase II: first Half between 18:00 and 18:45
- Phase III: half time break between 18:45 and 19:00
- Phase IV: second half between 19:00 and 19:45
- Phase V: leaving the arena between 19:45 and 20:30

The interesting sequences are the entering (Phase I) and the leaving (Phase V) of the promenade at the beginning and the end of the event. The pedestrian flow at the beginning of the event is given in Figure 6.3(a) and Figure 6.3(b). The sources for the occupancy of the section are the spectators coming from outside E and the spectators coming from other sections P_{12} and P_{11}. The sinks for the section are the spectators going to the tribune T and the spectators leaving to other sections P_{21} and P_{22}.

The contrary applies at the end of the event and the flow directions are inverted as presented in Figure 6.3(c) and Figure 6.3(d). The sources for the occupancy of the section are T pedestrians coming from the tribune together with the P_{11} and P_{12} spectators coming from other sections. The sinks for the section are the spectators going outside E and the spectators leaving to other sections P_{21} and P_{22}.

Let's assume the following values for a section S for an observation period Δt as provided by the counting system:

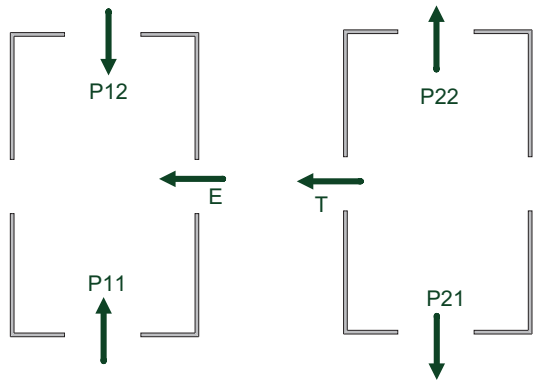

(a) Entering the section at the begin (b) Leaving the section at the begin

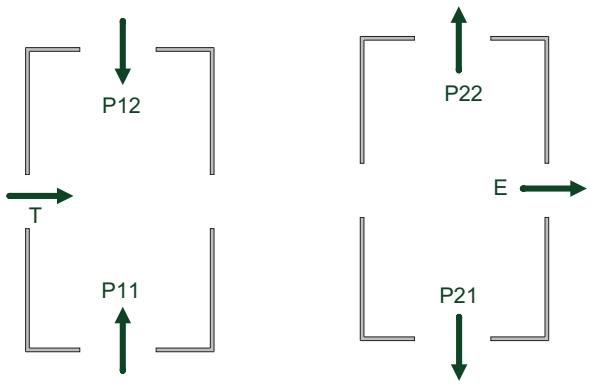

(c) Entering the section at the end (d) Leaving the section at the end

Figure 6.3: Model of a section of the promenade showing the pedestrian flow during a football event.

- E_1: the number of pedestrians coming from the outside and entering the section S.
- E_2: the number of pedestrians leaving the section S and going to the outside.
- T_1: the number of pedestrians coming from the tribune and entering the section S.
- T_2: the number of pedestrians leaving the section S and going to the tribune.
- $P_{11,12}$: the number of pedestrians entering the section S and coming from other sections.
- $P_{21,22}$: the number of pedestrians leaving the section S and going to other sections.

then the following effective values are derived for the section S during the period Δt:

- $E = E_1 - E_2$: the effective number of pedestrians coming from the outside.
- $T = T_1 - T_2$: the effective number of pedestrians entering the tribune.
- $P_{in} = P_{11} + P_{12}$: the effective number of pedestrians entering the section and coming from other sections.
- $P_{out} = P_{21} + P_{22}$: the effective number of pedestrians leaving the section and going to other sections.

At the beginning of the event, valid sources for the occupancy of the section S are E and P_{in}. The redundant data given by T_1 and E_2 are automatically eliminated by the subtraction. This is straightforward since for accessing the tribune area one first has to pass through the promenade, it means that those spectators are both accounted in T_1 and T_2 n-times they crossed the section. Thus, by subtracting both values from each other, they are accounted only once and the redundant data are eliminated. The same applies for spectators leaving the section for a small round outside. The sinks are T and P_{out}. These results are summarised by the flow given in Equation 6.1.

$$\begin{aligned} \Phi_{in}(\Delta t) &= E + P_{in} \\ \Phi_{out}(\Delta t) &= T + P_{out} \end{aligned} \tag{6.1}$$

The contrary applies at the end of the event. The valid sources are T and P_{in} and the valid sinks are P_{out} and E. The results are summarised in Equation 6.2.

$$\begin{aligned} \Phi_{in}(\Delta t) &= -T + P_{in} \\ \Phi_{out}(\Delta t) &= -E + P_{out} \end{aligned} \tag{6.2}$$

For both cases, we assume the approximative occupancy given in Equation 6.3. In an ideal case $\Phi_{in} = \Phi_{out}$. This is rather infeasible in this case since not all estimations take into account the initial occupancy of the section before the observation time. This is not necessarily zero. In addition, the accuracy of the counting system has to be accounted. Nevertheless, valid qualitative statements can be made with the defined value of Φ.

$$\Phi(\Delta t) \approx \frac{\Phi_{in}(\Delta t) + \Phi_{out}(\Delta t)}{2} \tag{6.3}$$

6.3.2 Section HRI020 of the promenade

Since this is the section connected to the train station (see Figure 6.2), we are awaiting the most traffic here at the beginning and the end of the football game. Observations also let

suppose that most of the spectators use the train station to access the arena.

6.3.2.1 Phase I: arrival

Figure 6.4 shows the exits usage by the pedestrians passing through the section HRI20 before the beginning of the game. The fill level of the bars shows the percentages usage of the corresponding exits. There is a bidirectional flow as expected, but the main flow direction is clear:

$$E = 6717 - 1035 = 5682$$
$$T = 2844 - 907 = 1937$$
$$P_{in} = 5160, P_{out} = 9623$$
$$\Phi = 11641$$

We can infer from the presented data that $\approx$ 11641 spectators entered the arena through this section. $\approx$ 16% of the spectators present in this section go in the tribune area directly connected to this section. The other $\approx$ 84% spectators are just transiting to other sections, the main flow direction being to the section HRI010. If we have a look at the individual exit usage, we note that 2 of the 6 exits at the main entrances show little to no usage at all (63 plus 3 pedestrians going in, 5 plus 4 pedestrians going out). One explanation for this little usage is that the doors must have been closed (but not locked) during that time, thus not inviting whereas the other doors were wide open.

6.3.2.2 Phase V: departure

Following values are recorded at the end of the events: $E = 3844$, $P_{in} = 4857$, $P_{out} = 2803$, $T = 1765$ and $\Phi = 6635$. The results are graphically displayed in Figure 6.5. Approximately 60% of the spectators used the main exits in this section to leave the arena, whereas 40% are transiting to other sections. The values do not take into account the initial occupancy of the section before 19:45. The individual main exits show similar usage.

This evenly use of the exit is correlated to the density during that leaving period. In contrast to the arriving period (which lasts 2 hours), the leaving period is effectively only 15 minutes. The density resp. jam at the exits are correspondingly higher. The relative low usage of the 4 side exits is due to their unfavourable location. Also, this section is less frequented at the end than at the beginning of the event (11200 compared to 6635).

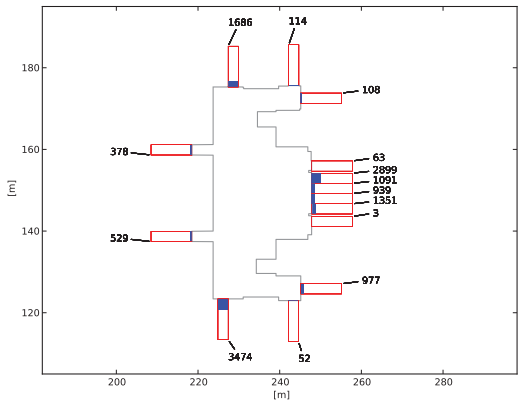

(a) Entering the section

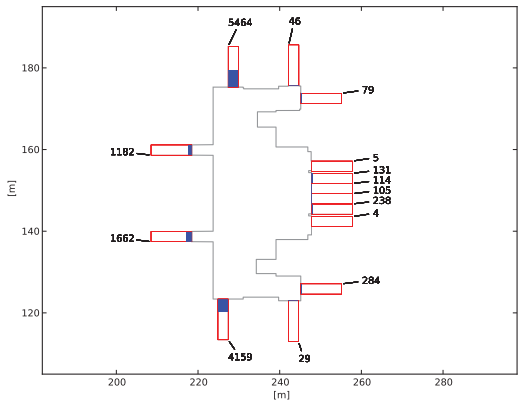

(b) Leaving the section

Figure 6.4: Pedestrians' profiles passing through the section HRI20 before the beginning of the game.

6.3.3 Section HRI030 of the promenade

6.3.3.1 Phase I: arrival

Figure 6.6 shows the accumulated values given by the counting system at the beginning of the event for the section HRI030. We have the following values: $E = 3979 - 2789 = 1190$, $P_{in} = 3620$, $P_{out} = 6323$, $T = 3260 - 894 = 2366$ and $\Phi = 8509$. It comes out that 27 % of the spectators in this section went into the tribune and for 73 % it was used to access other sections.

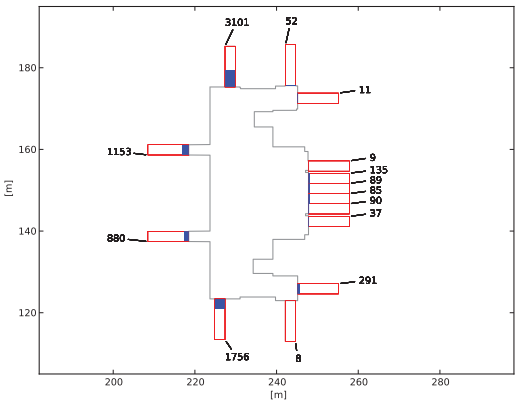

(a) Entering the section

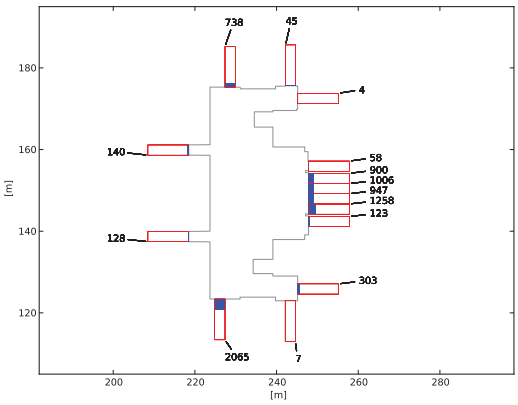

(b) Leaving the section

Figure 6.5: Pedestrians' profiles passing through the section HRI20 at the end of the game.

6.3.3.2 Phase V: departure

Following values are recorded at the end of the event for the section HRI030: $E = 4437-1143 = 3294$, $P_{in} = 3808$, $P_{out} = 3158$, $T = 2317 - 372 = 1945$ and $\Phi = 6102$. The graphical representation of the exit usage is given in Figure 6.7. In comparison to the status at the beginning, relatively more spectators go directly from this section to the outside without first transferring to the main exits in section HRI020. 3294 spectators ($\approx 54\%$ of the total who used this section) use this section reach outside, whereas only 1190 spectators used the section to enter the arena.

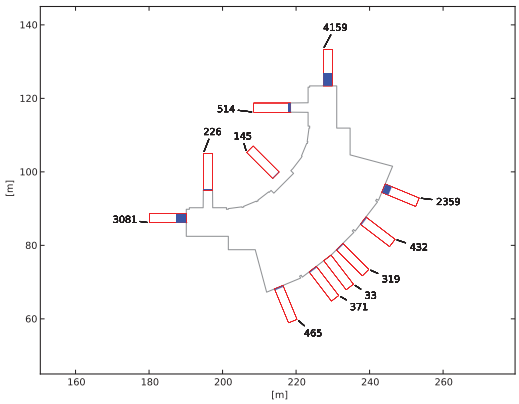

(a) Entering the section

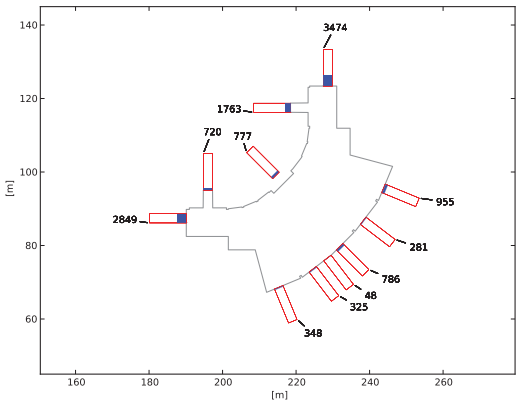

(b) Leaving the section

Figure 6.6: Pedestrians' profiles passing through the section HRI30 before the beginning of the game.

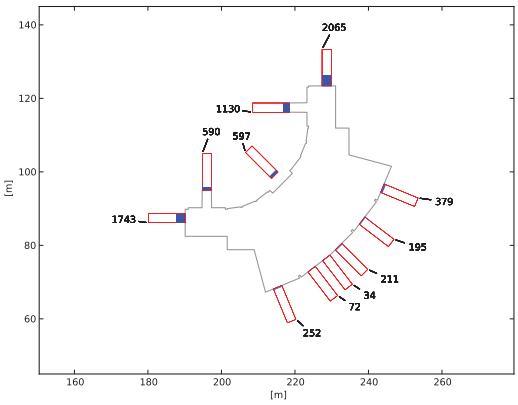

(a) Entering the section

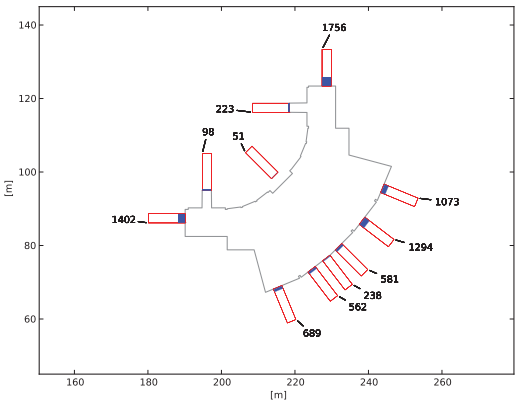

(b) Leaving the section

Figure 6.7: Pedestrians' profiles passing through the section HRI30 at the end of the game.

6.3.4 Section HRI050 of the promenade

6.3.4.1 Phase I: arrival

This section is the most close to the parking West (see Figure 6.2). Following values are recorded at the beginning of the game:

$$E = 906 - 858 = 48$$
$$T = 922 - 310 = 612$$
$$P_{in} = 4745, P_{out} = 4419$$
$$\Phi = 4912$$

The individual percentage usage of the exits is retrieved from Figure 6.8. This section shows the lowest traffic. In fact during that game, the stadium was only partially filled and the west part of the tribune was not full. Also, almost no pedestrians ($E = 48$) came into the tribune from the outside through this section. This implies that the pedestrians having their seats in the tribune area connected to this section come either from the parking west side or from the section HRI040.

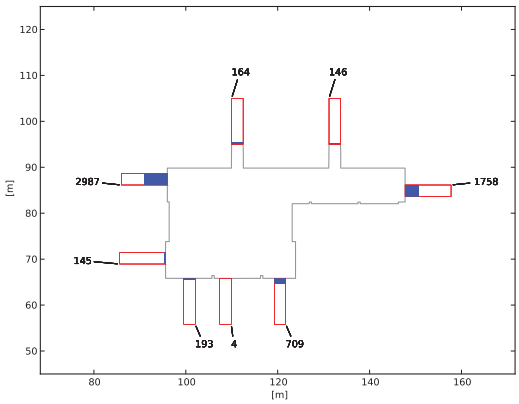

(a) Entering the section

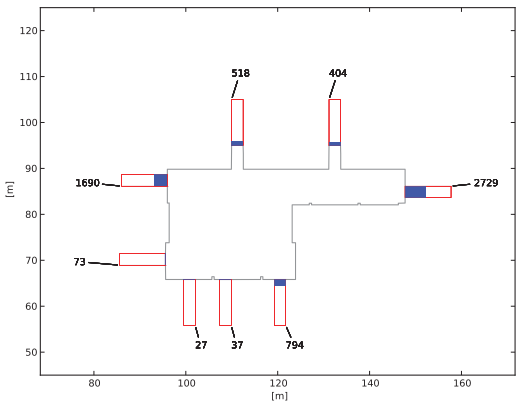

(b) Leaving the section

Figure 6.8: Pedestrians' profiles passing through the section HRI050 at the beginning of the game.

6.3.4.2 Phase V: departure

The recorded values at the end of the event for the section HRI050 are presented in Figure 6.9. The individual flow values are:

$$E = 1311 - 316 = 995$$
$$T = 782 - 189 = 593$$
$$P_{in} = 2280, P_{out} = 1987$$
$$\Phi = 2927$$

Similar to the data from the arrival phase, this section shows the lowest observed traffic for this event. Nevertheless, $E = 995$ spectators left the promenade through this section. This support the main idea that spectators first tend to go out at the end of the event and then find their way to the parking of the public transport stations.

6.3.5 Section HRI010 of the promenade

The behaviour of the spectators during the break has also been analysed for this section.

6.3.5.1 Phase I: arrival

Figure 6.10 shows the exits usage by the pedestrians passing through the section HR010 at the beginning of the game. 92.4 % of the spectators here are coming from other sections and $\approx 27\%$ of the spectators go directly to their seats in the tribune area directly connected to this section; the main direction being from the main entrances in the arena. There is also one particular strongly used exit. This is most likely because it is located near the main entrances. The flow values are:

$$E = 1643 - 1037 = 606$$
$$T = 3172 - 952 = 2220$$
$$P_{in} = 6510, P_{out} = 4766$$
$$\Phi = 8056$$

6.3.5.2 Phase III: half time break

There is little traffic during the break. The profiles are given in Figure 6.11. Approximately 177 spectators left the section to go outside the arena. By the beginning of the second half 168 spectators have returned. We should mention that the arena is a non-smoking area. This is an explanation for this number. Also, it can be inferred from the values of $T = 220$ that there are some spectators left in the section before the beginning of the second half. The number of

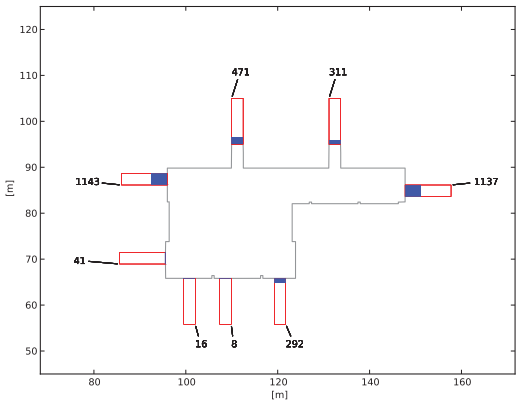

(a) Entering the section

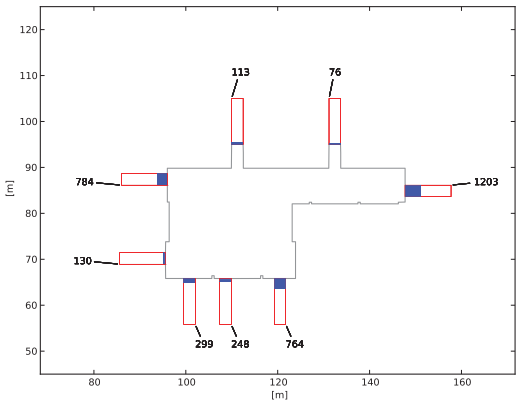

(b) Leaving the section

Figure 6.9: Pedestrians' profiles passing through the section HRI050 at the end of the game.

spectators coming from other sections and going to other sections is almost equal, which lets suppose that the spectators are not transiting to other sections but go into in the section and return to their seats places before the game is resumed. The recorded values during the break are:

$$E = 177 - 168 = 9$$
$$T = 922 - 702 = 220$$
$$P_{in} = 1025, P_{out} = 1066$$

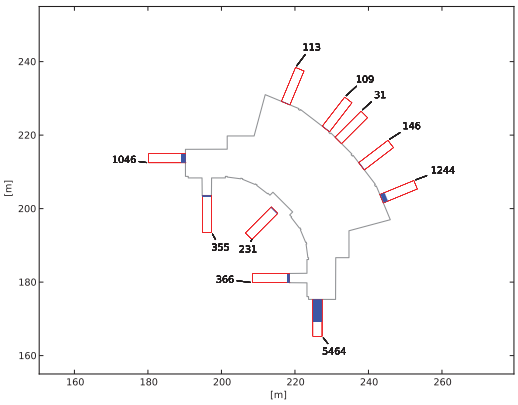

(a) Entering the section

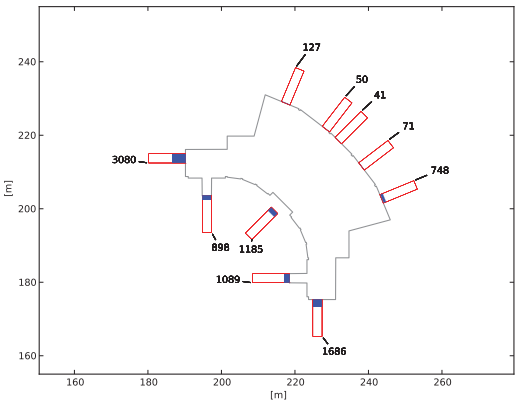

(b) Leaving the section

Figure 6.10: Pedestrians' profiles passing through the section HRI10 of the promenade before the beginning of the game.

6.3.5.3 Phase V: departure

At the end of the game, the obtained profiles are the opposite of the observations from the beginning. The results are summarised in Figure 6.12. The main flow direction is going out of the tribune and walking towards the main entrance. We should note at this point that there is also another possibility to leave this section by taking the elevator. Spectators taking the elevators are not counted. This may explain the discrepancies between the total number of

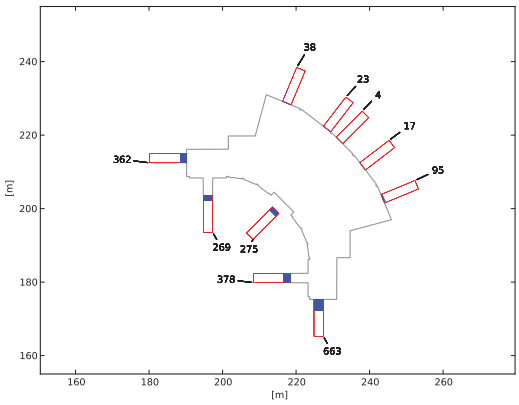

(a) Entering the section

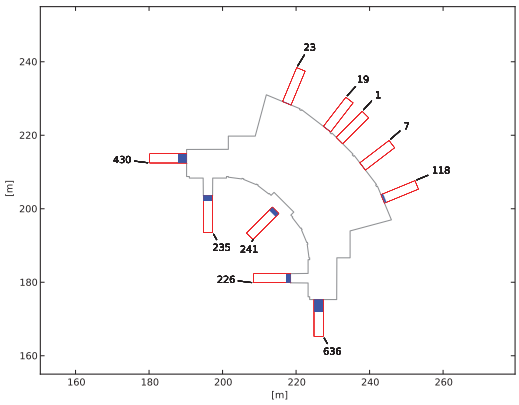

(b) Leaving the section

Figure 6.11: Pedestrians' profiles passing through the section HRI10 of the promenade during the half time break.

spectators entering the section and the total number leaving. The values are:

$$E = 1171 - 514 = 657$$
$$T = 2695 - 377 = 2318$$
$$P_{out} = 3789, P_{in} = 2750$$
$$\Phi = 4757$$

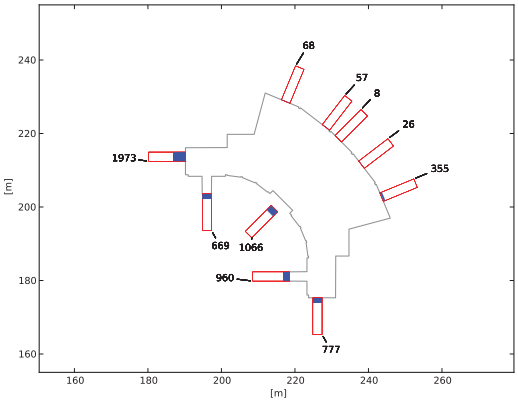

(a) Entering the section

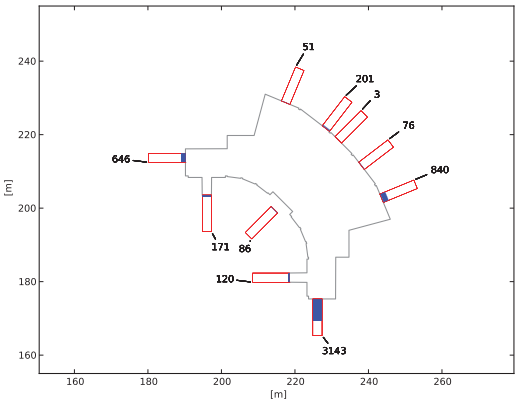

(b) Leaving the section

Figure 6.12: Pedestrians' profiles passing through the section HRI10 of the promenade at the end of the game.

6.3.6 Promenade area

6.3.6.1 Phase I: arrival

The profiles for entering the promenade before the beginning of the game are presented in Figure 6.13. Approximately 13,000 spectators have been registered by the counting system. The results are based upon the total occupancy of the promenade and do not take into consideration the different route choice options within the promenade itself. Also, we should mention here that this number is not the total number of spectators in the arena during that game, which was approximately 32,000 based on official sources. Under these considerations, it can be taken from the figure that more than the half of the spectators (58%) comes through the section HRI020 and distributes themselves into the other sections. They are using the train station to access the arena. HRI020 is directly connected to the train station and is also the main entrance to the arena. 15 % are coming from the direction parking West and 9.7 % are coming from the direction parking North. The values should be considered as lowest boundaries. For instance, it is unclear whether the 10.8% entering through section HRI030 came by train, although this would be the most reasonable assumption to consider here. The distribution to the tribune areas is then straightforward and is proportional to the capacity of the corresponding areas. The tribune areas connected to section HRI040 and HRI050 have the lowest capacity and accordingly fewer spectators are going there. 43.2 % of the spectators transfer to the other parts the arena, which are not covered by the counting system.

6.3.6.2 Phase V: departure

At this phase 11,000 spectators are recorded by the counting system. This number does not include the initial occupancy of the promenade before the end of the game since the data have been analysed in the period from 19:45 from 20:30 (see Section 6.3.1 about filtering the data). The profiles are presented in Figure 6.14. At the end of the event many spectators (about 33%) still leave the promenade through the section HRI020 directly accessing the train station. But this is far less than the original percentage of spectators (58%) who entered the arena through that section in the arrival phase. 9.7% came at the beginning from the direction parking North and 5.4% went in that direction at the end of the game. For the parking West direction the values are 15% for coming and 10% for going. We notice that the percentage at the end are lower that the percentage at the beginning. This is attributed to the fact that many spectators left the area through other sections. Also, the parking West is larger than the parking North, this is the reason why more spectators came from and went to that direction. In addition, at the end of the events, some of the exits which are normally closed during the arrival phase are opened. The greatest disparity between arrival and departure phases is observed in the sections HRI040 and HRI050. 15.9% left through that section whereas they were used by less than 1% in the arrival phase. This is a clear indicator that spectators do not necessarily choose

the same route for entering and for leaving a facility. This is also a clear indicator that the shortest path, as already assumed in many simulations tools, plays an important role. This idea is supported by the fact that all sections are relatively well used for leaving the arena independent on their locations.

To summarise, at the end of the game, there are more spectators who first go out of the promenade using the shortest path and then find their way back to the train station and the parking areas. This also implies that route choice behaviour outside the promenade has to be taken into account in simulations. From the presented data, it can be inferred that the common assumption that spectators choose the same route for accessing and leaving a facility is not necessarily true. Although it is not quantifiable from our data the shortest path to leave the building plays an important role and should be accounted. This is the preferred route from pedestrians unless motivated by other factors as analysed by Golledge [127].

6.3.7 Theoretical approach for route choice

The results presented in the previous sections do not give any details about the pedestrians' profiles within the promenade. For example, what percentage of the spectators who entered through the section HRI020 proceeds further to section HRI050? If we reconsider the main flow directions given in Figure 6.3, then the individual route choices inside a specific section during an observation period can be expressed as a system of linear equations. Considering the departure scenario at the end of the game, we have the route choices possibilities given in Figure 6.15. We read from the system that T spectators enter the section coming from the tribune and split in three groups (α_5, α_6 and α_7) according to the three possible routes. The spectators coming from other sections (for instance α_1 and α_2) have only two choices: transiting to the next section or going outside. These observations are summarised in Equation 6.4.

$$\begin{bmatrix} 1 & 1 & 0 & 0 & 0 & 0 & 0 \\ 0 & 0 & 1 & 1 & 0 & 0 & 0 \\ 0 & 0 & 0 & 0 & 1 & 1 & 1 \\ 0 & 1 & 0 & 0 & 1 & 0 & 0 \\ 0 & 0 & 0 & 1 & 0 & 0 & 1 \\ 1 & 0 & 1 & 0 & 0 & 1 & 0 \end{bmatrix} \times \begin{bmatrix} \alpha_1 \\ \alpha_2 \\ \alpha_3 \\ \alpha_4 \\ \alpha_5 \\ \alpha_6 \\ \alpha_7 \end{bmatrix} = \begin{bmatrix} P_{11} \\ P_{12} \\ T \\ P_{22} \\ P_{21} \\ E \end{bmatrix} \tag{6.4}$$

As expected, the system is under determined and the rank of the matrix is 5 implying 2 degrees of freedom. The solution domain should be restricted to positive integer values meaning $\alpha_i \in \mathcal{N}$. Since the matrix is totally unimodular, it is guaranteed that the solutions, if existing are integer. The system has a solution only under the condition stated by Equation 6.5 which essentially means that the number of pedestrians should be conserved.

$$\begin{aligned} E &= P_{11} + P_{12} - P_{21} - P_{22} + T \\ \Phi_{in} &= \Phi_{out} \end{aligned} \tag{6.5}$$

By considering α_1 and α_3 as the free variables, the solution space of the system is given in Equation 6.6.

$$\begin{bmatrix} \alpha_2 \\ \alpha_4 \\ \alpha_5 \\ \alpha_6 \\ \alpha_7 \end{bmatrix} = \alpha_1 \begin{bmatrix} -1 \\ 0 \\ 1 \\ -1 \\ 0 \end{bmatrix} + \alpha_3 \begin{bmatrix} 0 \\ -1 \\ 0 \\ -1 \\ 1 \end{bmatrix} + \begin{bmatrix} P_{11} \\ P_{12} \\ P_{22} - P_{11} \\ P_{11} + P_{12} - P_{21} - P_{22} + T \\ P_{21} - P_{12} \end{bmatrix} \tag{6.6}$$

If we apply the system to the scenario given in Figure 6.7(a) with the following values (to ensure the condition in Equation 6.5)

$$\begin{aligned} &T = 1945, \\ &E = 4159 + 3081 - 2849 - 3474 + 1945 = 2862, \\ &P_{11} = 4159, \\ &P_{12} = 3081. \\ &P_{21} = 3474, \\ &P_{22} = 2849 \end{aligned}$$

then we have the solution space defined by:

$$\begin{bmatrix} \alpha_2 \\ \alpha_4 \\ \alpha_5 \\ \alpha_6 \\ \alpha_7 \end{bmatrix} = \alpha_1 \begin{bmatrix} -1 \\ 0 \\ 1 \\ -1 \\ 0 \end{bmatrix} + \alpha_3 \begin{bmatrix} 0 \\ -1 \\ 0 \\ -1 \\ 1 \end{bmatrix} + \begin{bmatrix} 4159 \\ 3081 \\ -1310 \\ 2862 \\ 393 \end{bmatrix}$$

A possible distribution of the pedestrians in this section of the promenade is therefore given by the solution

$$\alpha^T = [2000, 2159, 500, 2581, 690, 362, 893].$$

The linear system can then be extended to the complete arena.

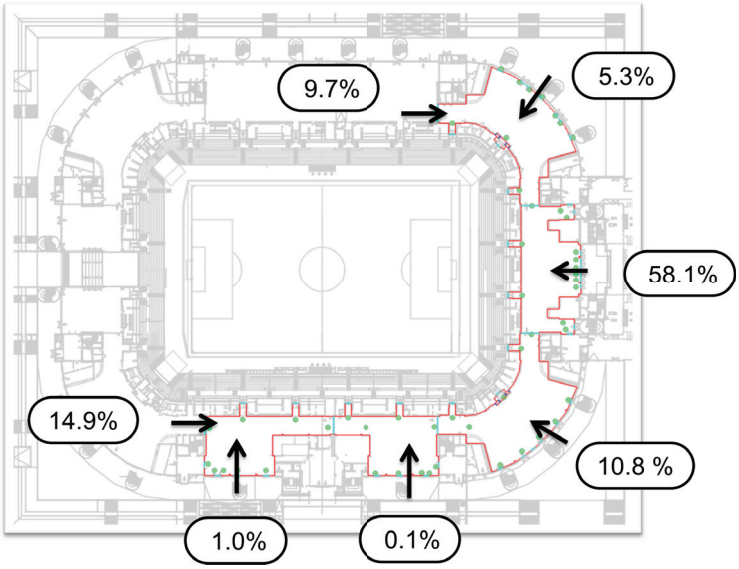

(a) Spectators coming from the outside and entering the promenade

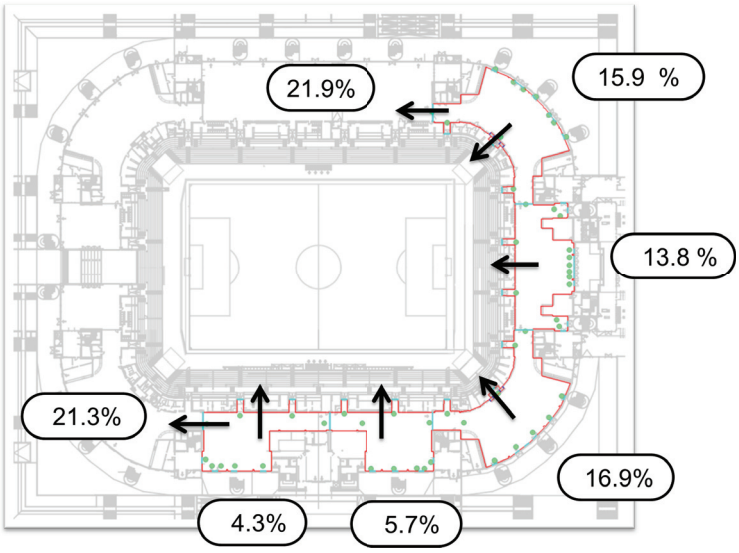

(b) Spectators leaving the promenade towards the tribune and other sections

Figure 6.13: Pedestrians' profiles passing through the promenade at the beginning of the game. 13,000 spectators are recorded by the counting system.

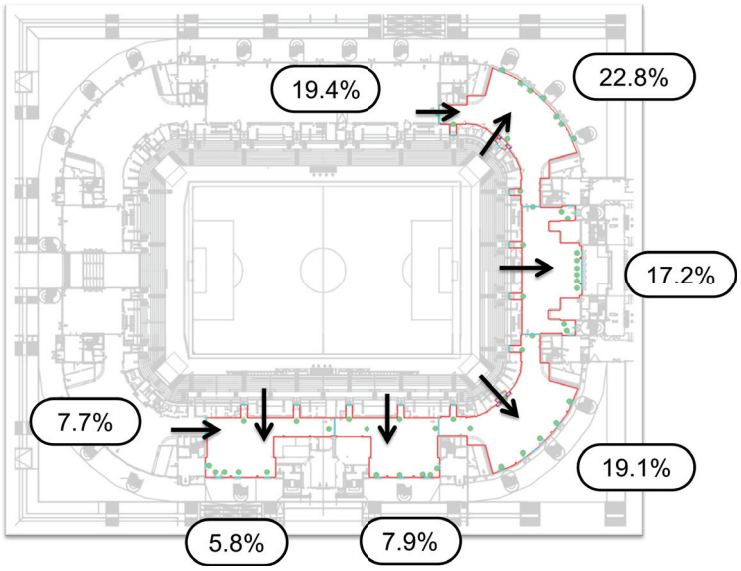

(a) Spectators entering the promenade coming from the tribune areas

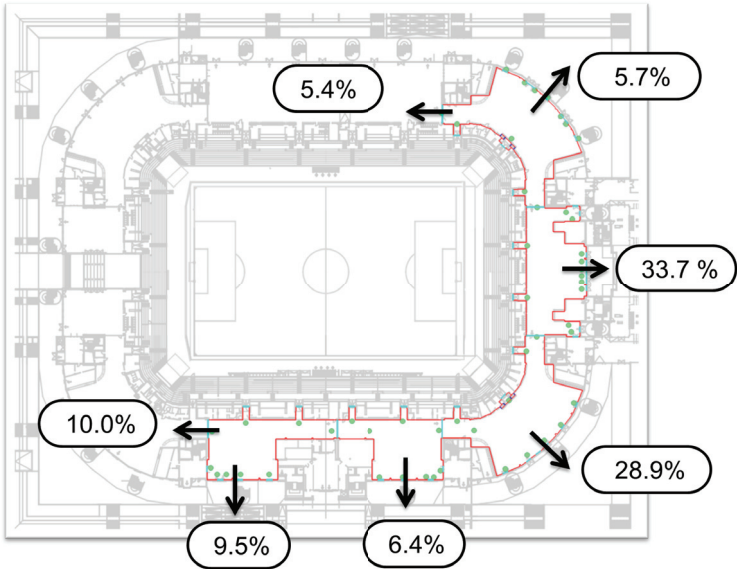

(b) Spectators leaving the promenade to the outside

Figure 6.14: Pedestrians' profiles passing through the promenade at the end of the game. 11,000 spectators are recorded by the counting system. This number does not consider the initial occupancy of the promenade before the end.

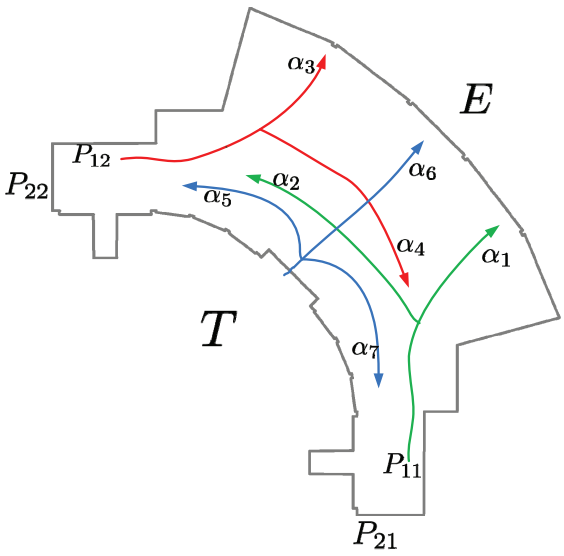

Figure 6.15: Determination of pedestrians' profiles in the section HRI010 of the promenade.

6.4 Analysis of Football Games

In the previous section the detailed analysis of route choice patterns and exits choosing behaviour of spectators for a specific football game has been presented. In the following a comparison across different football games is performed. We only analysed the profiles for entering and leaving the promenade during the arrival and the departure phase. The same filtering process described in Section 6.3.1 is applied. A total of 9 games has been recorded in the time ranging from July 2011 to November 2011. The average number of recorded spectators is 13,000 and the average number of total spectators in the arena during the games is 30,000 except for the game on the 2011-10-11 where more than 50.000 spectators were present in the arena (and 15,000 were recorded by the counting system). The game on the 2011-10-11 was a national game opposing Germany and Belgium accounting for the European Cup qualifiers 2012. All other games were games from the 2^{nd} division of the German *Bundesliga* involving the regional team Fortuna Düsseldorf. Recall that the data are recorded in the ESPRIT arena in Düsseldorf. Also, 2 games were played at 13:00, 4 games at 18:00, 2 games at 19:00 and one game at 20:15. Thus, a certain distribution of the games, even though very scarce, can be assumed.

The usage of the different sections (expressed in % of the total occupancy) for entering the promenade in the arrival phase are given in Figure 6.16(a). The first noticeable pattern here is the clustering of the data independent of the events. The data all shows similar patterns. 50 to 60 % of the spectators always gain access to the investigated promenade area via the section connected to the train station. This number is very low (less than 5%) for the sections HRI010, HRI040 and HRI050. Also, the number of spectators coming from the direction parking North and parking West is uniform between 10 and 15 %. Only the national game shows some outliers. The figure infers that no pedestrian has entered the promenade through the sections HRI010 and HRI030. A closer look at the data however has shown that during the analysis period from 17:00 to 19:00, almost 3800 pedestrians left the promenade and 3840 came in, resulting in a $\sim 0\%$ usage by applying the filtering process. The discrepancies can be attributed to the general audience during that national game which differs from the other events. This assumption is also supported by the fact that more spectators (than usual) came by cars from the parking West side. For all other events the same audience can be assumed mostly made of the local supporters of Fortuna and some supporters from the visiting team.

The distribution of the spectators inside the promenade is presented in Figure 6.16(b). In this case as well, a clustering is observed. This distribution to the tribune area is of course proportional to the capacity of the tribune. Consequently, fewer spectators go to the sections HRI040 and HRI050. Similar to the previous analysis outliers are found in the national game. More than 70% of the spectators go to other sections in the directions of parking West and parking North. Correspondingly, the occupancy rate for the other sections drops. This behaviour is once more attributed to the audience type. During the national game, the

spectators were more distributed in the arena, which was full. That is the reason why many spectators need to access their seats through the aforementioned directions.

At the end of the game, the spectators populate the promenade according to Figure 6.17(a). The general trend is that most of them (15 to 25%) come from the direction parking North. These values are also in accordance with Figure 6.16(b) where in the arrival phase the majority of the spectators went in that direction. They are now coming back, at least many of them. This observation does not apply for the parking West side. An interesting pattern is here that less spectators come from the parking West direction, although relatively the same percentage went to the direction parking North and parking West during the arrival phase. It means that those pedestrians have chosen a different way for leaving the arena.

The profiles for leaving the promenade during the departure phase are given in Figure 6.17(b). The data shows a strong clustering of the section usage. Similar to the observations during the other phases, the outliers are also from the national game. There are more spectators going to the parking West direction, probably to their cars. By fading out the outliers, we can make following general assumptions about the egress of this section of the arena during football games. The sections HRI020 and HRI030 are relatively equally used. Whereas the sections HRI020 is directly connected to the train station and is additionally the main entrance, the section HRI030 provides a more attractive view to the outside. Once in that section, spectators are more probable to directly go out. The other sections HRI010, HRI040 and HRI050 are also well used (from 5 to 10%) compared to the data from the arrival phase, where they were used by less than 5%. This also expresses the trend of first going to the outside at the end of the event and from there to take new orientation steps, while having more overview. Also, we can assume that the data are not related to the period of the day, since some games were played at noon and the others in the evening.

The implications of these results for an evacuation scenario are straightforward. The audience type plays an important role and mostly their familiarity with the location. We have seen from the data that the behaviour was almost identical across the games attended by the same audience. We have assumed the same audience because of a local team during home games which is very likely. The data were not collected during an actual evacuation, but the similarity between the data suggests that even in a case of a real evacuation with the same audience, the egress pattern might be similar. Also, the strategy of preferring the local shortest path to the outside in simulation tools is to some extent supported by the data. A considerable percentage of spectators went out during the departure phase through sections that were not used during the arrival phase, implying that they have preferred the shortest path out and then orientated themselves towards their final destinations. In the next sections sample data from concert performances are analysed. In that case, the audience is usually not the same.

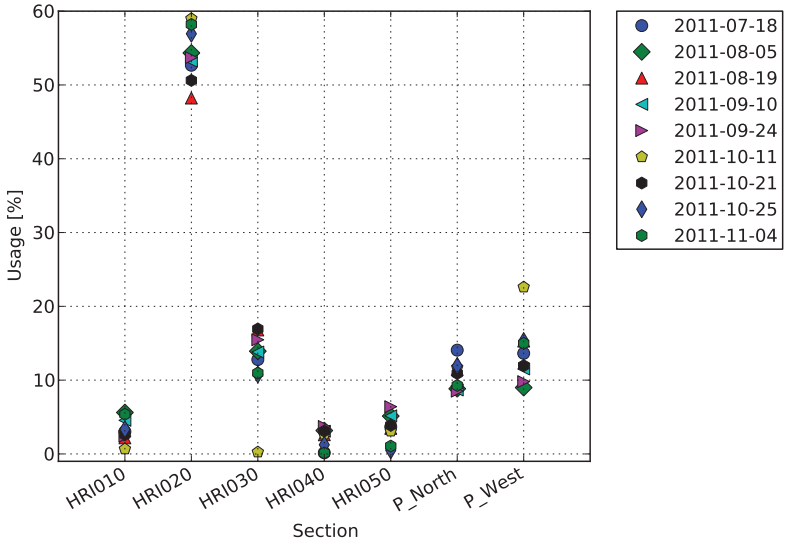

(a) Spectators coming from the outside and entering the promenade

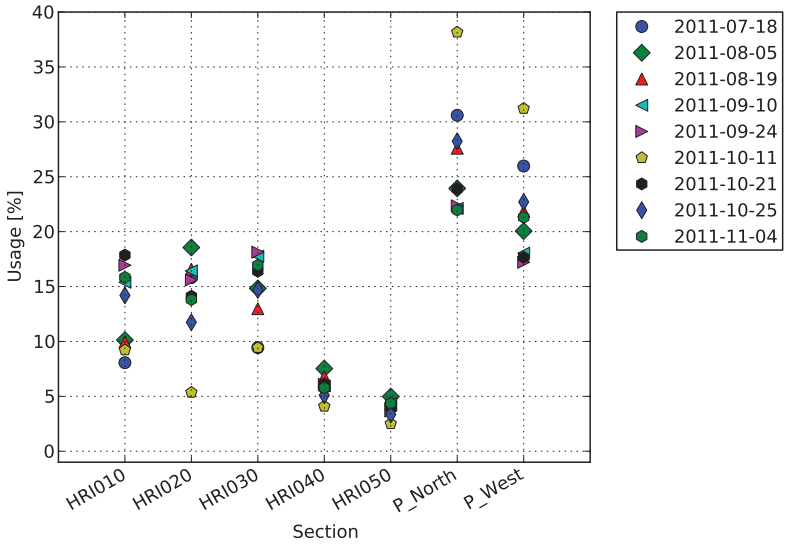

(b) Spectators leaving the promenade towards the tribune and other sections

Figure 6.16: Pedestrians' profiles for different football events during the arrival phase.

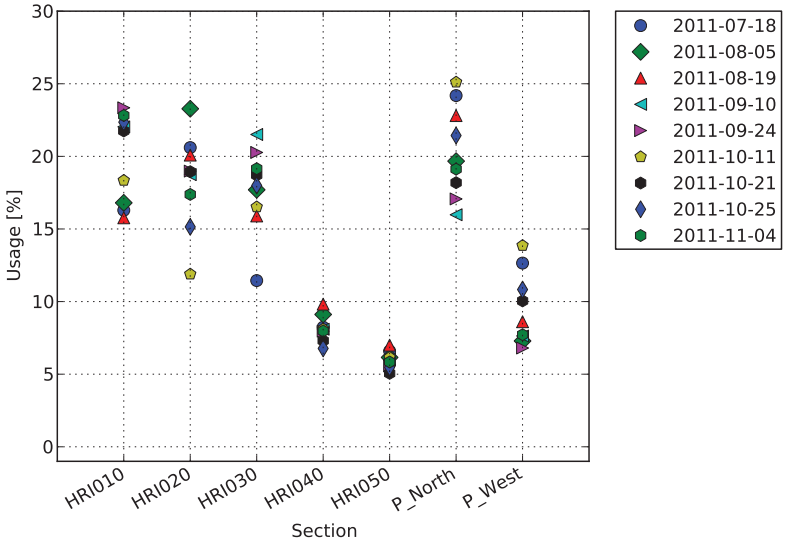

(a) Spectators entering the promenade coming from the tribune areas

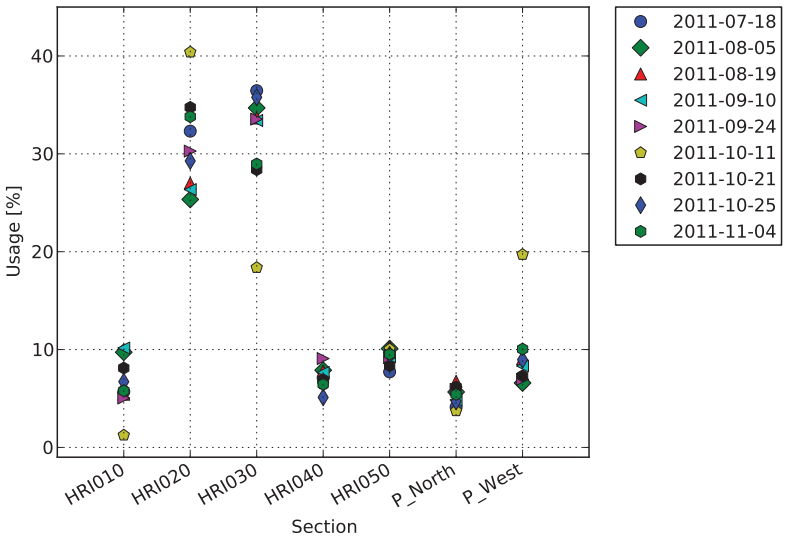

(b) Spectators leaving the promenade to the outside

Figure 6.17: Pedestrians' profiles for different football games during the departure phase.

6.5 Analysis of Concert Performances

For concert performances, only the departure phase has been analysed. This is due to the many artefacts present in the data during the arrival phase. Firstly, the entrance configuration always varies from performance to performance, using barricades and other type of barriers. Secondly, the arrival phase lasts longer, due to the different check stations and the spectators coming early to have the best places. All these factors lead to a lot a back and forth patterns, from people mainly looking for their seats, making the use of the filtering process used for football games impracticable. The departure phase is more stable and the extracted profiles for 4 different performances are presented in Figure 6.18. They were held in the time from 20:00 to 23:00.

The occupancy percentage of the section HRI010 through HRI050 for entering the promenade are (just like in the case of football games) proportional to the size of the connected tribune area. Therefore, the lowest values are observed for the sections HRI040 and HRI050. The data are presented in Figure 6.18(a). The direction parking West is blocked. This explains the value of 0% for both the arrival and the departure phases. The passage blocking is due to the position of the performance stages. For all performances, the stage was disposed along the playing field, such that the view to the artists was only possible starting from the tribune area connected to the section HRI050.

The data obtained during the departure phase are presented in Figure 6.18(b). Concerning the general shape of the data samples and their relative positions to each other, there are some similarities with the data from the football games. The patterns however are less clustered. This may be an indicator for a different behaviour but can also be attributed to the number of samples (4 concert events compared to 9 football events). The most used sections for exiting are HRI020 and HRI030 with usage ranging from 20 to 35 %. Similar values were obtained for football games. The less used section is HRI010, but the usage is slightly larger than the football case. The same applies for the sections HRI040 and HRI050. Here, the usage is between 10 and 15% whereas they were under 10% for the football case. The number of spectators leaving through the parking North direction is also slightly higher in comparison implying that more people came by cars. It is generally the case for concerts that many attendees travel by cars. The main outcome from the analysis of these concerts performances is that the use of the shortest path for leaving the promenade is amplified for all sections. The main factor is the type of the audience which can be assumed to be different for all performances.

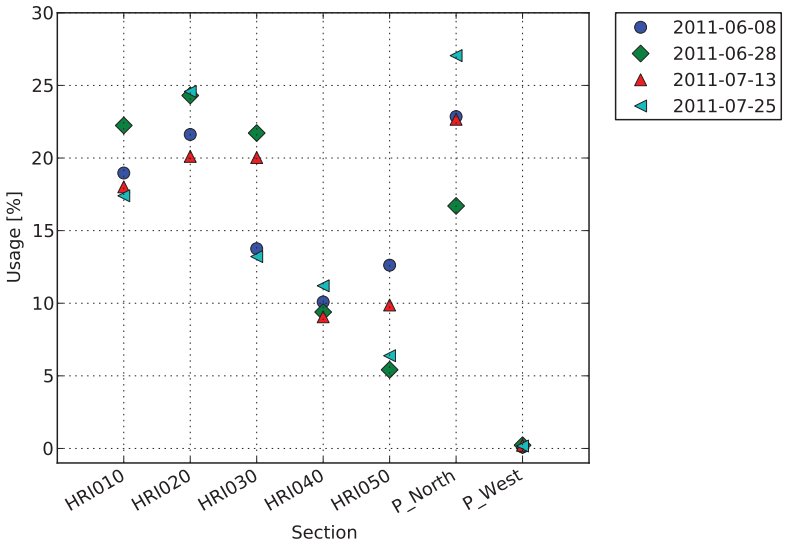

(a) Spectators entering the promenade coming from the tribune areas

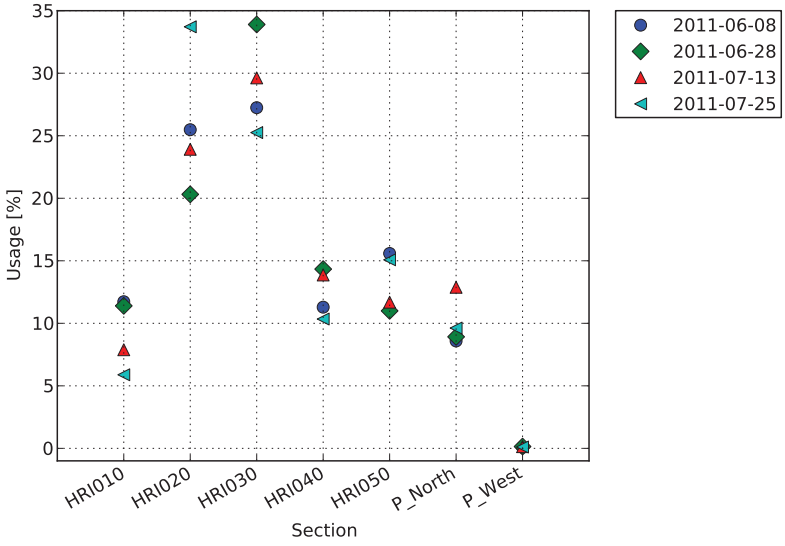

(b) Spectators leaving the promenade to the outside

Figure 6.18: Pedestrians' profiles during the departure phase at the end of 4 concert performances.

6.6 Modelling the Route Choice of Pedestrians

In the previous sections the pedestrians' route choice profile for entering and leaving the promenade part of the arena has been analysed for various football games and concert performances. In this section, we compare the results with our route choice modelling approach. The modelling and simulation framework has been presented in Chapter 2. The route choice model has been discussed in Chapter 4. For the simulation the model uses the navigation graph presented in Chapter 5. As already mentioned at the beginning of this chapter, we are only simulating an emergency clearing. This has two major impacts on the simulation. The first impact is that all pedestrians only have the same goal which is exiting from the facility. In a routine clearing, at the end of an event for instance, they may have a preferred destination, the parking lots or the train station for instance as demonstrated by the previous study. The second impact is that the pedestrians will choose the quickest path to reach the outside. The quickest path will result in a strictly unidirectional flow. The main output of profiles analysis was that the shortest path in the departure phase played an important role, even in the case of a routine clearing. Therefore, we can assume that this effect will be reinforced in the case of an emergency evacuation. If the aim is to simulate a routine clearing the output from the previous study can be used as input for the route choice model with some restrictions. The study did not provide the route choice patterns inside the promenade itself, for instance how many spectators move from one section to the other. Another restriction is that the type of the event has to be taken into account.

For the initial configuration of the simulation, 2800 pedestrians are homogeneously distributed in the promenade and another 9000 pedestrians are homogeneously distributed in the tribune. Similar to the empirical study the investigated values are E which denotes the number of using this section to reach the outside, P which is the number of pedestrians transiting through this section and T the number of pedestrians coming from the tribune. The route choice strategy applied is the quickest path and the analysis will mainly focus on the exit choosing behaviour.

6.6.1 Section HRI010

In the first stage the overall pedestrian flow is analysed. As the Figure 6.19(a) suggests, the flow is strictly unidirectional and leads straight from the tribune to the outside and almost all pedestrians are coming from the tribune area. The initial number of pedestrians in this section is ≈ 550. The obtained flow values are:

$$
\begin{aligned}
&E = 1972\\
&T = 1957\\
&P_{in} = 0, P_{out} = 536\\
&\Phi = T + 550 = 2507
\end{aligned}
$$

Pedestrians in the simulation are using the quickest path which can be simplified to the local shortest path in the case there are no congestions. This behaviour is demonstrated by the exit usage in percentage shown in Figure 6.19(b).The fill level of the bars is proportional to the overall number of pedestrians leaving through that section. The exit on the top left is the most used by 923 pedestrians. Those pedestrians are coming from the left aisle of the tribune. The exit on the top right is the less used (by only 101 pedestrians). This is due to the fact that most of the pedestrians coming from the right aisle of the tribune who would have used that exit transferred to the other section. There are two exits not far from each other, but which denotes different usages (472 and 130 pedestrians). This behaviour is also attributed to the absence of congestion in front of the exit. The absence of congestions is easy to understand. Since most of the pedestrians are coming from the tribune and the flow out of the tribune is smaller than the flow out of the promenade, the pedestrians are almost walking with their desired maximal velocity. The low outflow from the tribune is due to the geometrical restrictions and the connecting gates. In addition, the evacuation process in the simulation lasts approximately 10 minutes.

6.6.2 Section HRI020

For this section, a direct comparison between the simulation and the empirical data has been made. We focus however only on the exit choosing behaviour as it shows some interesting patterns. The exit choosing behaviour is given in Figure 6.20. If we first concentrate on the main six front exits on Figure 6.20(a), the first behaviour we notice is that not all exits are well used. The two exits on the outer part (used by 123 and 58 pedestrians) are not used. This typically occurs whenever a door a closed (not locked) and near another exit is open. The tendency is to walk towards the open exit as it is more inviting. The behaviour can be reversed if one spectator opens one of the exits, then other spectators will also start using it. This behaviour is not taken into account in our model and this is shown by the balanced usage of the main front exits (see Figure 6.20(b)). The second noticeable difference is the usage of the four side exits. They are used by pedestrians in our simulation following the quickest path. They lead in a shorter way to the outside than the other exits, although their position is not favourable. These discrepancies can be mitigated for instance by extending the model and adding an attractiveness parameter for all exits. Also, the network outside the building has to be considered as well.

6.6.3 Complete arena

The stage of the simulation for the investigated part of the arena after 5 seconds is presented in Figure 6.21. All exits are well used at this stage due to the high density in the different sections of the promenade. There are still no congestions as can be inferred from the pedestrians' colour which encodes the velocity. They are mostly green, meaning moving at their desired

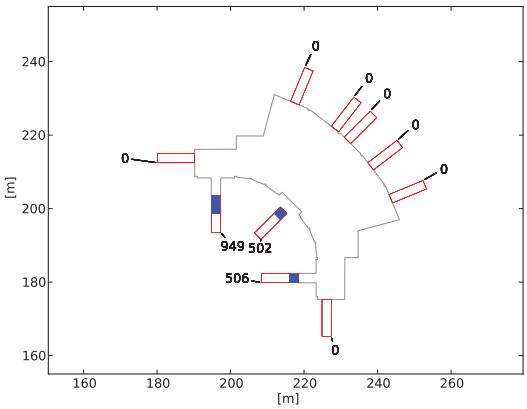

(a) Entering the section

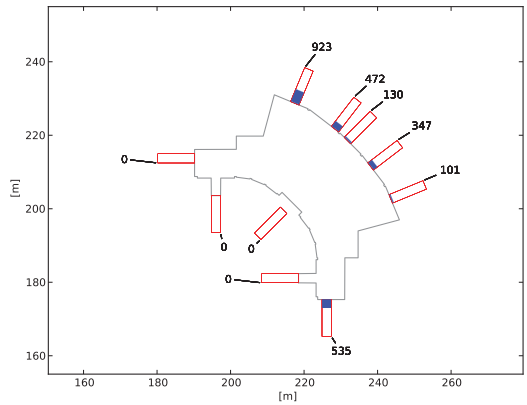

(b) Leaving the section

Figure 6.19: Pedestrians' profiles passing through the section HRI010 of the promenade in the simulation.

velocity. After 2 minutes, the situation is completely different as displayed in Figure 6.22. The congestions are only present in the tribune and pedestrians in the promenade only move towards the nearest exit. This is also the explication of the relatively high usage of some exits. In the absence of congestions, the quickest path is reduced to the shortest path which is the unique depending on the location.

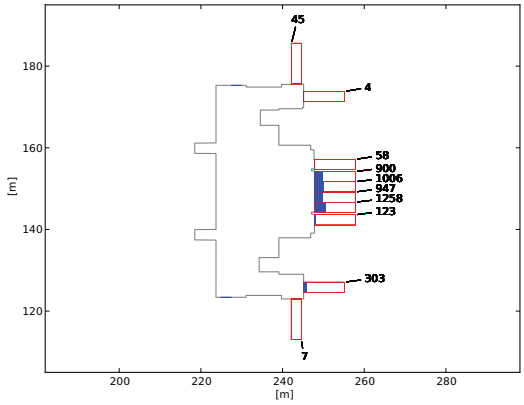

(a) Observation: leaving the section at the end of the football game

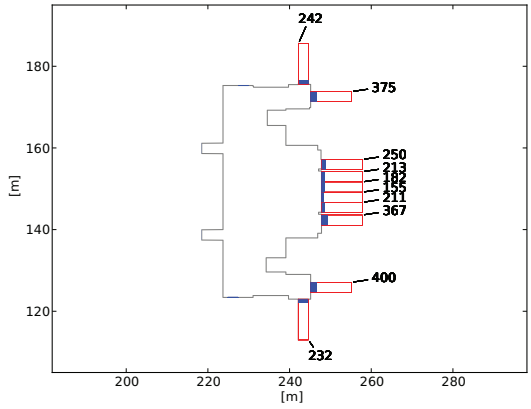

(b) Simulation: leaving the section

Figure 6.20: Comparison of pedestrians' profiles passing through the section HRI020 of the promenade.

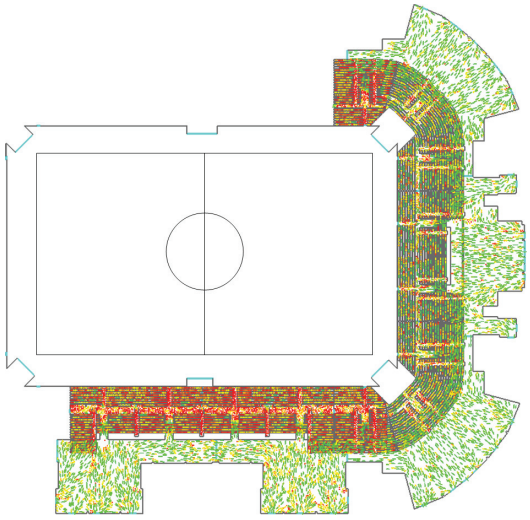

Figure 6.21: Status of the simulation after 5 seconds. The exits are evenly used.

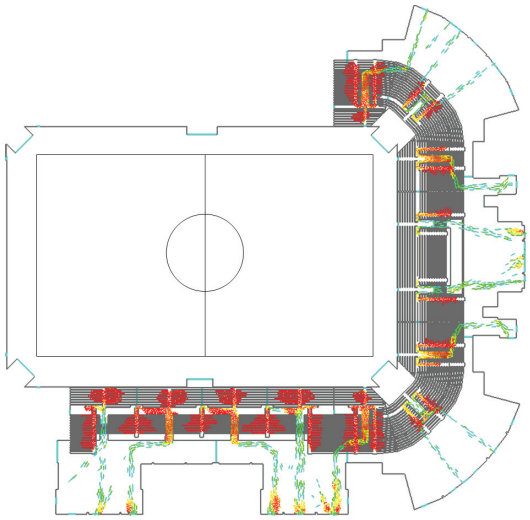

Figure 6.22: Status of the simulation after 2 minutes. The density is low in the promenade area and there is no congestion at all. The local nearest exits are preferred by the pedestrians.

6.7 Summary

In this chapter, an empirical study of pedestrians' route choice in an arena has been presented. The study has been done for different football games and concert performances. Usually it is assumed in evacuation simulations that evacuees choose the shortest path to leave the facility. In this study, we have shown that even not in an evacuation scenario, people tend to choose the shortest path to leave the facility. These results may be an argument for the use of that strategy in evacuation software. It has also been found that the same type of spectators, regular supporters of a local team for instance, has the same route choice pattern. The results were the same across different football games played at different times in the day. After evaluating the shortest path strategy as suitable for an evacuation scenario, a simulation has been performed and with some restrictions compared with data from the empirical study. The exit choosing behaviour has shown some discrepancies where some exits giving the impression of being closed were not well used by spectators, whereas they were used in the simulation. By extending the pedestrian model to recognise attractive exits, this gap can be closed. Finally, it is necessary to also consider the network outside the facility for a more accurate route choice.

Chapter 7

Conclusions and Outlooks

7.1 Summary

In this dissertation, three topics in the pedestrian dynamics field have been elaborated. These are the runtime optimisation of force based models, the modelling of route choice in a complex facility and an empirical study of pedestrians' route choice. The developed ideas have been applied in the ESPRIT arena in Düsseldorf, Germany where they have been implemented in an evacuation assistant. The main motivation behind these topics is the improvement of safety during mass events. The evacuation assistant developed for this purpose has been presented in the first chapter. The requirements for the assistant and the associated challenges have been discussed. The first challenge was to achieve a faster than real time simulation of an evacuation process in the arena with a force based model. The second challenge was the development of a route choice model for evacuation in a complex geometry. The second chapter presented the force based pedestrian model used at the operational level and an analysis of different other pedestrians models with respect to the runtime. With modifications including a smoothing algorithm at sharp turns, the model was applicable in the structure of the arena. Besides, the model has been integrated in an open source framework for developing pedestrian models. The third chapter presented different optimisation techniques for short range force based systems. The first technique was the use of neighbourhood lists. The second technique was the use of parallelisation on a computer cluster. The performance has been evaluated using the speedup. For the investigated part of the arena, a simulation with 20,000 pedestrians for a total evacuation time of 508 seconds was performed in 130 seconds. The time will further drops if the route choice strategies are optimised with respect to the runtime. It was therefore possible to achieve a faster than real time simulation. During the test phase of the system in the arena during the summer 2011, the occupancy was usually lower, so that the simulations were faster. With the available computational resources, the simulation program can be scaled to the targeted 50,000 spectators within the required time of 2 minutes. The fourth chapter presented the main idea of the thesis: newly developed route choice strategies for evacuation.

The classical shortest path has been combined with a quickest path based on observation. The idea behind the strategy is that in the case of emergency evacuation people will choose the quickest path to egress from the building. In order to detect the quickest path, pedestrians analyse their current situation. This has been modelled by observing the evolution of the different queues (if any) in the location and by systematically deciding for the fastest one. This choice takes into consideration the visibility range of the individual pedestrians and the efforts bounded to the change of a route expressed in terms of gain. The final decision whether or not to change the current route is regulated by a cost benefit analysis function, which takes as arguments the self-estimated travel times through alternative routes and a gain threshold. A good and plausible dynamics in the evacuation simulation process with reduced evacuation times have been the results of the modelling approach. We restrict ourselves to the term plausible in this case because no empirical data about evacuations are available to properly validate the idea. In addition, criteria to assess the criticality of an evacuation process have been elaborated. We investigated the evacuation time distribution, the time in jam distribution and the average jam size of pedestrians during an evacuation simulation. The jam size itself is not critical as long as it disappears quickly. An evacuation process should therefore not only minimise the jam size, but also to reduce the duration of jamming situations. Also, during the analysis of the data parameters such as the surrounding conditions (weather for instance) must be taken into consideration. The route choice algorithm operates on a navigation graph. Techniques for generating navigation graphs were presented in the fifth chapter. The techniques use a polygonal decomposition of the geometry and operate on the vertices of the polygons to generate visibility and navigation graphs. For a complex structure like the tribune of a stadium, these approaches were found to be infeasible in combination with the pedestrian force based model used. Besides, force based models are very sensitive to the direction of the desired velocity. The solution was to manually insert navigation lines at strategic locations and to use standard algorithms like Dijkstra to generate the navigation graph. The idea was successfully implemented and a simulation of the arena was possible.

The automated person counting system installed in the arena has provided data about spectators route choice patterns for an empirical study. The empirical data have presented and analysed in the sixth chapter. Two types of events have been investigated: football games and concert performances. In this study, we have shown that even not in the case of an evacuation scenario, spectators tend to choose the shortest path to egress from the building at the end of the event. This may be a good support for the assumption that even in the case of a real evacuation with the same type of audience; the route choice pattern will not be very different. Additionally, we have shown that for the same type of spectators, regular supporters of a local team for instance (during a home game), displays an identical route choice pattern across different games. This seems to be a routine behaviour. Slightly varying results were obtained by analysing concert performances, where the use of the shortest path for leaving the arena was amplified. The route choice model has been compared with the empirical data with some restrictions. Since the route choice model was optimised for evacuation and the observed data were rather obtained from a routine clearing, some discrepancies have been observed. In the

model all pedestrians used the quickest path to egress from the facility. This does not apply to a routine clearing. Nevertheless, if the aim is to simulate a routing clearing, output data from the counting system can now be used as input for the route choice model. This step is expected to be straightforward since a strong correlation between the different football games has been found. This was also due to the little varying configurations for entering and leaving the arena during the games. For concerts, the configurations of the entrances vary depending on the events and the use of the output data may be achieved after further investigations. The exact distribution of spectators with respect to their route choice inside the arena could not be determined from the provided data. Nevertheless, we have demonstrated with a theoretical approach using a system of linear equations describing the route choice pattern that the solution space is not very large and has a finite number of solutions. A possible solution has been provided for a section of the promenade.

7.2 Outlooks and Future Works

Some problems encountered during the development of the model can easily be solved by integrating a basic flood field model as a layer on the bottom of the navigation graph. This idea has already been broached by some hybrid models. Also, additional speedup will be gained by further optimising the route choice algorithms. The presented route choice model did not include a deep consideration of the psychological state of the pedestrians. Although the patience time in jam and the observation features can be considered as first steps in this direction. More investigations should be done for integrating psychological features in pedestrian model in general. However, the main question will remain the validation of such models. This could be a motivation for the development of new validation techniques. The key point is the need of more empirical studies in this area. Also, the idea presented in this work is only applicable for two-dimensional structures. If we think of shopping malls or a train stations with different levels, which are usually equipped with walls made of glass, the necessity for investigating visibility and route choice in three-dimensional structures becomes obvious.

Bibliography

[1] W. M. Predtetschenski and A. I. Milinski, *Personenströme in Gebäuden - Berechnungsmethoden für die Projektierung.* Verlagsgesellschaft Rudolf Müller, Köln-Braunsfeld, 1971.

[2] E. R. Galea, S. Gwynne, P. Lawrence, L. Filippidis, D. Blackspields, and D. Cooney, *buildingEXODUS V 4.0 - User Guide and Technical Manual*, 2004, www.fseg.gre.ac.uk.

[3] TraffGo HT GmbH, *Handbuch PedGo 2, PedGo Editor 2*, 2005, www.evacuation-simulation.com.

[4] *Benutzerhandbuch Aseri, Version 4.6*, I.S.T. Integrierte Sicherheits-Technik GmbH.

[5] P. A. Thompson and E. W. Marchant, "A Computer Model for the Evacuation of Large Building Populations," *Fire Safety Journal*, vol. 24, pp. 131–148, 1995.

[6] R. M. Tavares and E. Galea, "Evacuation modelling analysis within the operational research context: A combined approach for improving enclosure designs," *Building and Environment*, vol. 44, no. 5, pp. 1005 – 1016, 2009.

[7] D. Thalmann and S. R. Musse, *Crowd Simulation.* Springer London, 2007.

[8] H. Choset, K. Lynch, S. Hutchinson, G. Kantor, W. Burgard, L. Kavraki, and S. Thrun, *Principles of Robot Motion: Theory, Algorithms and Implementation.* MIT Press, 2005.

[9] M. de Berg, O. Cheong, M. van Kreveld, and M. Overmars, *Computational Geometry: Algorithms and Applications*, 3rd ed. Springer, 2008.

[10] G. F. Mulligan and J. P. Crampton, "Population growth in the world's largest cities," *Cities*, vol. 22, no. 5, pp. 365 – 380, 2005.

[11] Un-Habitat, "State of the world's cities 2008/2009," *Cities*, vol. 12, no. 5, 2008.

[12] S. Holl and A. Seyfried, "Hermes - an Evacuation Assistant for Mass Events," *inSiDe*, vol. 7, no. 1, pp. 60–61, 2009.

[13] A. U. Kemloh Wagoum, M. Chraibi, J. Mehlich, A. Seyfried, and A. Schadschneider, "Efficient and validated simulation of crowds for an evacuation assistant," *Computer Animation and Virtual Worlds*, vol. 23, no. 1, pp. 3–15, 2012.

[14] A. Schadschneider, W. Klingsch, H. Klüpfel, T. Kretz, C. Rogsch, and A. Seyfried, *Encyclopedia of Complexity and System Science.* Springer, Berlin, Heidelberg, 2009, vol. 5, ch. Evacuation Dynamics: Empirical Results, Modeling and Applications, pp. 3142–3176.

[15] M. Boltes and A. Seyfried, "Collecting pedestrian trajectories," *Neurocomputing*, vol. 100, pp. 127 – 133, 2013.

[16] J. J. Fruin, *Pedestrian Planning and Design*. Elevator World, New York, 1971.

[17] M. Chraibi, U. Kemloh, A. Seyfried, and A. Schadschneider, "Force-based models of pedestrian dynamics," *Networks and Heterogeneous Media*, vol. 6, no. 3, pp. 425 – 442, 2011.

[18] S. P. Hoogendoorn, P. Bovy, and W. Daamen, "Microscopic Pedestrian Wayfinding and Dynamics Modelling," in *Pedestrian and Evacuation Dynamics*, M. Schreckenberg and S. Sharma, Eds., 2002, pp. 123–155.

[19] A. Schadschneider, D. Chowdhury, and K. Nishinari, *Stochastic Transport in Complex Systems From Molecules to Vehicles*. Elsevier Amsterdam, Oxford, 2011.

[20] V. J. Blue and J. L. Adler, "Cellular automata microsimulation for modeling bidirectional pedestrian walkways," *Transportation Research Part B*, vol. 35, pp. 293–312, 2001.

[21] A. Kirchner and A. Schadschneider, "Simulation of evacuation processes using a bionics-inspired cellular automaton model for pedestrian dynamics," *Physica A*, vol. 312, pp. 260–276, 2002.

[22] K. Nishinari, K. Sugawara, and Kaza, "Modelling of self-driven particles: Foraging ants and pedestrians," *Physica A*, vol. 372, no. 1, pp. 132–141, Dec 2006.

[23] D. Helbing and P. Molnár, "Social force model for pedestrian dynamics," *Phys. Rev. E*, vol. 51, pp. 4282–4286, 1995.

[24] W. J. Yu, L. Chen, R. Dong, and S. Dai, "Centrifugal force model for pedestrian dynamics," *Phys. Rev. E*, vol. 72, no. 2, 2005.

[25] A. Treuille, S. Cooper, and Z. Popović, "Continuum crowds," *ACM Trans. Graph.*, vol. 25, pp. 1160–1168, 2006.

[26] N. Pelechano, J. M. Allbeck, and N. I. Badler, "Controlling individual agents in high-density crowd simulation," in *Proceedings of the 2007 ACM SIGGRAPH/Eurographics symposium on Computer animation*, ser. SCA '07. Aire-la-Ville, Switzerland: Eurographics Association, 2007, pp. 99–108.

[27] L. Gonçalves, M. Kallmann, and D. Thalmann, "Defining behaviors for autonomous agents based on local perception and smart objects," *Computers & Graphics*, vol. 26, no. 6, pp. 887–897, 2002.

[28] A. Kirchner, H. Klüpfel, K. Nishinari, A. Schadschneider, and M. Schreckenberg, "Discretization effects and the influence of walking speed in cellular automata models for pedestrian dynamics," *J. Stat. Mech.*, vol. 10, p. P10011, 2004.

[29] D. Hartmann, "Adaptive pedestrian dynamics based on geodesics," *New Journal of Physics*, vol. 12, p. 043032, 2010.

[30] X. Zheng, T. Zhong, and M. Liu, "Modeling crowd evacuation of a building based on seven methodological approaches," *Building and Environment*, vol. 44, no. 3, pp. 437–445, 2009.

[31] R. L. Hughes, "A continuum theory for the flow of pedestrians," *Transportation Research Part B*, vol. 36, pp. 507–535, 2002.

[32] S. Chenney, "Flow tiles," in *Proceedings of the 2004 ACM SIGGRAPH/Eurographics symposium on Computer animation*, ser. SCA '04. Aire-la-Ville, Switzerland, Switzerland: Eurographics Association, 2004, pp. 233–242.

[33] U. Weidmann, "Transporttechnik der Fussgänger - Transporttechnische Eigenschaften des Fussgängerverkehrs (Literaturstudie)," Institut für Verkehrsplanung, Transporttechnik, Strassen- und Eisenbahnbau IVT an der ETH Zürich, ETH-Hönggerberg, CH-8093 Zürich, Literature Research 90, March 1993, in German.

[34] P. J. DiNenno, *SFPE Handbook of Fire Protection Engineering*, 3rd ed. Quincy MA: National Fire Protection Association, 2002.

[35] M. Chraibi, A. Seyfried, and A. Schadschneider, "Generalized centrifugal force model for pedestrian dynamics," *Physical Review E*, vol. 82, p. 046111, 2010.

[36] P. Molnár, "Modellierung und Simulation der Dynamik von Fußgängerströmen," Dissertation, Universität Stuttgart, 1995.

[37] S. Burghardt, "Analyse und vergleichende Untersuchung zum Fundamentaldiagramm auf Treppen," Masterthesis, Bergische Universität Wuppertal, Dec 2009.

[38] A. Meunders, "Kalibrierung eines Mikroskopischen Modells für Personenströme zur Anwendung im Projekt Hermes," Masterthesis, Bergische Universität Wuppertal, Sep 2011.

[39] "RIMEA-Richtlinie für Mikroskopische Entfluchtungs-Analysen," www.rimea.de.

[40] *Interim Guidelines for Evacuation Analyses for New and Existing Passenger Ships*, IMO, London, 2002, mSC/Circ. 1033.

[41] J. Zhang, W. Klingsch, A. Schadschneider, and A. Seyfried, "Transitions in pedestrian fundamental diagrams of straight corridors and t-junctions," *Journal of Statistical Mechanics: Theory and Experiment*, vol. 2011, no. 06, p. P06004, 2011.

[42] ——, "Ordering in bidirectional pedestrian flows and its influence on the fundamental diagram," *Journal of Statistical Mechanics: Theory and Experiment*, vol. 2012, no. 02, p. P02002, 2012.

[43] C. Burstedde, K. Klauck, A. Schadschneider, and J. Zittartz, "Simulation of pedestrian dynamics using a two-dimensional cellular automaton," *Physica A: Statistical Mechanics and its Applications*, vol. 295, no. 3-4, pp. 507–525, 2001.

[44] A. Schadschneider, C. Eilhardt, S. Nowak, and R. Will, "Towards a calibration of the floor field cellular automaton," in *Pedestrian and Evacuation Dynamics*, R. D. Peacock *et al.*, Eds. Springer, 2011, pp. 557–566.

[45] T. Kretz, "Pedestrian traffic - simulation and experiments," Dissertation, Universität Duisburg-Essen, 2007.

[46] T. Kretz and M. Schreckenberg, "The F.A.S.T.-Model," in *Cellular Automata*, ser. Lecture Notes in Computer Science, vol. 4173/2006. Springer Berlin/Heidelberg, 2006, pp. 712–715.

[47] K. M. W. Schroeder and B. Lorense, *Visualization Toolkit: An Object-Oriented Approach to 3D Graphics*. Kitware Inc., 2006, vol. 4th edition.

[48] M. Summerfield, *Advanced Qt Programming: Creating Great Software with C++ and Qt 4*, ser. Prentice Hall Open Source Software Development Series. Addison Wesley Professional, 2010.

[49] B. Steffen, A. U. Kemloh Wagoum, M. Chraibi, and A. Seyfried, "Parallel real time computation of large scale pedestrian evacuations," in *The Second International Conference on Parallel, Distributed, Grid and Cloud Computing for Engineering*, 2011.

[50] M. P. Allen and D. J. Tildesley, *Computer simulation of liquids*, M. P. Allen and D. J. Tildesley, Eds. Oxford University Press, 1989, vol. 18, no. 195.

[51] G. Sutmann and V. Stegailov, "Optimization of neighbor list techniques in liquid matter simulations," *Journal of Molecular Liquids*, vol. 125, no. 2-3, pp. 197–203, 125 2006.

[52] J. Mehlich, "Laufzeitoptimierung von Simulationen raumkontinuierlicher Modelle der Fußgängerdynamik mithilfe von Nachbarschaftslisten," Masterthesis, Fachhochschule Aachen, Aug 2009.

[53] A. Seyfried, M. Chraibi, J. Mehlich, U. Kemloh, and A. Schadschneider, "Runtime optimization of force based models within the hermes project," in *Pedestrian and Evacuation Dynamics 2010*, 2011.

[54] P. Richmond and D. Romano, "A High Performance Framework For Agent Based Pedestrian Dynamics On GPU Hardware," in *Proceedings of EUROSIS ESM 2008 (European Simulation and Modelling)*, Oct. 2008.

[55] C. Reynolds, "Big fast crowds on PS3," in *Proceedings of the 2006 ACM SIGGRAPH symposium on Videogames*, 2006.

[56] M. Griebel, S. Knapek, and G. Zumbusch, *Numerical Simulation in Molecular Dynamics: Numerics, Algorithms, Parallelization, Applications*, 1st ed. Springer Publishing Company, Incorporated, 2007.

[57] M. J. Quinn, R. A. Metoyer, and K. Hunter-zaworski, "Parallel implementation of the social forces model," in *in Proceedings of the Second International Conference in Pedestrian and Evacuation Dynamics*, 2003, pp. 63–74.

[58] J. Pettré, P. d. H. Ciechomski, J. Maïm, B. Yersin, J.-P. Laumond, and D. Thalmann, "Real-time navigating crowds: scalable simulation and rendering: Research articles," *Comput. Animat. Virtual Worlds*, vol. 17, pp. 445–455, July 2006.

[59] J. Janak and P. Pattnaik, "Protein calculations on parallel processors. ii. parallel algorithm for the forces and molecular dynamics," *Journal of Computational Chemistry*, vol. 13, no. 9, pp. 1098–1102, 1992.

[60] T. Clark, R. von Hanxleden, J. McCammon, and L. Scott, "Parallelizing molecular dynamics using spatial decomposition," in *Proceedings of the Scalable High-Performance Computing Conference*, 1994, pp. 95–102.

[61] S. Plimpton and B. Hendrickson, "Parallel molecular dynamics algorithms for simulation of molecular systems," in *T. G. Mattson (ed) Parallel Computing in Computational Chemistry*. Washington, D.C.: American Chemical Society, 1995, pp. 114–132.

[62] D. Hegarty, M. Kechadi, and K. Dawson, "Dynamic domain decomposition and load balancing for parallel simulations of long-chained molecules," in *Applied Parallel Computing Computations in Physics, Chemistry and Engineering Science*, ser. Lecture Notes in Computer Science, J. Dongarra, K. Madsen, and J. Wasniewski, Eds. Springer Berlin / Heidelberg, 1996, vol. 1041, pp. 303–312.

[63] F. Baiardi, A. Bonotti, L. Ferrucci, L. Ricci, and P. Mori, "Load balancing by domain decomposition: the bounded neighbour approach," in *Proceeding of 17th European Simulation Multiconference*, 2003, pp. 9–11.

[64] S. Wang and M. P. Armstrong, "A quadtree approach to domain decomposition for spatial interpolation in grid computing environments," *Parallel Comput.*, vol. 29, pp. 1481–1504, October 2003.

[65] Message Passing Interface Forum, "MPI2: A message passing interface standard," *High Performance Computing Applications*, vol. 12, no. 1–2, pp. 1–299, 1998.

[66] R. Chandra, L. Dagum, D. Kohr, D. Maydan, J. McDonald, and R. Menon, *Parallel programming in OpenMP*. San Francisco, CA, USA: Morgan Kaufmann Publishers Inc., 2001.

[67] G. M. Amdahl, "Validity of the single processor approach to achieving large scale computing capabilities," in *Proceedings of the April 18-20, 1967, spring joint computer conference*, ser. AFIPS '67 (Spring). New York, NY, USA: ACM, 1967, pp. 483–485.

[68] Redbooks, IBM, *Programming the Cell Broadband Engine Architecture: Examples and Best Practices*. Vervante, 2008.

[69] Wikipedia, "Xeon — wikipedia, the free encyclopedia," 2012, [Online; accessed 22-January-2012].

[70] www.hpcwire.com, 2009 (accessed 15 Feb. 2012). [Online]. Available: http://www.hpcwire.com/hpcwire/2009-10-27/will_roadrunner_be_the_cells_last_hurrah.html

[71] www.heise.de, 2009 (accessed 15 Feb. 2012). [Online]. Available: http://www.heise.de/newsticker/meldung/SC09-IBM-laesst-Cell-Prozessor-auslaufen-864497.html

[72] A. U. Kemloh Wagoum, B. Steffen, and A. Seyfried, "Runtime optimisation approaches for a real-time evacuation assistant," in *Parallel Processing and Applied Mathematics*, ser. Lecture Notes in Computer Science, R. Wyrzykowski, J. Dongarra, K. Karczewski, and J. Wasniewski, Eds. Springer Berlin/Heidelberg, 2012, vol. 7203, pp. 386–395.

[73] *Juropa-JSC - HPC-FF*, August 2009. [Online]. Available: http://www.fz-juelich.de/portal/EN/Research/InformationTechnology/Supercomputer/JUROPA.html

[74] M. Geimer, F. Wolf, B. J. N. Wylie, E. Ábrahám, D. Becker, and B. Mohr, "The scalasca performance toolset architecture," *Concurrency and Computation: Practice and Experience*, vol. 22, no. 6, pp. 702–719, 2010.

[75] S. E. Asch, *Effects of group pressure upon the modification and distortion of judgments*. Carnegie Press, 1951, vol. 27, no. 3, pp. 177–190.

[76] F. Allport, *Social psychology*. Houghton Mifflin, 1924.

[77] R. Turner and L. Killian, *Collective behavior*. Prentice-Hall, 1972.

[78] J. Sime, "Crowd psychology and engineering," *Safety Science*, vol. 21, no. 1, pp. 1–14, 1995.

[79] S. R. Musse and D. Thalmann, "Hierarchical model for real time simulation of virtual human crowds," *IEEE Transactions on Visualization and Computer Graphics*, vol. 7, pp. 152–164, 2001.

[80] H. Xi and Y.-J. Son, "Two-level modeling framework for pedestrian route choice and walking behaviors," *Simulation Modelling Practice and Theory*, vol. 22, pp. 28–46, 2012.

[81] N. Pelechano and N. I. Badler, "Modeling crowd and trained leader behavior during building evacuation," *IEEE Computer Graphics and Applications*, vol. 26, pp. 80–86, 2006.

[82] B. G. Silverman, "Toward realism in human performance simulation," in *The science and simulation of human performance*, ser. Advances in human performance and cognitive engineering research, J. Ness, V. Tepe, and D. Ritzer, Eds., vol. 5. Emerald Group Publishing Limited, 2004, pp. 469–498.

[83] ——, *PMFserv (Version 2.1.0)[Computer Software]*, Edutainiacs: LLC, Philadelphia, PA, 2006.

[84] C. M. Henein and T. White, "The microscopic model and the panicking ball-bearing," in *Pedestrian and Evacuation Dynamics 2008*, W. W. F. Klingsch, C. Rogsch, A. Schadschneider, and M. Schreckenberg, Eds. Springer Berlin Heidelberg, 2010, pp. 569–575.

[85] R. Geraerts and M. H. Overmars, "The corridor map method: A general framework for real-time high-quality path planning." *Computer Animation and Virtual Worlds*, vol. 18, pp. 107–119, 2007.

[86] J. Barraquand, L. Kavraki, J.-C. Latombe, T.-Y. Li, R. Motwani, and P. Raghavan, "A random sampling scheme for path planning," *International Journal of Robotics Research*, vol. 16, pp. 759–774, 1996.

[87] J. Dijkstra and H. Timmermans, "Towards a multi-agent model for visualizing simulated user behavior to support the assessment of design performance," *Automation in Construction*, vol. 11, no. 2, pp. 135–145, feb 2002.

[88] G. Løvås, "Modelling and simulation of pedestrian traffic flow," *Transpn. Res. B*, vol. 28, pp. 429–443, 1998.

[89] M. Asano, T. Iryo, and M. Kuwahara, "Microscopic pedestrian simulation model combined with a tactical model for route choice behaviour," *Transportation Research Part C: Emerging Technologies*, vol. 18, no. 6, pp. 842–855, 2010.

[90] M. Höcker, V. Berkhahn, A. Kneidl, A. Borrmann, and W. Klein, "Graph-based approaches for simulating pedestrian dynamics in building models," in *8th European Conference on Product & Process Modelling (ECPPM)*, University College Cork, Cork, Ireland, 2010.

[91] H. Alt and E. Welzl, "Visibility graphs and obstacle-avoiding shortest paths," *Mathematical Methods of Operations Research*, vol. 32, pp. 145–164, 1988.

[92] E. W. Dijkstra, "A note on two problems in connexion with graphs." *Numerische Mathematik*, vol. 1, pp. 269–271, 1959.

[93] R. W. Floyd, "Algorithm 97: shortest path," *Communications of the ACM*, vol. 5-6, p. 345, 1962.

[94] P. Svestka and M. H. Overmars, "Coordinated path planning for multiple robots," *Robotics and Autonomous Systems*, vol. 23, pp. 125–152, 1998.

[95] M. H. Overmars and E. Welzl, "New methods for computing visibility graphs," in *Proceedings of the fourth annual symposium on Computational geometry*, ser. SCG '88. New York, NY, USA: ACM, 1988, pp. 164–171.

[96] U. Chattaraj, A. Seyfried, and P. Chakroborty, "Comparison of Pedestrian Fundamental Diagram Across Cultures," *Advances in Complex Systems*, vol. 12, no. 3, pp. 393–405, 2009.

[97] J. Klewer, "Die Wahrnehmung von Besuchern von Großveranstaltungen auf ihren Wegen in Stadien," Masterthesis, Rheinische Friedrich-Wilhelms-Universität Bonn, Sep 2009.

[98] E. S. Kirik, T. B. Yurgel'yan, and D. Krouglov, "The Shortest Time and/or the Shortest Path Strategies in a CA FF Pedestrian Dynamics Model," *Journal of Siberian Federal University. Mathematics & Physics*, vol. 2, no. 3, pp. 271–278, 2009.

[99] H. Zhao and Z. Gao, "Reserve capacity and exit choosing in pedestrian evacuation dynamics," *Journal of Physics A: Mathematical and Theoretical*, vol. 43, 2010.

[100] S. M. Lo, H. C. Huang, P. Wang, and K. K. Yuen, "A game theory based exit selection model for evacuation," *Fire Safety Journal*, vol. 41, pp. 364–369, 2006.

[101] R.-Y. Guo and H.-J. Huang, "Route choice in pedestrian evacuation: formulated using a potential field," *Journal of Statistical Mechanics: Theory and Experiment*, vol. P04018, 2011.

[102] T. Kretz, "Pedestrian traffic: on the quickest path," *Journal of Statistical Mechanics: Theory and Experiment*, vol. P03012, 2009.

[103] S. Russell and P. Norvig, *Artificial Intelligence: A Modern Approach*, 2nd ed. Prentice-Hall, Englewood Cliffs, NJ, 2003.

[104] K. Nishinari, A. Kirchner, A. Namazi, and A. Schadschneider, "Extended Floor Field CA Model for Evacuation Dynamics," *IEICE Transactions*, vol. 87-D, no. 3, pp. 726–732, 2004.

[105] Z. Fang, Q. Li, Q. Li, L. D. Han, and D. Wang, "A proposed pedestrian waiting-time model for improving space time use efficiency in stadium evacuation scenarios," *Building and Environment*, vol. 46, no. 9, pp. 1774–1784, 2011.

[106] A. Borgers and H. Timmermans, "A model of pedestrian route choice and demand for retail facilities within inner-city shopping areas," *Geogr. Anal.*, vol. 18, p. 115, 1986.

[107] H. Timmermans, X. van der Hagen, and A. Borgers, "Transportation systems, retail environments and pedestrian trip chaining behavior: modelling issues and applications," *Transportation Research*, vol. 26B, no. 1, pp. 45–59, 1992.

[108] H. Ehtamo, S. Heliövaara, S. Hostikka, and T. Korhonen, "Modeling Evacuees' Exit Selection with Best Response Dynamics," in *Pedestrian and Evacuation Dynamics 2008*, W. W. F. Klingsch, C. Rogsch, A. Schadschneider, and M. Schreckenberg, Eds. Springer-Verlag Berlin Heidelberg, 2010.

[109] K. Teknomo and P. Fernandez, "Simulating optimum egress time," *Safety Science*, vol. 50, no. 5, pp. 1228–1236, 2012.

[110] A. U. Kemloh Wagoum, A. Seyfried, and S. Holl, "Modelling dynamic route choice of pedestrians to assess the criticality of building evacuation," *Advances in Complex Systems*, vol. 15, no. 3, 2012.

[111] A. U. Kemloh Wagoum and A. Seyfried, "Optimizing the evacuation time of pedestrians in a graph-based navigation," in *Developments in Road Transportation*, M. Panda and U. Chattaraj, Eds. Macmillian Publishers India Ltd, 2010, pp. 188–196.

[112] A. Seyfried, A. Portz, and A. Schadschneider, "Phase coexistence in congested states of pedestrian dynamics," in *Cellular Automata*, ser. Lecture Notes in Computer Science, S. Bandini, S. Manzoni, H. Umeo, and G. Vizzari, Eds., vol. 6350, 9th International Conference on Cellular Automata for Reseach and Industry, ACRI 2010 Ascoli Piceno, Italy, September 2010. Springer-Verlag Berlin / Heidelberg, 2010.

[113] G. Løvås, "On the importance of building evacuation system components," *IEEE Transact. on Eng. Man.*, vol. 45, pp. 181–191, 1998.

[114] W. Chow, "[']waiting time' for evacuation in crowded areas," *Building and Environment*, vol. 42, no. 10, pp. 3757–3761, 2007.

[115] H. E. Nelson and F. W. Mowrer, "Emergency Movement," in *SFPE Handbook of Fire Protection Engineering*, 3rd ed., P. J. DiNenno, Ed. Quincy MA: National Fire Protection Association, 2002, ch. 14, pp. 367–380.

[116] A. Seyfried, B. Steffen, and T. Lippert, "Basics of modelling the pedestrian flow," *Physica A*, vol. 368, pp. 232–238, 2006.

[117] N. Biggs, E. Lloyd, and R. Wilson, *Graph theory, 1736-1936*. Clarendon Press, 1999.

[118] P. Stucki, *Obstacles in pedestrian simulations*. ETH, Eidgenössische Technische Hochschule Zürich, Department of Computer Science, 2003.

[119] D.-T. Lee, "Proximity and reachability in the plane." Dissertation, University of Illinois at Urbana-Champaign, Champaign, IL, USA, 1978, aAI7913526.

[120] E. Welzl, "Constructing the visibility graph for n-line segments in o(n2) time," *Information Processing Letters*, vol. 20, no. 4, pp. 167 – 171, 1985.

[121] S. K. Ghosh and D. M. Mount, "An output-sensitive algorithm for computing visibility graphs," *SIAM Journal on Computing*, vol. 20, no. 5, pp. 888–910, 1991.

[122] J. Kitzinger, "The visibility graph among polygonal obstacles: a comparison of algorithms," Masterthesis, University of New Mexico, 2003.

[123] B. Steffen and A. Seyfried, "Modelling of pedestrian movement around 90° and 180° bends," in *Proceedings of the First International Conference on Soft Computing Technology in Civil, Structural and Environmental Engineering*, B. H. V. Topping and Y. Tsompanakis, Eds. Civil-Comp Press, Stirlingshire, UK, 2009.

[124] F. Giannotti and D. Pedreschi, Eds., *Mobility, Data Mining and Privacy - Geographic Knowledge Discovery*. Springer, 2008.

[125] S. Leitinger, S. Gröchenig, S. Pavelka, and M. Wimmer, *Erfassung von Personenströmen mit der Bluetooth-Tracking-Technologie. In: Angewandte Geoinformatik 2010*, 15th ed. New York: Addison Wesley Longman Inc., 2010.

[126] T. Liebig and A. U. Kemloh Wagoum, "Modelling microscopic pedestrian mobility using bluetooth," in *ICAART (2)*, 2012, pp. 270–275.

[127] R. Golledge, "Path selection and route preference in human navigation: A progress report," in *Spatial Information Theory A Theoretical Basis for GIS*, ser. Lecture Notes in Computer Science, A. Frank and W. Kuhn, Eds. Springer Berlin / Heidelberg, 1995, vol. 988, pp. 207–222.

Résumé

"No man should escape our universities without knowing how little he knows." – J. Robert Oppenheimer

Personal Information

First Name	Armel Ulrich
Last Name	Kemloh Wagoum
Date of Birth	September 08, 1983
Place of Birth	Mbo Bandjoun, Cameroon

Education

Oct.2012-Dec.2012	**Research Associate**, *Dept. Computer sciences, University of North Carolina at Chapel Hill, USA*.
2009–present	**Research Associate**, *Dept. Civil Security and Traffic, German Research Centre Jülich GmbH, Germany*.
2002–2008	**Certified Degreed Engineer (Dipl.-Ing.)** , *grade 1.5 (Very Good)*, Hamburg University of Technology (TUHH), Computer Science and Engineering. Concentrations: Scientific Calculation and Communication in Networks
2004	**Pre Diploma (Vordiplom)**, *TUHH*, grade 1.8 (Good).
1993–2001	**High School**, *Government Bilingual High School*, Bafoussam, Cameroon. School Leaving Certificate (Baccalauréat C) with distinctions
1987–1993	**Grammar School**, *École Publique de Banengo*, Bafoussam, Cameroon.

Theses

Diploma Thesis

title	*Implementation of a Data Mining Approach for the Flood Risk Management Domain*
supervisors	Prof. Dr. F. Mayer-Lindenberg, Prof. Dr.-Ing. E. Pasche, Dr.-Ing. P. Owotoki, M.Sc. N. Manojlovič
description	A web-based advisory system for flood prone areas with a data mining back-end as business logic of the system

Student Research Project (Joint work with Airbus Germany GmbH)

title	*Optimization of System Validation in Aircraft Systems*
supervisors	Prof. Dr.-Ing. W. Krautschneider, Dr.-Ing. T. Selchert

Academic Honours and Awards

2004–2005	Scholarship for Students with Outstanding Academic Performance
2006–2008	Friedrich-Naumann Stiftung für die Freiheit fellowship

2010 "Tracking, Analysis and Simulation of Crowds", Maik Boltes, Ulrich Kemloh, Mohcine Chraibi and Jack Liddle. Best Poster Award, ASIM Workshop 2010 Forschungszentrum Jülich GmbH

Teaching Experience

2005–2006 Undergraduate in electronics

2007 Tutorial in C-Programming and electronics, Spring 2007

2003–2005 Supervisor by the DLR SCHOOL LAB at the Hamburg University of Technology, Physics experiments with high school students

Internships

2007 **Weinmann Medical Systems**, *Hamburg*, Germany.
Software and hardware development, firmware for medical devices

2004 **Philips Semiconductors**, *Hamburg*, Germany.

2004 **Siemens AG**, *Hamburg*, Germany.

2002 **Informix SARL Cameroon**, *EDV: Operating systems Windows and UNIX/Linux.*

Languages

French **Native Language**

German **proficient**

English **proficient**

Miscellaneous Activities

2011–present Chief Information Officer by Koegni-eHealth, Innovation for Development e.V. (registered association)

2002–present Membership of the ASTO TUHH (African Student Organisation at the TUHH)

2006–2008 Responsible for the Education section at the Cameroonian Association Hamburg (ACH e.V, Registered Association)

2000–2001 Co-founder and chairman of the computer science club in Government Bilingual High School Bafoussam

Updated

April 16, 2013

Schriften des Forschungszentrums Jülich
IAS Series

1. **Three-dimensional modelling of soil-plant interactions: Consistent coupling of soil and plant root systems**
by T. Schröder (2009), VIII, 72 pages
ISBN: 978-3-89336-576-0
URN: urn:nbn:de:0001-00505

2. **Large-Scale Simulations of Error-Prone Quantum Computation Devices**
by D. B. Trieu (2009), VI, 173 pages
ISBN: 978-3-89336-601-9
URN: urn:nbn:de:0001-00552

3. **NIC Symposium 2010**
Proceedings, 24 – 25 February 2010 | Jülich, Germany
edited by G. Münster, D. Wolf, M. Kremer (2010), V, 395 pages
ISBN: 978-3-89336-606-4
URN: urn:nbn:de:0001-2010020108

4. **Timestamp Synchronization of Concurrent Events**
by D. Becker (2010), XVIII, 116 pages
ISBN: 978-3-89336-625-5
URN: urn:nbn:de:0001-2010051916

5. **UNICORE Summit 2010**
Proceedings, 18 – 19 May 2010 | Jülich, Germany
edited by A. Streit, M. Romberg, D. Mallmann (2010), iv, 123 pages
ISBN: 978-3-89336-661-3
URN: urn:nbn:de:0001-2010082304

6. **Fast Methods for Long-Range Interactions in Complex Systems**
Lecture Notes, Summer School, 6 – 10 September 2010**,** Jülich, Germany
edited by P. Gibbon, T. Lippert, G. Sutmann (2011), ii, 167 pages
ISBN: 978-3-89336-714-6
URN: urn:nbn:de:0001-2011051907

7. **Generalized Algebraic Kernels and Multipole Expansions for Massively Parallel Vortex Particle Methods**
by R. Speck (2011), iv, 125 pages
ISBN: 978-3-89336-733-7
URN: urn:nbn:de:0001-2011083003

8. **From Computational Biophysics to Systems Biology (CBSB11)**
Proceedings, 20 - 22 July 2011 | Jülich, Germany
edited by P. Carloni, U. H. E. Hansmann, T. Lippert, J. H. Meinke, S. Mohanty, W. Nadler, O. Zimmermann (2011), v, 255 pages
ISBN: 978-3-89336-748-1
URN: urn:nbn:de:0001-2011112819

9. **UNICORE Summit 2011**
Proceedings, 7 - 8 July 2011 | Toruń, Poland
edited by M. Romberg, P. Bała, R. Müller-Pfefferkorn, D. Mallmann (2011), iv, 150 pages
ISBN: 978-3-89336-750-4
URN: urn:nbn:de:0001-2011120103

10. **Hierarchical Methods for Dynamics in Complex Molecular Systems**
Lecture Notes, IAS Winter School, 5 – 9 March 2012, Jülich, Germany
edited by J. Grotendorst, G. Sutmann, G. Gompper, D. Marx (2012), vi, 540 pages
ISBN: 978-3-89336-768-9
URN: urn:nbn:de:0001-2012020208

11. **Periodic Boundary Conditions and the Error-Controlled Fast Multipole Method**
by I. Kabadshow (2012), v, 126 pages
ISBN: 978-3-89336-770-2
URN: urn:nbn:de:0001-2012020810

12. **Capturing Parallel Performance Dynamics**
by Z. P. Szebenyi (2012), xxi, 192 pages
ISBN: 978-3-89336-798-6
URN: urn:nbn:de:0001-2012062204

13. **Validated force-based modeling of pedestrian dynamics**
by M. Chraibi (2012), xiv, 112 pages
ISBN: 978-3-89336-799-3
URN: urn:nbn:de:0001-2012062608

14. **Pedestrian fundamental diagrams: Comparative analysis of experiments in different geometries**
by J. Zhang (2012), xiii, 103 pages
ISBN: 978-3-89336-825-9
URN: urn:nbn:de:0001-2012102405

15. **UNICORE Summit 2012**
Proceedings, 30 - 31 May 2012 | Dresden, Germany
edited by V. Huber, R. Müller-Pfefferkorn, M. Romberg (2012), iv, 143 pages
ISBN: 978-3-89336-829-7
URN: urn:nbn:de:0001-2012111202

16. **Design and Applications of an Interoperability Reference Model for Production e-Science Infrastructures**
by M. Riedel (2013), x, 270 pages
ISBN: 978-3-89336-861-7
URN: urn:nbn:de:0001-2013031903

Schriften des Forschungszentrums Jülich
IAS Series

17. **Route Choice Modelling and Runtime Optimisation for Simulation of Building Evacuation**
by A. U. Kemloh Wagoum (2013), xviii, 122 pages
ISBN: 978-3-89336-865-5
URN: urn:nbn:de:0001-2013032608

Increasing number of visitors at large-scale events combined with the increasing complexity of modern buildings set a major challenge for planners, operators and emergency services. Examples include multi-purpose arenas, large railway stations and airports. In this dissertation the use of modern parallel hardware in combination with optimised algorithms are for the first time used on site to speed up the simulation of large crowds. The aim is to perform real-time forecasts of pedestrian traffic. For this purpose, special neighbourhood lists and a two-stage hybrid parallelisation are used. The second part of this dissertation deals with route choice in complex structures, which plays an important role in achieving realistic computer simulations of pedestrian flows. The developed route choice process is based on visibility and perception of the local environment by the simulated agents. It has as basis a navigation graph. The generation of the graph, especially in complex structures, has also been performed within the framework of this thesis. The work is closed with an empirical study in which the route choice profiles of spectators during various football games and concert performances are analysed and compared with the proposed model.The runtime optimisation strategies and route choice algorithms have been successfully tested in the ESPRIT arena in Düsseldorf (Germany), where they have been integrated in an evacuation assistant.

This publication was edited at the Jülich Supercomputing Centre (JSC) which is an integral part of the Institute for Advanced Simulation (IAS). The IAS combines the Jülich simulation sciences and the supercomputer facility in one organizational unit. It includes those parts of the scientific institutes at Forschungszentrum Jülich which use simulation on supercomputers as their main research methodology.

IAS Series
Volume 17
ISBN 978-3-89336-865-5

JÜLICH
FORSCHUNGSZENTRUM